Quiambao, J., Hess, K., Johnston, S., El Hayek, E.; Noureddine, A., Ali, A.S., Spilde, M., Brearley, A., Cerrato, J.M., Howe, K.J. and Jorge Gonzalez-Estrella, J. (2023) Interfacial interactions of uranium and arsenic with microplastics: from field detection to controlled laboratory tests. Environmental Engineering Science https://doi.org/10.1089/ees.2023.0054

Environmental Engineering Science

Environmental Engineering Science Manuscript Central: http://mc.manuscriptcentral.com/environmental

Interfacial interactions of Uranium and Arsenic with Microplastics: from field detection to controlled laboratory tests

Journal:	Environmental Engineering Science
Manuscript ID	EES-2023-0054
Manuscript Type:	Special issue: Microbial and Chemical Processes
Date Submitted by the Author:	24-Feb-2023
Complete List of Authors:	Quiambao, Jasmine; University of New Mexico Hess, Kendra; Oklahoma State University, School of Civil and Environmental Engineering Johnston, Emily; Oklahoma State University, School of Civil and Environmental Engineering Noureddine, Achraf; University of New Mexico, Department of Chemical & Biological Engineering El Hayek, Eliane; University of New Mexico, Department of Pharmaceutical Sciences Ali, Abdul-Mehdi; University of New Mexico, Department of Earth and Planetary Sciences Spilde, Michael; University of New Mexico, Department of Earth and Planetary Sciences Brearley, Adrian; University of New Mexico, 5Department of Earth and Planetary Sciences Cerrato, Jose; University of New Mexico, Civil, Construction, & Environmental Engineering; Howe, Kerry; University of New Mexico Gonzalez-Estrella, Jorge; Oklahoma State University College of Engineering Architecture and Technology, Civil and Environmental Engineering
Keyword:	Sorption < Groundwater Quality, Surface Water < Hydrology and Water Resources, Hazardous Materials, characterization < Hazardous Materials, Radioactive Materials
Manuscript Keywords (Search Terms):	microplastics, freshwater, uranium, arsenic, surface precipitation

SCHOLARONE™ Manuscripts



688x205mm (150 x 150 DPI)

Interfacial interactions of Uranium and Arsenic with Microplastics: from field detection to

2 controlled laboratory tests

- 3 Jasmine Quiambao¹, Kendra Hess²⁺, Sloane Johnston², Eliane El Hayek³; Achraf Noureddine⁴,
- 4 Abdul-Mehdi S. Ali⁵, Michael Spilde⁵, Adrian Brearley⁵, José M. Cerrato¹⁺, Kerry J. Howe¹⁺,
- 5 and Jorge Gonzalez-Estrella*2+

- 7 *Corresponding email addresses: jorgego@okstate.edu
- 8 +AEESP members
- 9 Department of Civil, Construction & Environmental Engineering, MSC01 1070, University of
- 10 New Mexico, Albuquerque, New Mexico 87131, USA
- ²School of Civil & Environmental Engineering, 248 Engineering North, Oklahoma State
- 12 University, Stillwater, Oklahoma 74078
- ³ Department of Pharmaceutical Sciences, MSC09 5360, University of New Mexico, College of
- 14 Pharmacy, Albuquerque, New Mexico 87131, USA
- ⁴ Department of Chemical & Biological Engineering, MSC01 1120, 1 University of New Mexico
- 16 Albuquerque, NM 87131, USA
- ⁵Department of Earth and Planetary Sciences, MSC03 2040, University of New Mexico,
- 18 Albuquerque, New Mexico 87131, USA

- 20 ABSTRACT: We studied the co-occurrence of microplastics (MPs) and metals in field sites and
- 21 further investigated their interfacial interaction in controlled laboratory conditions. First, we
- detected MPs in freshwater co-occurring with metals in rural and urban areas in New Mexico.
- Automated particle counting and fluorescence microscopy indicated that particles in field
- samples ranged from 7 to 149 particles L⁻¹. The urban location contained the highest count of
- confirmed MPs including polyester, cellophane, and rayon as indicated by Fourier Transform
- 26 Infrared Attenuated Total Reflection (FTIR-ATR) analyses. Metal analyses using inductively
- coupled plasma (ICP) revealed that bodies of water in a rural site affected by mining legacy
- contained up to 332.8 µg L⁻¹ of U, while all bodies of water contained As concentrations below
- 29 11.4 μg L⁻¹. These field findings motivated experiments in laboratory conditions reacting MPs
- with 0.02 0.2 mM of As or U solutions at acidic and neutral pH with poly(methyl-

methacrylate), polyethylene, and polystyrene MPs. In these experiments, As did not interact with any of the MPs tested at pH 3 and pH 7, nor U with any MPs at pH 3. Experiments supplied with U and MPs at pH 7 indicated that MPs served as substrate surface for the adsorption and nucleation of U precipitates. Chemical speciation modeling and microscopy analyses (e.g., TEM) suggest that U precipitates resemble sodium-compreignacite and schoepite. These findings have relevant implications to further understanding the occurrence and interfacial interaction of MPs and metals in freshwater.

Keywords: microplastics, freshwater, uranium, arsenic, surface precipitation

1. Introduction

Microplastics (MPs), plastic materials <5mm, are widely distributed in the marine environment; however, more information is needed to understand the prevalence of MPs in freshwater (Blettler et al., 2018, Carbery et al., 2018, Ateia et al., 2022). According to previous studies, MPs concentrations in surface water range from 10⁻⁵ to 1000 particles L⁻¹ (Li et al., 2018). Microplastics contamination in freshwater is closely related to anthropogenic activities and enters freshwater ecosystems via several sources, including littering, leaching and runoff from landfills, or water treatment plants (Eerkes-Medrano et al., 2015). Higher concentrations of MPs prevail in areas with high population density or proximity to urban centers(Wong et al., 2020, Yonkos et al., 2014); nevertheless, MPs occur even in remote locations (Yang et al., 2021). In freshwater, MPs interact with other contaminants (e.g., heavy metals). For example, aged polyvinyl chloride (PVC) MPs found in seawater showed traces of copper (Cu) and zinc (Zn).(Brennecke et al., 2016) Various metals were found sorbed in polyethylene terephthalate (PET), high-density polyethylene (HDPE), polyvinyl chloride (PVC), low-density polyethylene (LDPE), and polypropylene (PP) (Rochman et al., 2014); plastic materials such as PVC, HDPE,

and LDPE adsorbed trace metals of Cu, Zn, Cd, and Pb in nine urban intertidal regions in Canada (Munier and Bendell, 2018). Microplastics evidently react with heavy metals; therefore, the reactivity between MPs and heavy metals increases in waters contaminated with heavy metals. However, we have limited information about the status of MP contamination in freshwater with known elevated concentrations of heavy metals. The interaction between MPs and heavy metals is driven by physicochemical properties of MPs, chemical characteristics of heavy metals, and environmental conditions (Tourinho et al., 2019, Ateia et al., 2022). Properties of contaminants such as pKa, hydrophobicity, planarity, chain, ring structure, and functional groups affect the adsorption of contaminants on MPs. Organic matter, pH, ionic strength, salinity, contact time, and temperature affect the adsorption behavior of different contaminants on MPs as well (Nafiaah, 2020). Uranium and As undergo a wide range of complexation, dissociation, and precipitation reactions in water (Gonzalez-Estrella et al., 2020, Meza et al., 2023) and likely affect the typical sorption mechanisms between other metals and MPs observed in previous studies. Thus, more information is needed to understand the interfacial interactions of U and As with MPs. Our study assessed the prevalence of MPs in urban and rural freshwater with known elevated U and As concentrations documented since 2014 and affected by U mining for a few decades (Blake et al., 2015, Blake et al., 2017). The field results motivated the evaluation of the interactions of As and U with polyethylene (PE), polystyrene (PS), and polymethyl(meta)acrylate (PMMA) MPs in controlled laboratory conditions. The novelty of our study is rooted in integrating field and laboratory methods to better understand the mechanisms affecting the interaction of metals and MPs. We provide new insights into the role of interfacial processes affecting the reactivity of

metals and MPs in freshwater containing these constituents.

2. Materials and Methods

- **2.1. Field sampling and analyses.**
- 79 2.1.1. Experimental procedures to avoid MP contamination in field and laboratory
- **methodologies.** The use of plastic materials was reduced as much as possible to avoid MP
- background contamination. All experimental instruments and glassware were sonicated for 30
- min in an ultrasonic bath with ultra-pure water (18 M Ω) and covered with aluminum foil
- between sonication and use. All benchtops were carefully cleaned, and all laboratory procedures
- were conducted in a fume hood. Field controls were included to monitor any airborne
- 85 contamination. In laboratory procedures, a control containing only ultra-high purity water during
- 86 filtering and digestion was included to account for any background MP interference.
- 2.1.2. Sampling Methodology. For MPs analyses, three 1L samples were collected from six
- 88 locations along Paguate River and freshwater reservoirs near the Jackpile Mine of Laguna
- 89 Pueblo, NM. These sites were selected based on their proximity to the mine and the Laguna
- 90 community. Additionally, three locations on the Rio Grande, and three on Tingley Beach,
- Albuquerque, NM, were selected to compare occurrence of MPs in a rural and an urban
- 92 community (Table S1). Samples were taken from the surface to avoid sediment interference. A
- 93 separate set of samples were taken from 20 bodies of water in the area to confirm elevated
- oncentrations of U and As reported in previous studies from our group (Blake et al., 2015,
- 95 Blake et al., 2017). Note that less samples were taken for MP analyses due to the complexity of
- 96 the extraction procedures.
- 97 2.1.3 Extraction of MPs. To extract MPs and ensure the quality of visual assessment and
- 98 polymer identification, the procedure recommended by Koelmans et al. (2019) was followed.

- Details about the extraction of microplastics are provided in the supplementary information (SI) document.
- 2.1.4 Analyses of MPs and Metals in Field Samples. The extracted particles were examined and imaged using a stereomicroscope (AmScope 7X-180X Trinocular Zoom Stereo Microscope) for initial visual assessment. The filters were imaged using a fluorescence microscope (Cytation 5 Cell Imaging Multi Mode Reader, Agilent Technologies) with Gen5® software. For quantification, each filter's overall image was run through the MPVAT 2.0 macros using ImageJ (Prata et al., 2020). Each filter was then analyzed using a FTIR spectrometer (micro-FTIR, Thermo Nicolet iN10 MX). For each filter, the number of particles examined with Attenuated Total Reflectance (ATR) was 10% of the particles identified during fluorescence microscopy quantification, or a minimum of five (whichever was greater). Further details of the fluorescence and FTIR-ATR analyses are provided in the supplementary SI document.
- 2.2 Controlled laboratory experiments.
 - **Reagents.** Sodium arsenate dibasic heptahydrate, Na₂HAsO₄7H₂O reagent (\geq 98%) was purchased from Sigma Aldrich. Uranyl nitrate hexahydrate reagent, UO₂(NO₃)₂6(H₂O) (98-102%) was purchased from IBI Labs. Three types of common, high-production-volume MPs were used in these experiments: PE, PS, and PMMA (Table S2). Polyethylene is considered the "largest volume polymer produced globally" (Demirors, 2011) while PMMA has a wide range of applications where it is used as a substitute for glass products like aircraft canopies, windows, and aquariums (Ali et al., 2015). Polyethylene (0.96 g/cc, $10-63 \mu m$) and PMMA MPs (1.2 g/cc, 1-45 µm) were purchased from Cospheric (California, USA). Polystyrene is used for packaging, disposable cups, and many other uses (Veerappapillai & Muthukumar, 2015). Polystyrene beads (200-300µm) were purchased from Polysciences. Glass microfiber filters (Advantec GC-50

borosilicate diameter, 47mm; Pore Size: 0.5 µm) were purchased from Cole-Parmer. The main characteristics of these MPs are provided in Table S2.

2.2.2 Sorption experiments. These series of experiments were performed to assess the

sorption of different concentrations of As and U onto PE, PS, and PMMA commercial MPs at pH 3 and pH 7. pH adjustments were made with 0.1 M HNO₃ or NaOH. A mass of 0.1 g of Polyethylene, PS, and PMMA commercial MPs were added into a borosilicate glass beaker containing a volume of 100 mL of DI water resulting in a concentration of MP of 1 g L⁻¹. Isotherms were carried out for 48h by separately exposing the MPs to 0.05, 0.1, and 0.2 mM of U or As. All experimental conditions were run in triplicates in a VWR Advanced Orbital Shaker Model 15000 at 150 rpm at room temperature (25°C) for 48h. After 48h. the solutions were vacuum filtered through a 0.5 μm glass microfiber filter and glass frit filter unit. The filtered water samples were transferred into centrifuge tubes and the filters were placed in a petri dish and stored at 4°C. Metal adsorption was determined by quantifying the soluble concentration of U and As with ICP-OES and ICP-MS. Each filter paper was slowly rinsed with ultra-pure water (18 MΩ) to avoid additional compounds precipitating as the remaining water evaporated from the filter surface and preserved for spectroscopy analyses.

2.2.3 Interaction of MPs with filtered solutions of U. An additional set of experiments were conducted to isolate the interactions between soluble U and MPs at pH 7. In these experiments 0.02 and 0.06mM U were used and all U solutions were filtered prior to exposure to the MPs to eliminate U precipitates from the solution. Polypropylene centrifuge tubes were used instead of glass to ensure that the glass was not providing a surface for heterogenous precipitation. The isotherms were run with the same parameters and conditions explained above. A control with no MPs was also included in the experiment.

- **2.2.4 Characterization of MPs.** Polyethylene, PMMA, and PS MPs exposed to U and As were analyzed with various spectroscopy techniques to identify any precipitation reaction on the surface. Transmission Electron Microscopy (TEM), Scanning Electron Microscopy (SEM), and Energy Dispersive Spectroscopy (EDS) were used to examine the MPs morphology and quantify heavy metals binding onto the surface. Zeta potential ζ was used to measure the surface charge of MPs at pH 3 and pH 7. Details of sample preparation and SEM and TEM analyses parameters are provided in SI.
- 152 3. Results and Discussion
- 153 3.1 Occurrence of MPs in freshwater
- Quantification and Characterization of MPs. All locations contained a similar range of 3.1.1 particle concentrations (Table 1). In Laguna Pueblo, NM, a range from 7 to 149 particles L⁻¹ was detected in the water samples taken from six different locations (Fig. S1A-F and Table 1). Water samples taken from three different locations of Tingley Beach, Albuquerque, NM, showed a range of 18 to 127 particles L⁻¹. Finally, a range from 12 to 101 particles L⁻¹ were detected in water samples taken from three different locations of Rio Grande, Albuquerque, NM. Following quantification, FTIR-ATR analyses were performed to analyze the chemical composition of the particles. A total of 25, 23, and 25 particles were analyzed from the Laguna Pueblo, Tingley Beach, and Rio Grande samples, respectively. Fig. 1 shows representative particles analyzed with FTIR-ATR, Table 1 shows the spectra match of each particle analyzed, and all data from these analyses are available in the supporting information file (Table S4-S6). The 25 particles analyzed from the Laguna Pueblo samples indicated spectra matching from 21% to 72% relative to pure polymers. The most common polymer found in Laguna Pueblo was cellophane (CP) with spectra matches ranging from 30 to 67%, followed by

poly(styrene:vinylidene chloride) (37–48%), and rayon (32-72%) (Table 1). Analysis of 23 particles randomly selected from the Tingley Beach samples indicated their spectra matched from 25% to 73% to pure polymers (Table 1). The most common polymers found in these samples were cellophane (29-64%), followed by polyester (PES) (73%), and rayon (56-67%). Finally, the analyses of 25 particles selected from the Rio Grande samples indicated their spectra matched from 20% to 73% relative to pure polymers. The most common spectra match found in these samples were cellophane (33-72%) followed by rayon (38-52%) and poly(styrene) (28–50%).

The results presented above include all matches, but the criteria used in this study require spectra matches greater than 60% for a particle to be considered a confirmed MP. Confirmed MPs are bolded in Table 1. Of the 25 particles examined with FTIR-ATR from the Laguna Pueblo location, two MPs were identified- rayon (72%) and cellophane (67%), meaning that 8% of the particles match with a polymer spectrum. On the other hand, from the 23 particles analyzed in Tingley Beach, two polyester (both 73%), two rayon (67 and 63%), one polytetrafluoroethylene #4 (65%), and three cellophane (64, 63, and 60%) MPs were identified, meaning that 32% of the particles match with a polymer spectrum. Finally, out of the twenty-five particles analyzed from Rio Grande, one polyamide 6 + polyamide 6,6 (73%) particle and one cellophane (72%) particle were identified as MPs, indicating that 8% of the particles analyzed matched with a polymer spectrum. This analysis indicates that Tingley beach, a stagnant freshwater body located in an urban center, contained the highest number of particles confirmed as MPs.

However, a distinction must be made that the FTIR-ATR analysis provides insight specifically into MPs greater than 20 μ m. While this is limiting, it is important to recall that larger MPs can continue to break down in the environment potentially releasing micro- and nanoplastics

below this 20 μ m threshold, thus an analysis of larger MPs still provides valuable insight. Many of the particles on each filter, especially fibers, had at least one dimension below the 20 μ m detection limit of the μ -FTIR, but above the 0.5 μ m detection limit of the fluorescence microscopemeaning they could be quantified, but were not eligible for FTIR-ATR analysis. An example of fibrous particles, potentially MPs, that were below the detection limit are shown in Fig. S1.

Previous studies have also found similar polymer types including PES, PA, rayon, or CP and a similar particle content in freshwater. For example, a range from 3.4 to 25.8 particles L⁻¹ were found in Lake Taihu in China. The most common polymer types identified were CP, polyethylene terephthalate (PET), PES, polypropylene (PP), and polyamide (PA) (Su et al., 2016). Fibrous and fragmented MPs were found along the middle and lower reaches of the Yangtze River Basin with concentrations varying from 0.24 to 1.8 particles L⁻¹ and 0.5 to 3.1 particles L⁻¹, respectively (Li et al., 2019, Su et al., 2018). Mainly PP, polyethylene (PE), and polycarbonate (PC) were found in the middle of the Yangtze River Basin (Li et al., 2019), while the most dominant polymers were PES (33%), PP (19%), and PE (9%) in the lower basin area (Su et al., 2018). Similarly, a range from 0.9 to 2.4 particles L⁻¹ were identified in Suzhou River, Huangpu River, and the urban creeks of Shanghai where the dominant polymer was PES (Luo et al., 2019). Microplastic Functional Chemistry. The degradation of MPs in the environment due to ultraviolet and physical weathering has become well documented in recent years (Liu et al., 2020). In this work, the functional chemistry of weathered environmental MPs are compared with pristine and pure polymer spectral reference libraries. The FTIR-ATR spectra of selected MPs found in field samples compared to the reference spectra are shown in Fig. 2. All examined spectra including library references are found in from Table S4 to S6. Changes in the spectra of the MPs found in the samples compared to the reference spectrum may be explained due to weathering patterns and

reactions with other elements in the environment can be observed in the rayon particles (T1-1 and T2-3) in O-H region (3700-3000 cm⁻¹) and C-H peaks (2900 cm⁻¹). Cellophane particles (T1-2 and T1-3) showed changes in the C-H bending signal (1450-1500 cm⁻¹). Other examples include the polyester MPs (T2-1 and T22) with modifications in the O-H (3700-3000 cm⁻¹) and C-H peaks (2900 cm⁻¹) compared to the reference. Discrepancy in functional chemistry between the pristine reference spectra and weathered environmental MPs likely leads to the misidentification or underidentification of MPs by current spectral identification tools. The current challenges of spectral identification highlight the need to generate more environmentally relevant spectral libraries that contain mechanically weathered and UV aged polymers.

Quantification of U and As in freshwater. Our analyses confirmed occurrence of U and As in all freshwaters that were sampled to detect MPs (Table S3). In Laguna Pueblo, the concentration of U and As ranged from 0.45 to 332.80 μg L⁻¹ and from 0.66 to 5.54 μg L⁻¹, respectively. These analyses agree with previous findings (Blake et al., 2015, Blake et al., 2017). The concentration of U and As of the samples collected from Tingley Beach ranged from 2.16 to 2.35 μg L⁻¹ of U and 10.75 to 11.40 μg L⁻¹ of As. Samples collected from Rio Grande showed a concentration of U from 1.07 to 1.43 μg L⁻¹ while the concentration of As ranged from 2.32 to 3.05 μg L⁻¹.

In our study, it was not possible to detect accumulation of U and As on the surface of MPs due to the methodologies used for extraction of MPs, i.e., in bodies of water with higher content of organic matter and suspended solids, chemical treatment is necessary to remove excess of particulate material. The high content of organic matter and inorganic particles in the samples interfered with the direct analysis of MPs without any sample treatment. These field observations motivated additional experiments in controlled laboratory conditions to assess interactions of metals with MPs.

3.2 Interfacial interactions of metals and MP in controlled laboratory conditions.

Uranium Precipitation and Reactivity with the MPs surface at pH7. The reactivity of U and MPs depended on the pH. In assays supplied with PMMA and PE carried out at pH 7, the soluble concentration of U decreased significantly (p < 0.05) from 0.05 mM to \sim 0.003 mM after 48h of reaction (Fig. 3A-C). The soluble U concentration exposed to the three types of MPs and the control remained close to the initial concentration (0.05 mM) after the 48h exposure (Fig. 3D-F). Surface SEM EDS analyses revealed that U precipitated on the surface of PMMA (Fig. 4A). Further SAED TEM analyses of both the surface of the MPs and precipitates formed in the control suggest that the solid phase formed resemble Na-compreignacite on the surface of PMMA (Fig. 4B). Chemical equilibrium analyses were conducted and indicated that the solution was supersaturated with respect to schoepite and Na-compreignacite; both uranyl oxide hydrates. The Na-bearing U solids were the primary phases in our study because NaOH was used to adjust the pH. The decrease in U observed in the control without MPs at pH 7 was likely caused by homogenous precipitation of uranyl solids. Heterogenous precipitation took place with the presence of MPs which provided surface sites for U solids to deposit and precipitate. These results suggest that U homogenous and heterogenous precipitation processes are relevant mechanisms that may be observed in aquatic environments supersaturated with U. Past studies have confirmed Na-compreignacite and schoepite precipitates formed at pH 7 in a similar concentration used in our study (Gorman-Lewis, Burns, et al., 2008; Gorman-Lewis, Fein, et al., 2008; Kanematsu et al., 2014). To further investigate the surface interaction mechanism of U and MPs, PMMA MPs

PMMA MPs were selected for these experiments because they have the smallest particle size (1-

were exposed to three different U concentrations (0.05, 0.1, and 0.2 mM) at pH 7 for 48 h.

 μ m), largest surface area (0.86 ± 0.87 m²/g), most negatively charged surface (-42.83 ± 5.17 mV) compared to PE and PS at pH 7 (Table S2 and Fig. S2) and the concentration of U decreased the most in the sorption experiments amended with PMMA MPs. The soluble U concentration significantly (p < 0.05) decreased in assays supplied with and control without PMMA MPs (Fig. 5). These findings show that homogenous and heterogenous precipitation of U onto the surface of the MPs are key mechanism for U reactivity in the system studied.

Interaction of MPs with Prefiltered U Solutions. Additional experiments were run with U concentrations of 0.02 and 0.06 mM that were prefiltered to ensure that U precipitates was the conduct in which U reacted with MP and not the soluble fraction. The filtered U solution exposed to the three MPs and the control at pH 7 slightly decreased (Fig. S3). The use of glass vials was eliminated in this section as it can influence precipitation reactions; polypropylene tubes was used instead. These findings imply that homogenous and heterogenous precipitation are still occurring in the system even with the substitution from glass to plastic and with the extra filtration step to remove U precipitate before MP exposure. Although U precipitated homogenously in the control without MPs, the SEM analyses confirmed U mineral precipitated heterogeneously on the MPs surface. The EDS analyses also showed U and Na compositions and did not show any silica (Si) (Fig. 4). A paired-samples t-test showed the decrease of U concentration is significantly different, t(2) = 64.27, p = 0.0002, (p < 0.05). These results demonstrate that the precipitation process drives the interaction between the MPs and uranium, and not the soluble ions in the system. Other studies have reported that metals reacted with MPs. Most of the interactions reported in these studies are attributed to adsorption reactions between cations and MPs.

Lack of reactivity of As (pH 3 and 7) and U (pH 3) with MPs. All experiments supplied with As and PE, PS, and PMMA MPs at pH 3 and pH 7 remained close to the initial concentration (0.05 mM) after the 48 h of exposure (Fig. 3D-F). Similar results were found for the assays supplied with U at pH 3. The controls showed no change in the concentration as well. Although sorption of As (III) onto polytetrafluoroethylene (PTFE) and PS MPs at pH ranging from 3 to 7 has been reported (Dong et al., 2019, 2020), we found no sorption of As (V) onto MPs at pH 3 and 7. Lack of sorption of As (V) may be explained by difference of charges; that is, As (V) is predominantly negative at this pH range (H₂AsO₄- and HAsO₄²-), whereas As (III) species are uncharged (Benjamin, 2015). Lack of sorption of U at pH 3, predominantly UO₂²⁺ at acidic pH, likely results from the lack of electrostatic attraction as well. Previous studies have stated that hydrophobic and electrostatic interactions are two predominant mechanisms for the sorption of contaminants on MPs (Tourinho et al., 2019).

3.3 Environmental Implications

Freshwater samples containing MPs and taken from a location that has been historically affected by U mining highlights the importance of detecting MPs on sites also affected by other contaminants of concern. Accumulation of contaminants on MPs can facilitate the transport and localized consumption of contaminants by various trophic groups. Moreover, the batch experiment data indicated that heterogeneous precipitation could be a key reaction mechanism between MPs and U which is relevant in sites with elevated concentrations of metals (Blake et al., 2017, Donahue and Hendry, 2003, Ruiz et al., 2016). Actual environmental conditions (e.g., pH, organic matter composition, ionic strength, salinity, contact time, and temperature) may affect these reactions; therefore, future research should observe the behavior of MPs and U with weathered MPs and in various aqueous media like samples collected from freshwater and

seawater. A better understanding of the relationship and behavior of metals and MPs would provide valuable information about the transport of contaminants sorbed onto MPs and potential toxicity synergies.

4 Conclusions

Our findings indicate that heavy metal contaminated in freshwater rural communities can be also affected by MP occurrence. Although urban sites contained more confirmed MPs, freshwater in the rural community also contained MPs. Fluorescence quantification of MPs indicated that all water samples contained MPs in the range of 7 to 149 particles L⁻¹. Further FTIR-ATR analyses of some of the detected particles confirmed their chemical compositions match with known polymer spectra and displayed clear discrepancies in surface chemistry likely due to environmental exposure. Tingley beach, a stagnant water reservoir located in an urban center, contained the highest amount of confirmed MP particles. Laboratory experiments evidenced the formation of U precipitates on the surface of MPs at pH 7; indicating that MPs can serve as a surface for U adsorption and nucleation. Chemical speciation modeling and TEM analyses suggest that the U solids formed are sodium-compreignacite and schoepite. The lack of interfacial interaction of As and U with commercial MPs (i.e., PMMA, PE, and PS) at pH 3 is explained by unstable surface charge of the MPs. Lack of interaction of As and MPs at pH 7 is likely explained by the charge repulsion of As (anionic metalloids) and the negative surface of MPs. Our study provides insights about occurrence of MPs, the interfacial interaction of U and As with MPs in laboratory-controlled conditions, and information about their fate, mobility, and potential synergies in the environment.

5 Acknowledgments

- This work was funded by the Center for Water and the Environment (National Science
- Foundation CREST Grant Number 1914490), National Institute of Environmental Health

Sciences (NIEHS) Superfund Research Program (Award 1 P42 ES025589), the National Institute
on Minority Health and Health Disparities (NIMHD) Award Number P50MD015706, and the
New Mexico Water Resources Research Institute, the NM State Legislature (NMWRRI-SG-
2020). The content, opinions, findings, conclusions, and recommendations are those of the
authors and do not necessarily represent the official views of any of these institutions.

Authorship Contribution Statement

Jasmine Quiambao: Investigation, Formal analysis, Writing - Original Draft; Kenara Hess:
Investigation, Formal analysis, Writing - Review & Editing; Sloane Johnston: Investigation
Eliane El Hayek: Investigation; Achraf Noureddine: Investigation, Resources; Mehdi Ali:
Resources; Michael Spilde: Resources; Adrian Brearley: Resources; José M. Cerrato:
Conceptualization, Methodology, Writing - Review & Editing, Supervision, Resources, Funding
acquisition; Kerry J. Howe: Conceptualization, Methodology, Writing - Review & Editing,
Supervision, Resources, Funding acquisition; Jorge Gonzalez-Estrella: Conceptualization,
Methodology, Writing - Review & Editing, Supervision, Resources, Project administration,
Funding acquisition.
Mary Ann Liebert, Inc., 140 Huguenot Street, New Rochelle, NY 10801

ATEIA, M., ERSAN, G., GAR ALALM, M., BOFFITO, D. C. & KARANFIL, T. 2022. Emerging investigator series: Microplastics Sources, Fate, Toxicity, Detection, and Interactions with Micropollutants in Aquatic Ecosystems – A Review of Reviews. *Environ. Sci-Proc. Imp.*

- BLAKE, J. M., AVASARALA, S., ARTYUSHKOVA, K., ALI, A.-M. S., BREARLEY, A. J., SHUEY, C., ROBINSON, W. P., NEZ, C., BILL, S., LEWIS, J., HIRANI, C., PACHECO, J. S. L. & CERRATO, J. M. 2015. Elevated Concentrations of U and Cooccurring Metals in Abandoned Mine Wastes in a Northeastern Arizona Native American Community. *Environ. Sci. Technol.*, 49, 8506-8514.
- BLAKE, J. M., DE VORE, C. L., AVASARALA, S., ALI, A.-M., ROLDAN, C., BOWERS, F., SPILDE, M. N., ARTYUSHKOVA, K., KIRK, M. F., PETERSON, E., RODRIGUEZ-FREIRE, L. & CERRATO, J. M. 2017. Uranium mobility and accumulation along the Rio Paguate, Jackpile Mine in Laguna Pueblo, NM. *Environ. Sci-Proc. Imp.*, 19, 605-621.
- BLETTLER, M. C. M., ABRIAL, E., KHAN, F. R., SIVRI, N. & ESPINOLA, L. A. 2018. Freshwater plastic pollution: Recognizing research biases and identifying knowledge gaps. *Water Res.*, 143, 416-424.
- BRENNECKE, D., DUARTE, B., PAIVA, F., CAÇADOR, I. & CANNING-CLODE, J. 2016. Microplastics as vector for heavy metal contamination from the marine environment. *Estuar. Coast Shelf S.*, 178, 189-195.
- CARBERY, M., O'CONNOR, W. & PALANISAMI, T. 2018. Trophic transfer of microplastics and mixed contaminants in the marine food web and implications for human health. *Environ. Intl.*, 115, 400-409.
- DONAHUE, R. & HENDRY, M. J. 2003. Geochemistry of arsenic in uranium mine mill tailings, Saskatchewan, Canada. *Appl. Geochem.*, 18, 1733-1750.
- EERKES-MEDRANO, D., THOMPSON, R. C. & ALDRIDGE, D. C. 2015. Microplastics in freshwater systems: a review of the emerging threats, identification of knowledge gaps and prioritisation of research needs. *Water Res.*, 75, 63-82.
- GONZALEZ-ESTRELLA, J., MEZA, I., BURNS, A. J., ALI, A.-M. S., LEZAMA-PACHECO, J. S., LICHTNER, P., SHAIKH, N., FENDORF, S. & CERRATO, J. M. 2020. Effect of Bicarbonate, Calcium, and pH on the Reactivity of As(V) and U(VI) Mixtures. *Environmental Science & Technology*, 54, 3979-3987.
- KOELMANS, A. A., MOHAMED NOR, N. H., HERMSEN, E., KOOI, M., MINTENIG, S. M. & DE FRANCE, J. 2019. Microplastics in freshwaters and drinking water: Critical review and assessment of data quality. *Water Res.*, 155, 410-422.
- LI, J., LIU, H. & PAUL CHEN, J. 2018. Microplastics in freshwater systems: A review on occurrence, environmental effects, and methods for microplastics detection. *Water Res.*, 137, 362-374.
- LI, L., GENG, S., WU, C., SONG, K., SUN, F., VISVANATHAN, C., XIE, F. & WANG, Q. 2019. Microplastics contamination in different trophic state lakes along the middle and lower reaches of Yangtze River Basin. *Environ. Pollut.*, 254, 112951.
- LIU, P., ZHAN, X., WU, X., LI, J., WANG, H. & GAO, S. 2020. Effect of weathering on environmental behavior of microplastics: Properties, sorption and potential risks. *Chemosphere*, 242, 125193.

- LUO, W., SU, L., CRAIG, N. J., DU, F., WU, C. & SHI, H. 2019. Comparison of microplastic pollution in different water bodies from urban creeks to coastal waters. *Environ. Pollut.*, 246, 174-182.
- MEZA, I., GONZALEZ-ESTRELLA, J., BURNS, P. C., RODRIGUEZ, V., VELASCO, C. A., SIGMON, G. E., SZYMANOWSKI, J. E. S., FORBES, T. Z., APPLEGATE, L. M., ALI, A.-M. S., LICHTNER, P. & CERRATO, J. M. 2023. Solubility and Thermodynamic Investigation of Meta-Autunite Group Uranyl Arsenate Solids with Monovalent Cations Na and K. *Environmental Science & Technology*, 57, 255-265.
- MUNIER, B. & BENDELL, L. I. 2018. Macro and micro plastics sorb and desorb metals and act as a point source of trace metals to coastal ecosystems. *PLOS One*, 13, e0191759-e0191759.
- NAFIAAH, N. 2020. Interaction of freshwater microplastics with biota and heavy metals: a review. *Environmental chemistry letters*, v. 18, pp. 1813-1824-2020 v.18 no.6.
- PRATA, J. C., ALVES, J. R., DA COSTA, J. P., DUARTE, A. C. & ROCHA-SANTOS, T. 2020. Major factors influencing the quantification of Nile Red stained microplastics and improved automatic quantification (MP-VAT 2.0). *Sci. Total Environ.*, 719, 137498.
- ROCHMAN, C. M., HENTSCHEL, B. T. & TEH, S. J. 2014. Long-Term Sorption of Metals Is Similar among Plastic Types: Implications for Plastic Debris in Aquatic Environments. *PLOS One*, 9, e85433.
- RUIZ, O., THOMSON, B. M. & CERRATO, J. M. 2016. Investigation of in situ leach (ISL) mining of uranium in New Mexico and post-mining reclamation. *New Mexico Geology*, 38.
- SU, L., CAI, H., KOLANDHASAMY, P., WU, C., ROCHMAN, C. M. & SHI, H. 2018. Using the Asian clam as an indicator of microplastic pollution in freshwater ecosystems. *Environ. Pollut.*, 234, 347-355.
- SU, L., XUE, Y., LI, L., YANG, D., KOLANDHASAMY, P., LI, D. & SHI, H. 2016. Microplastics in Taihu Lake, China. *Environ. Pollut.*, 216, 711-719.
- TOURINHO, P. S., KOČÍ, V., LOUREIRO, S. & VAN GESTEL, C. A. M. 2019. Partitioning of chemical contaminants to microplastics: Sorption mechanisms, environmental distribution and effects on toxicity and bioaccumulation. *Environmental Pollution*, 252, 1246-1256.
- WONG, J. K. H., LEE, K. K., TANG, K. H. D. & YAP, P. S. 2020. Microplastics in the freshwater and terrestrial environments: Prevalence, fates, impacts and sustainable solutions. *Sci. Total Environ.*, 719, 137512.
- YANG, L., LUO, W., ZHAO, P., ZHANG, Y., KANG, S., GIESY, J. P. & ZHANG, F. 2021. Microplastics in the Koshi River, a remote alpine river crossing the Himalayas from China to Nepal. *Environmental Pollution*, 290, 118121.
- YONKOS, L. T., FRIEDEL, E. A., PEREZ-REYES, A. C., GHOSAL, S. & ARTHUR, C. D. 2014. Microplastics in Four Estuarine Rivers in the Chesapeake Bay, U.S.A. *Environ. Sci. Technol.*, 48, 14195-14202.

Table 1 Number of particles detected and analyzed by FTIR-ATR including the polymer type and their percentage matches in Laguna Pueblo, Tingley Beach, and the Rio Grande, New Mexico.

Site	Particles Quantified	Particles Analyze d	Particle Tag	Polymer Type	Match (%)
			L1-1	Polyamide - Nylon 6/12	50
Laguna Pueblo			L1-2	1-2 Urethane Alkyd, Linseed Oil-Rich	
Fishing Pond	25	5	L1-3	Precipitated Silica	42
(L1)			L1-4	Acrylonitrile Butadiene Styrene Terpolymer #6	39
			L1-5	Aromatic Hydrocarbon Resin	37
			L2-1	Cellophane	67
			L2-2	Ponomer Resin #2	50
Laguna Pueblo, Rio	34	75	L2-3	Poly(Styrene:Vinylidene Chloride)	37
Paguate (L2)			L2-4	Precipitated Silica	37
			L2-5	Di-(Methylthio) Toluene Diamine	29
		15	L3-1	Cellophane	44
			L3-2	Poly(Styrene:Vinylidene Chloride)	44
			L3-3	Cellophane	43
			L3-4	Cellophane	41
	149		L3-5	Cellophane	40
			L3-6	Cellophane	37
Laguna			L3-7	Cellophane	37
Pueblo,			L3-8	Cellophane	37
Wetland (L3)			L3-9	Cellophane	34
(L3)			L3-10	Polystyrene #4	33
			L3-11	Rayon	32
			L3-12	Poly(Styrene:4-Vinylpyridine)	32
			L3-13	Cellophane	30
			L3-14	2-(2-Hydroxy-3,5-(1,1 Dimethylbenzylphenyl)Benzotri azole)	28
			L3-15	Zinc Borate Hydrate	25
			L4-1	Rayon	50
Laguna Pueblo, Wetland	82	8	L4-2	Titanium Oxide (98%), Aluminum Oxide (2%)	44
Creek (L4)			L4-3	Titanium Oxide (98%), Aluminum Oxide (2%)	44

			L4-4	Poly(Styrene:Vinyldiene Chloride)	42
			L4-5	Styrene Derived Plasticizer	42
			L4-6	Titanium Oxide (98%), Aluminum Oxide (2%)	39
			L4-7	Poly(Styrene:Vinylidene Chloride)	38
			L4-8	Propylene Glycol Dibenzoate #1	29
			L5-1	Rayon	72
Laguna Pueblo. Creek			L5-2	Poly(Styrene:Vinyldiene Chloride)	48
near to Jackpile Mine	7	5	L5-3	Acrylonitrile Butadiene Styrene Terpolymer #6	46
(L5)			L5-4	Cellophane	36
			L5-5	Cellophane	33
			L6-1	Cellophane	50
			L6-2	Cellophane	50
			L6-3	Cellophane	50
			L6-4	Cellophane	48
Laguna			L6-5	Cellophane	48
Pueblo. Creek	110	10	L6-6	Cellophane	47
near to Jackpile Mine	119	12	L6-7	Zinc Borate Hydrate	35
(L6)			L6-8	Barium Metaborate	33
			L6-9	Polyol Acetal	28
			L6-10	Barium Metaborate	27
			L6-11	Fluorocarbon	23
			L6-12	5-Phenyltetrazole, Calcium Salt	21
			T1-1	Rayon	67
Tingley			T1-2	Cellophane	64
Beach,	18	5	T1-3	Cellophane	63
Albuquerque (T1)	10		T2-4	Cellophane	51
(11)			T2-5	Basic Lead Carbonate	35
			T2-1	Polyester	73
Tingley			T2-2	Polyester	73
Tingley Beach, Albuquerque	40	~	T2-3	Rayon	63
	43	5	T2-4	Cellophane	53
(T2)			T2-5	2-Amino-2-Methyl-1-Propanol #1	47
Tinalar			T3-1	Polytetrafluoroethylene #4	65
Tingley Beach,			T3-2	Cellophane	60
Albuquerque	127	13	T3-3	Cellophane	58
(T3)			T3-4	Rayon	56
				114 5 011	20

		T3-5	Cellophane	56
		T3-6	Cellophane	55
		T3-7	Cellophane	54
		T3-8	Cellophane	49
		T3-9	Cellophane	41
		T3-10	Cellophane	35
		T3-11	Cellophane	35
		T3-12	Cellophane	29
		T3-13	Coal Tar Oil	25
·····		R4-1	Poly(Styrene), Atactic	50
		R4-2	Poly(Styrene:Vinyldiene Chloride)	41
		R4-3	Rayon	38
Rio		R4-4	Cellophane	38
Grande	10	R4-5	Endothermic Foaming Agent #2	33
Albuquerqu 101	10	R4-6	5-Phenyltetrazole, Calcium Salt	31
e (R4)		R4-7	Poly(Styrene), Atactic	28
		R4-8	N,N-Diphenyl-P- Phenylenediamine	28
		R4-9	Zinc Borate #1	27
		R4-10	 Basic Lead Carbonate 	20
		R5-1	Rayon	52
Rio Grande,		R5-2	Cellophane	44
Albuquerqu 12	5	R5-3	Poly(Styrene), Atactic	42
e (R5)		R5-4	Rayon	38
		R5-5	Cellophane	33
		R6-1	Polyamide 6 + Polyamide 6,6	73
		R6-2	Cellophane	72
		R6-3	Polytetrafluoroethylene #4	58
Rio		R6-4	Cellophane	53
Grande		R6-5	Zinc Molybdate on Talc	46
Albuquerq 96	10	R6-6	Rayon	41
ue (R6)		R6-7	Polystyrene #1	38
. ,		R6-8	Poly(Styrene:Vinyldiene Chloride)	37
		R6-9	Poly(Styrene:4-Vinylpyridine)	36
		R6-10	Benzyl Alcohol	32
		Lab Ctrl	Titanium Oxide (98%),	55
Laborator 18	5	- 1	Aluminum Oxide (2%)	33
y Control	5	Lab Ctrl	Titanium Oxide (98%),	50
•		- 2	Aluminum Oxide (2%)	20

		Lab Ctrl	Titanium Oxide (98%),	47
		- 3 Lab Ctrl	Aluminum Oxide (2%) Titanium Oxide (98%),	4.6
		- 4	Aluminum Oxide (2%)	46
		Lab Ctrl - 5	Titanium Oxide (98%), Aluminum Oxide (2%)	41.35
		Ctrl - 1	Cellophane	50
		Ctrl - 2	Poly(Styrene:4-Vinylpyridine)	34
		Ctrl - 3	Poly(Styrene:Vinylidene Chloride)	32
Field	15 5		2,2-Ethylidene-Bis(4,6-Di-t-	
Control		Ctrl - 4	Butyl-Phenyl) Fluorophosphonite	25
			Bis [2-Hydroxy-5-T-Octyl-3-	
		Ctrl - 5	(Benzotriazol-2-Phenyl]	25
			Methane	
	Mary Ann Liebert, Inc	., 140 Huguenot S	Street, New Rochelle, NY 10801	

Figure Captions

- **Fig 1.** Representative images of plastic-like particles found in (A) Laguna Pueblo, New Mexico (Site L5), (B) Tingley Beach, Albuquerque, New Mexico (Site T1 & T2), and (C) the Rio Grande, Albuquerque, New Mexico (Site R1 & R3).
- Fig. 2. Confirmed MPs (A) and their respective IR spectra (B). Dotted lines indicate polymer reference spectra. Images of microplastic particles L5-1, T1-1, T2-3, R6-2, L2-1, T1-2, T1-3, T3-2, T2-1, T2-2, T3-1, and R6-1 are available in the SI file.
- Fig. 3. Soluble U concentration in batch experiments containing (A) PMMA, (B) PE, and (C) PS and soluble As concentration in batch experiments containing (D) PMMA, (E) PE, and (F) control without MPs at pH 3 and pH 7 at 0 and 48 h exposure. Assays were supplied with 0.05 mM U. Error bars indicate standard deviation obtained from duplicates. Asterisks represent the significant difference of soluble U concentration.
- Fig. 4. Spectroscopy analyses of PMMA MPs exposed to 0.06 mM of U for 48 h. Experiments were performed at pH 7 (A) TEM images of precipitates onto the commercial PMMA MP surface (B) SEM/EDS analyses confirming U accumulated on the MP surface.
- sed to very pitates onto cumulated on to the second Fig. 5. Soluble U concentration in batch experiments containing (A) PMMA and (B) control (no MPs) at pH 7 at 0 and 48 h exposure. Error bars indicate standard deviation obtained from triplicates.

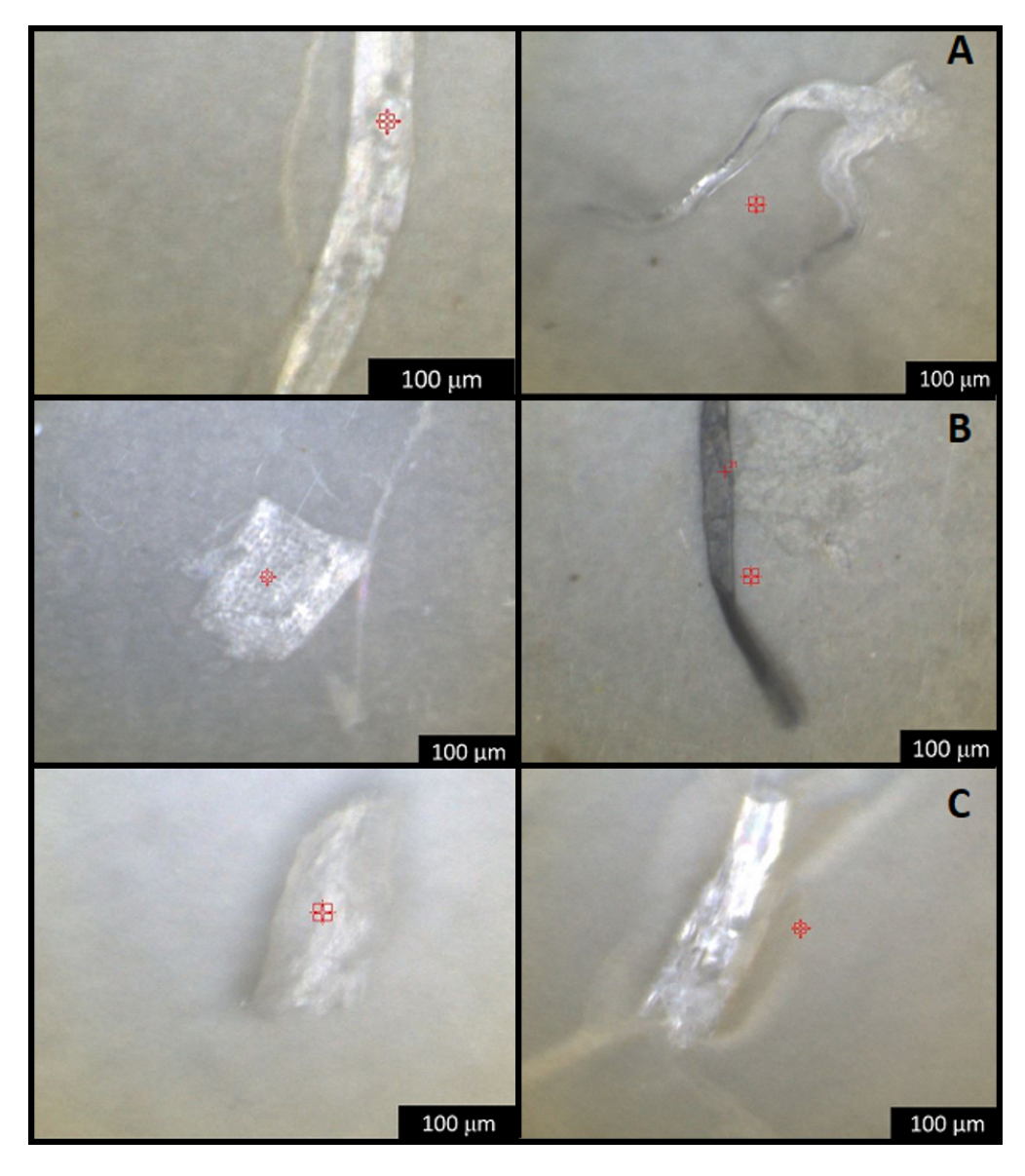


Fig. 1. Representative images of plastic-like particles found in (A) Laguna Pueblo, New Mexico (Site L5), (B)Tingley Beach, Albuquerque, New Mexico (Site T1 & T2), and (C) the Rio Grande, Albuquerque, New Mexico (Site R1 & R3).

162x186mm (150 x 150 DPI)

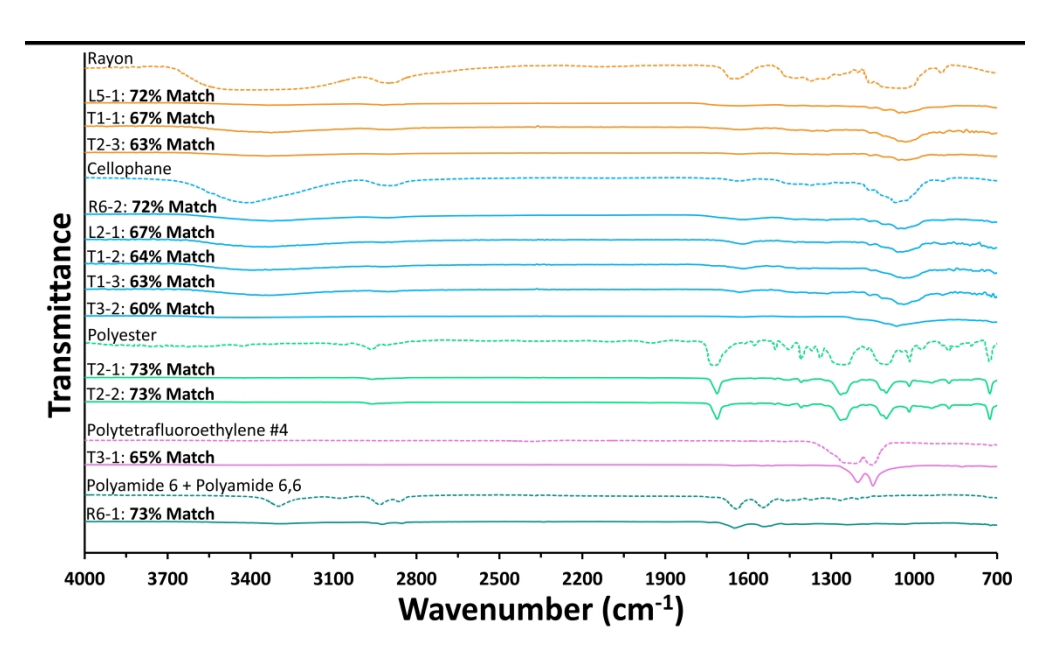


Fig. 2. Confirmed MPs (A) and their respective IR spectra (B). Dotted lines indicate polymer reference spectra. Images of microplastic particles L5-1, T1-1, T2-3, R6-2, L2-1, T1-2, T1-3, T3-2, T2-1, T2-2, T3-1, and R6-1 are available in the SI file.

1370x805mm (150 x 150 DPI)

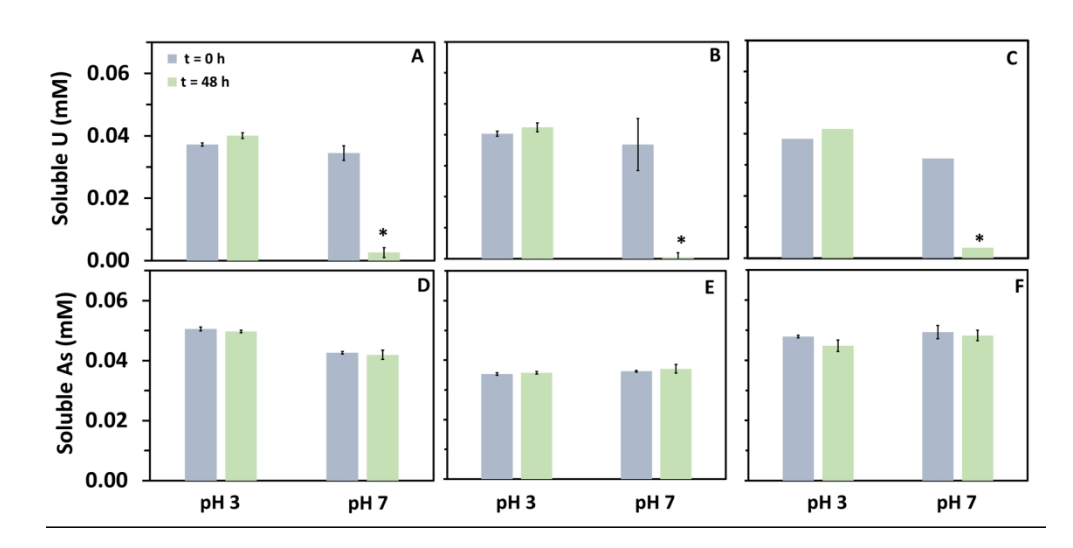


Fig. 3. Soluble U concentration in batch experiments containing (A) PMMA, (B) PE, and (C) PS and soluble As concentration in batch experiments containing (D) PMMA, (E) PE, and (F) control without MPs at pH 3 and pH 7 at 0 and 48 h exposure. Assays were supplied with 0.05 mM U. Error bars indicate standard deviation obtained from duplicates. Asterisks represent the significant difference of soluble U concentration

452x225mm (149 x 149 DPI)

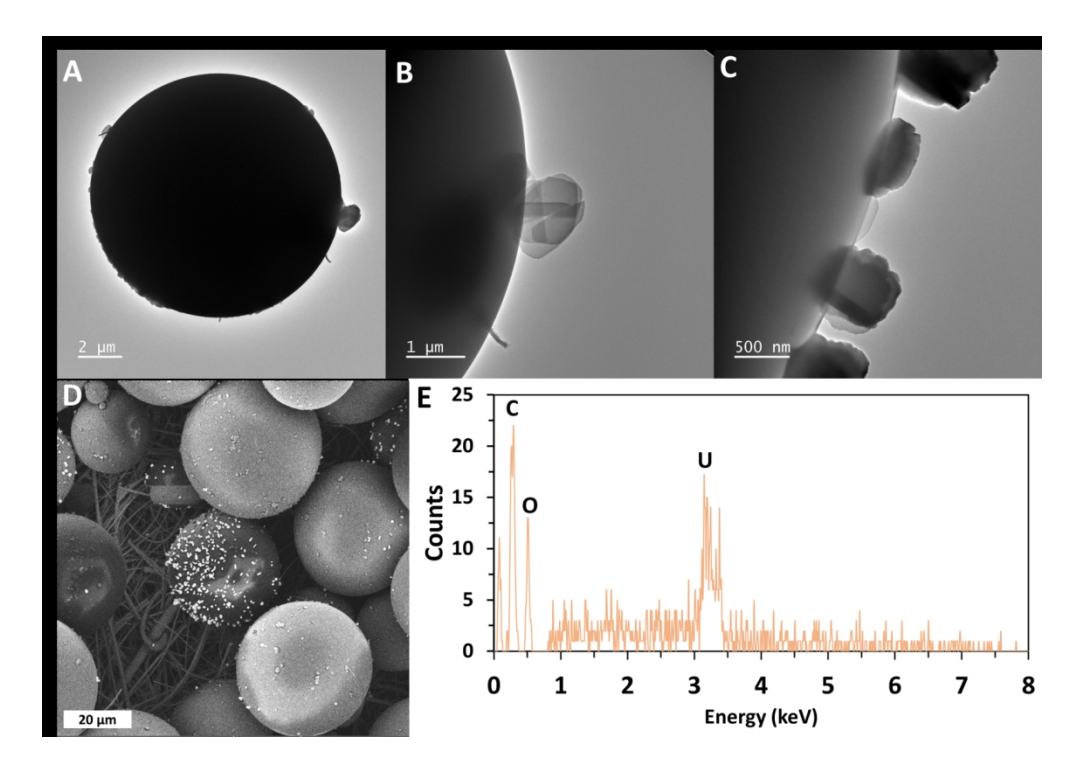


Fig. 4. Spectroscopy analyses of PMMA MPs exposed to 0.06 mM of U for 48 h. Experiments were performed at pH 7 (A) TEM images of precipitates onto the commercial PMMA MP surface (B) SEM/EDS analyses confirming U accumulated on the MP surface.

271x190mm (149 x 149 DPI)

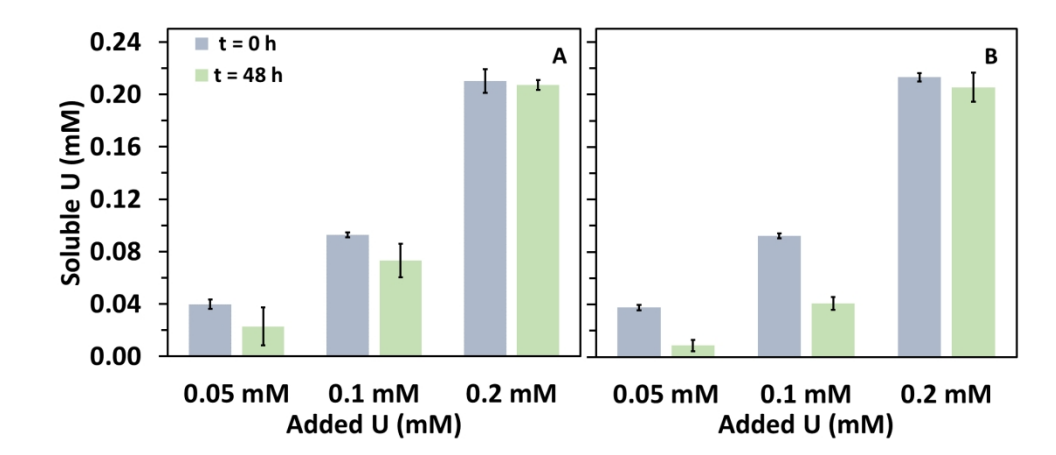


Fig. 5. Soluble U concentration in batch experiments containing (A) PMMA and (B) control (no MPs) at pH 7 at 0 and 48 h exposure. Error bars indicate standard deviation obtained from triplicates.

343x147mm (150 x 150 DPI)

Supplementary information: Interfacial interactions of Uranium and Arsenic with

Microplastics: from field detection to controlled laboratory tests.

Jasmine Quiambao¹, Kendra Hess², Sloane Johnston², Eliane El Hayek³; Achraf Noureddine⁴, Abdul-Mehdi S. Ali⁵, Michael Spilde⁵, Adrian Brearley⁵, José M. Cerrato¹, Kerry J. Howe¹, and Jorge Gonzalez-Estrella*2

*Corresponding email addresses: jorgego@okstate.edu

¹ Department of Civil, Construction & Environmental Engineering, MSC01 1070, University of New Mexico, Albuquerque, New Mexico 87131, USA

²School of Civil & Environmental Engineering, 248 Engineering North, Oklahoma State University, Stillwater, Oklahoma 74078

³ Department of Pharmaceutical Sciences, MSC09 5360, University of New Mexico, College of Pharmacy, Albuquerque, New Mexico 87131, USA

g, MSC01 11.
SC03 2040, University ⁴ Department of Chemical & Biological Engineering, MSC01 1120, 1 University of New Mexico Albuquerque, NM 87131, USA

⁵Department of Earth and Planetary Sciences, MSC03 2040, University of New Mexico, Albuquerque, New Mexico 87131, USA

Content:

Extraction of MPs

Analyses of MPs and Metals in Field Samples

Scanning electron microscopy and transmission electron microscopy methodologies

Table S1. Microplastic and Metal Sample Location and Site Description

Table S2 Physical and chemical characteristics of the commercial microplastics used in this study.

Table S3. Uranium and Arsenic concentration in water samples of Laguna Pueblo, NM.

Table S4. FTIR-ATR particle analyses of samples from Laguna Pueblo, NM.

Table S5. FTIR-ATR particle analyses of samples from Tingley Beach, Albuquerque, NM.

Table S6. FTIR-ATR particle analyses of samples from Rio Grande, Albuquerque, NM.

Fig. S1. Stereomicroscope images exemplifying fibers below the FTIR-ATR detection limit.

Figure S2. Zeta potential (mV) of the three commercial microplastics (PMMA, PE, and PS) at pH 3 and pH 7.

oatch exper.
.ics) at pH 7 at 6 Fig. S3. Soluble U concentration of filtered solutions in batch experiments containing (A) PMMA, (B) PE, (C) PS, and (D) control (no microplastics) at pH 7 at 0 and 48 h. Error bars indicate standard deviation obtained from triplicates.

Extraction of MPs

Water samples were vacuum filtered with a glass frit filter unit and 47 mm 0.45 μ m borosilicate glass microfiber filter (Whatman). The original sample bottle was rinsed three times with ultrapure water (18 M Ω) and vacuum filtered to maximize the MP extraction from the samples. Particles retained on the filter were washed with 100 mL of 30% (v/v) H₂O₂ into a serum bottle for digestion of organic matter. Digestion was carried out in an oscillation incubator at 50°C and 80 rpm for 48 h. After digestion, the H₂O₂ solution was vacuum filtered with a glass frit filter unit onto a 0.45 μ m borosilicate glass microfiber filter. Subsequently, filters were sonicated in 5.1 M ZnCl₂ with an ultrasonic processor to fully disperse all trapped particles and left overnight to separate by density. The supernatant was filtered through a 25 mm 0.2 μ m Al₂O₃ filter (Whatman Anodisc 25). The Al₂O₃ filter was rinsed with ultra-pure water (18 M Ω) to remove excess ZnCl₂ solution then stored in a petri dish for subsequent quantification and characterization of MPs.

Analyses of MPs and Metals in Field Samples.

The extracted particles were examined and imaged using a stereomicroscope (AmScope 7X-180X Trinocular Zoom Stereo Microscope) for initial visual assessment. To prepare for MPs imaging with fluorescence microscopy, each Al_2O_3 filter was placed in a clean glass petri dish where a few drops (less than $30\mu L$) of $10~\mu g$ Nile Red/L methanol solution was added to cover the filter flow-through area. The filters were left to react with the dye for 10~m min then were rinsed with $200\mu L$ of n-hexane on a glass filtration stack to remove excess dye before being placed in a Greiner 6-well plate. The filters were imaged using a fluorescence microscope (Cytation 5 Cell Imaging Multi Mode Reader, Agilent Technologies) with Gen5® software. The detection limit of Cytation 5 cell Imaging at this magnification is $\sim 0.5~\mu m$. Using the software, a series of images were taken at 4x magnification with an RFP filter cube (excitation 531~nm/emission 593~nm) to produce a stitched

image of each filter. Each image was preprocessed to reduce background fluorescence. When necessary, further reduction of background fluorescence was done by increasing image contrast and decreasing brightness. For quantification, each filter's overall image was run through the MPVAT 2.0 macros using ImageJ.(Prata et al., 2020) Each filter was run through MPVAT 2.0 three times and the average was reported. Only the filter flow-through area (13 mm diameter) was considered for quantification.

Each filter was then analyzed using a FTIR spectrometer (micro-FTIR, Thermo Nicolet iN10 MX) with a detection limit of 20 μm. For each filter, the number of particles examined with Attenuated Total Reflectance (ATR) was 10% of the particles identified during fluorescence microscopy quantification, or a minimum of five (whichever was greater). For examination of the filters with FTIR-ATR, each filter was mounted on a gold mirror slide. Using OMNIC Picta® software, a mosaic image of the filter flow-through area was taken. A reflectance map was acquired to guide in the selection of potential plastic particles for further examination with ATR. Using a cooled detector and Germanium tip, each measurement was taken using a 51s detection time with 256 scans, a spectral range of 4000-675 cm⁻¹, and a resolution of 8 cm⁻¹. Aperture size was adapted to fit each particle. The resulting spectra were searched against the HR Polymer Additives and Plasticizers, Hummel Polymer Sample Library, Polymer Laminate Films, and Synthetic Fibers by Microscope libraries. From the search, a percent match of the experimental spectra and reference spectra was acquired. This percent match was used to determine if a particle was a polymer. Following the procedure suggested by Yang et al. (2015), a match greater than 70% automatically indicates a polymer. A match between 60-70% requires manual comparison of experimental and reference spectra; similar absorption peaks are required to confirm a match. Any match less than 60% was automatically not considered a polymer.

Inductively Coupled Plasma-Mass Spectrometer (ICP-MS) Perkin Elmer Nex-ION 300D (Dynamic Cell Reaction) was used to quantify soluble U and As of the 20 sites samples. Prior to analysis samples were acidified with 5% HNO₃.

Scanning electron microscopy and transmission electron microscopy methodologies

Scanning Electron Microscopy (SEM) analyses were conducted on a Tescan Vega3 XMU variable pressure SEM (Tescan Orsay Holding a.s., Brno, Czech Republic). Samples were coated with silver at first. However, this created a spectral overlap with uranium M-alpha lines, thus gold coating was used on later samples. Accelerating voltage was set to 10 kV to reduce damage and potential charging on the polymer bead samples. Sample current used ranged from 10 to 30 pA with a spot size <100 nm. Transmission Electron Microscopy analyses (TEM) analyses were performed using a JEOL NEOARM 200CF aberration-corrected scanning TEM. Samples were prepared by brushing holey carbon TEM films on Cu grids gently across the filter papers. The spheres attached to the holey carbon film by electrostatic attraction. TEM was performed using a JEOL NEOARM 200CF aberration-corrected scanning transmission electron microscope operating at 200 kV in the Nanomaterials Characterization Facility at the University of New Mexico. A variety of electron microscopy techniques were used, including bright-field TEM (BF-TEM), bright-field scanning TEM (STEM), high-angle annular dark-field (HAADF) (STEM), SEM, selected area electron diffraction (SAED) and X-ray analysis in both spot and STEM mode. Bright-field TEM images and electron diffraction patterns were acquired using a GATAN OneView 4k x 4K digital camera and processed using GATAN Microscopy Suite® (GMS) imaging software. Background corrected full spectral X-ray maps and quantitative EDS data were obtained using twin JEOL 100mm2 SDD EDS detectors and processed using Oxford ng the AZtec X-ray analysis software. Quantification of EDS spectra was carried out using the Cliff-Lorimer thin film approximation using theoretical k-factors.

Table S1. Microplastic and Metal Sample Location and Site Description

	Microplastic		
Sample Location and Site Description	Sample Date	Site #	Coordinates
Laguna Pueblo, New Mexico. Fishing Pond	2/23/2020	Site L1	35°09'01.0"N 107°23'56.8"W
Laguna Pueblo, New Mexico. Rio Paguate	2/23/2020	Site L2	35°09'14.9"N 107°24'18.6"W
Laguna Pueblo, New Mexico. Wetland	2/23/2020	Site L3	35°04'00.2"N 107°19'34.7"W
Laguna Pueblo, New Mexico. Wetland Creek	2/23/2020	Site L4	35°03'56.1"N 107°19'36.8"W
Laguna Pueblo, New Mexico. Creek near to Jackpile Mine	2/23/2020	Site L5	35°07'24.0"N 107°20'10.3"W
Laguna Pueblo, New Mexico. Creek near to Jackpile Mine	2/23/2020	Site L6	35°07'22.1"N 107°20'10.4"W
Tingley Beach, Albuquerque, New Mexico. Recreational pond	7/9/2020	Site T1	35°05'08.7"N 106°40'25.2"W
Tingley Beach, Albuquerque, New Mexico. Recreational pond	7/9/2020	Site T2	35°05'03.5"N 106°'40"19.1W
Tingley Beach, Albuquerque, New Mexico. Recreational pond	7/9/2020	Site T3	35°04'59.9"N 106°40'17.6"W
Rio Grande, Albuquerque, New Mexico. River in urban center	7/9/2020	Site R4	35°05'16.5"N 106°40'41.7"W
Rio Grande, Albuquerque, New Mexico. River in urban center	7/9/2020	Site R5	35°05'26.3"N 106°41'04.2"W
Rio Grande, Albuquerque, New Mexico. River in urban center	7/9/2020	Site R6	35°05'22.4"N, 106°40'51.1"W
	Metals	X	
Sample Location and Site Description	Sample Date		Coordinates
Laguna Pueblo, New Mexico. Fishing Pond	2/23/2020		35°09'01.0"N 107°23'56.8"W
Laguna Pueblo, New Mexico. Rio Paguate	2/23/2020		35°09'14.9"N 107°24'18.6"W
Laguna Pueblo, New Mexico. Wetland	2/23/2020		35°04'00.2"N 107°19'34.7"W
Laguna Pueblo, New Mexico. Wetland Creek	2/23/2020		35°03'56.1"N 107°19'36.8"W
Laguna Pueblo, New Mexico. Creek near to Jackpile Mine	2/23/2020		35°07'24.0"N 107°20'10.3"W
Laguna Pueblo, New Mexico. Creek near to Jackpile Mine	2/23/2020		35°07'22.1"N 107°20'10.4"W
Tingley Beach, Albuquerque, New Mexico. Recreational pond	7/9/2020		35°05'08.7"N 106°40'25.2"W

Tingley Beach, Albuquerque, New	7/9/2020	35°05'03.5"N
Mexico. Recreational pond	77772020	106°'40"19.1W
Tingley Beach, Albuquerque, New	7/9/2020	35°04'59.9"N
Mexico. Recreational pond	1/9/2020	106°40'17.6"W
Rio Grande, Albuquerque, New	7/0/2020	35°05'16.5"N
Mexico. River in urban center	7/9/2020	106°40'41.7"W
Rio Grande, Albuquerque, New	- /0 /0 0 0 0	35°05'26.3"N
Mexico. River in urban center	7/9/2020	106°41'04.2"W
Rio Grande, Albuquerque, New		35°08'95.7"N
Mexico. River in urban center	7/9/2020	106°68'08.7"W
Rio Paguate Bridge in Jackpile Mine	9/21/2020	35°07'24.0"N
	9/21/2020	107°20'11.8"W
("ford") Die Degreete Duiden in Jeaknile Mine	9/26/2020	
Rio Paguate Bridge in Jackpile Mine	8/26/2020	35°07'24.0"N
("ford")	0.45.645.05.0	107°20'11.0"W
Rio Paguate Bridge in Jackpile Mine	8/26/2020	35°07'24.0"N
("ford")		107°20'11.0"W
Rio Paguate Bridge in Jackpile Mine	8/26/2020	35°07'23.9"N
(Stop 1) ("ford")		107°20'11.2"W
Rio Paguate Bridge in Jackpile Mine	8/26/2020	35°07'23.9"N
(Stop 1) ("ford")		107°20'11.2"W
Rio Paguate Bridge in Jackpile Mine	8/26/2020	35°07'23.9"N
(Stop 1) ("ford")		107°20'11.2"W
		35°08'04.2"N
Rio Moquino in Jackpile Mine	8/26/2020	107°20'50.6"W
		35°08'04.2"N
Rio Moquino in Jackpile Mine	8/26/2020	107°20'50.6"W

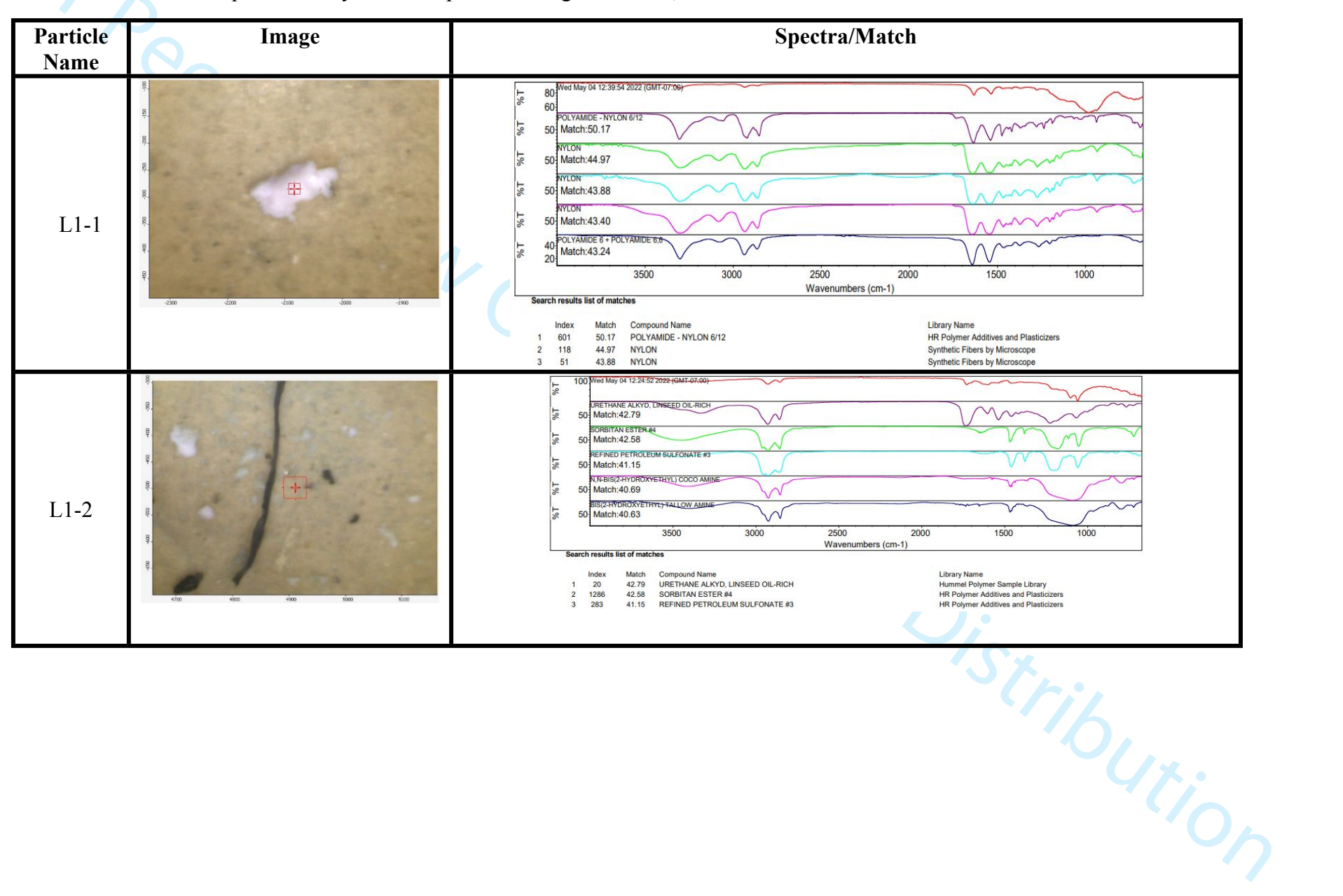
Table S2. Microplastic properties of commercial poly (methyl methacrylate) (PMMA), clear polyethylene (PE), and polystyrene (PS) including density, particle size, surface area, and ZETA potential at pH 3 and pH 7.

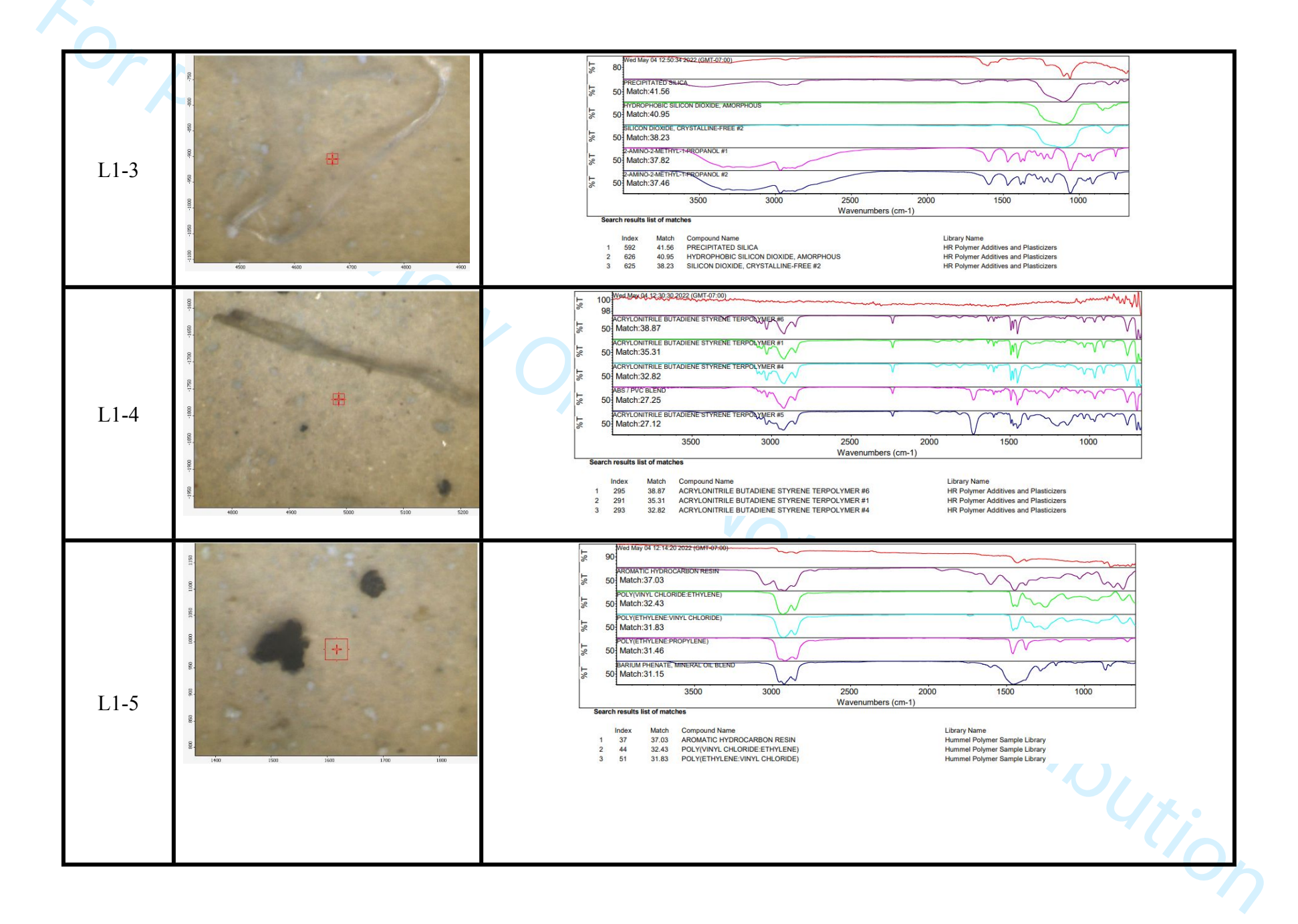
Commercial	Density	Particle	Surface Area	Zeta	Zeta
Microplastics	(g/c^3)	Size (µm)	(m^2/g)	Potential at	Potential at
				pH 3 (mV)	pH 7 (mV)
Poly (Methyl	1.2	1-45	0.86 ± 0.87	-4.88 ± 11.74	-42.83 ± 5.17
Methacrylate)					
Clear	0.96	10-63	0.21 ± 0.14	7.83 ± 16.95	-12.10 ± 8.92
Polyethylene					
Polystyrene	1.05	200-300	0.020 ± 0.0050	5.65 ± 6.64	-13.06 ± 4.94

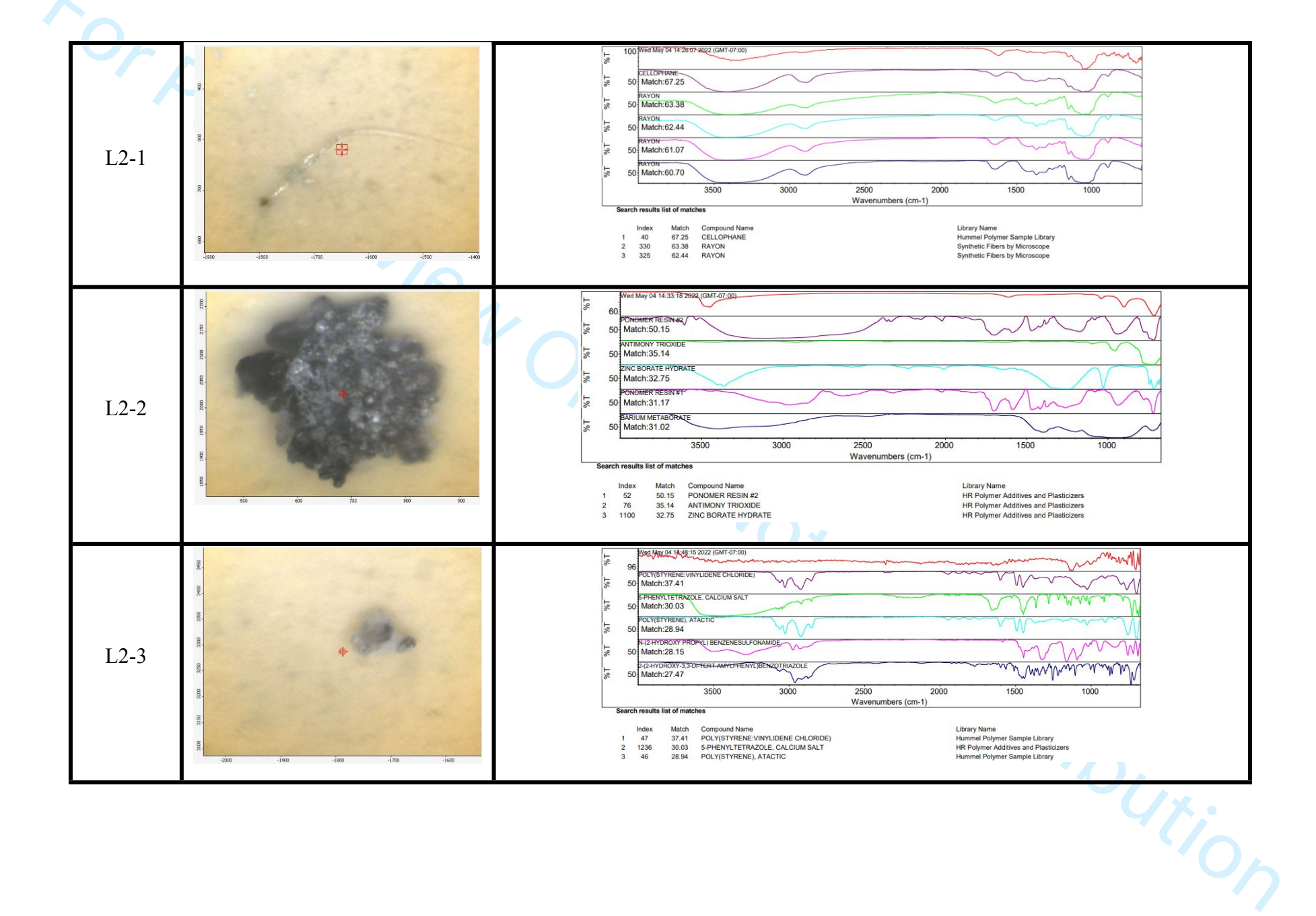
Table S3. Uranium and Arsenic concentration in water samples of Laguna Pueblo, NM.

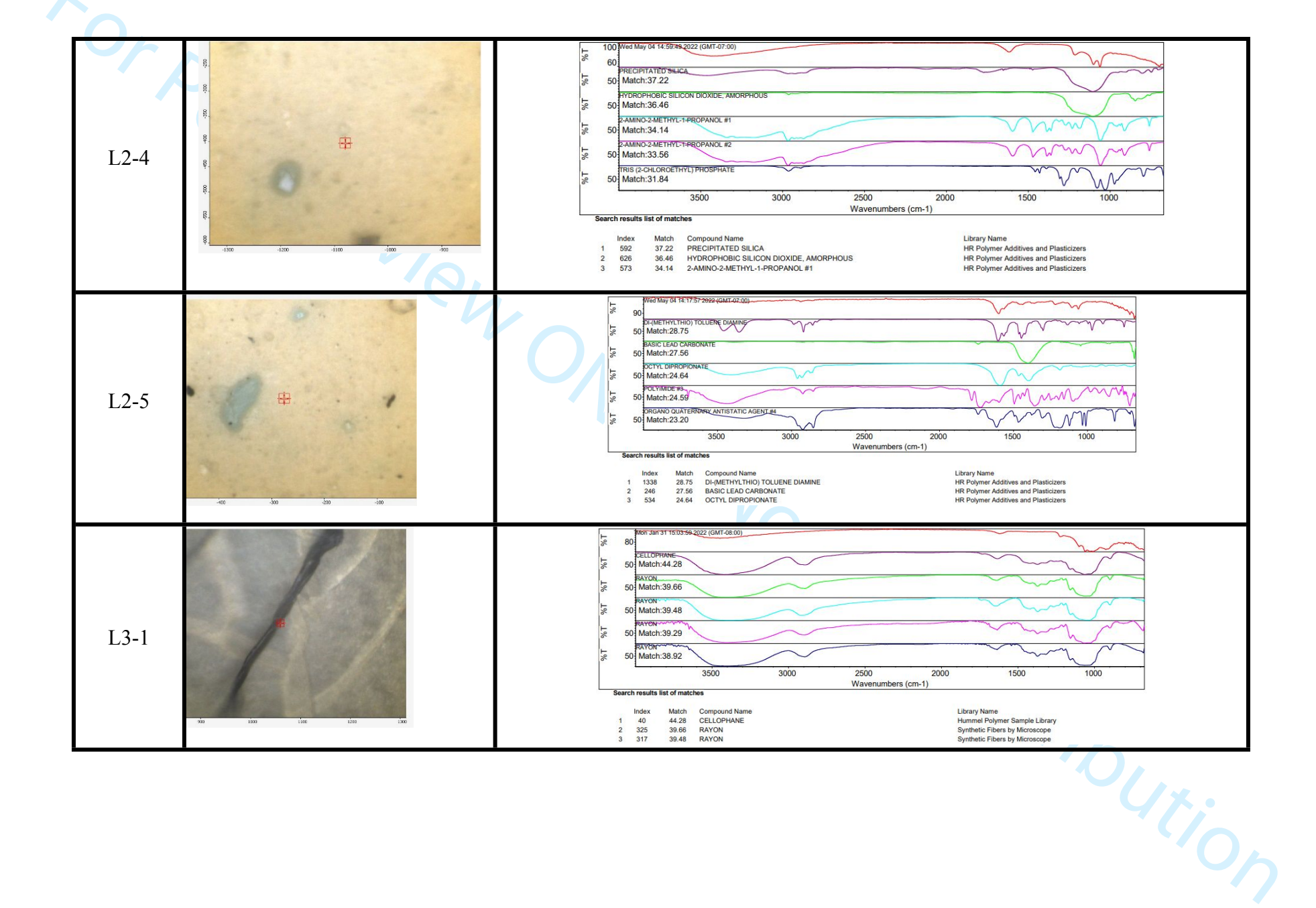
Location	As (va/L)	U
	(μg/L)	$\frac{(\mu g/L)}{0.12}$
Procedure Control	0.42	0.13
Field Control	0.43	0.13
Laguna Pueblo 1	2.27	0.65
Laguna Pueblo 2	1.45	0.45
Laguna Pueblo 3	0.81	1.85
Laguna Pueblo 4	0.66	36.53
Laguna Pueblo 5	1.43	28.27
Laguna Pueblo 6	1.3	29.65
Rio Grande 1	2.32	1.07
Rio Grande 2	3.01	1.43
Rio Grande 3	3.05	1.34
Tingley Beach 1	10.75	2.31
Tingley Beach 2	11.4	2.35
Tingley Beach 3	11.26	2.16
Rio Paguate Bridge in Jackpile Mine ("ford")	2.23	233.56
Rio Paguate Bridge in Jackpile Mine ("ford")	2.89	329.56
Rio Paguate Bridge in Jackpile Mine ("ford")	3.33	332.8
Rio Paguate Bridge in Jackpile Mine (Stop 1) ("ford")	1.4	274.06
Rio Paguate Bridge in Jackpile Mine (Stop 1) ("ford")	1.75	296.56
Rio Paguate Bridge in Jackpile Mine (Stop 1) ("ford")	1.75	280.1
Rio Moquino in Jackpile Mine	5.54	40.38
Rio Moquino in Jackpile Mine	1.46	31.41

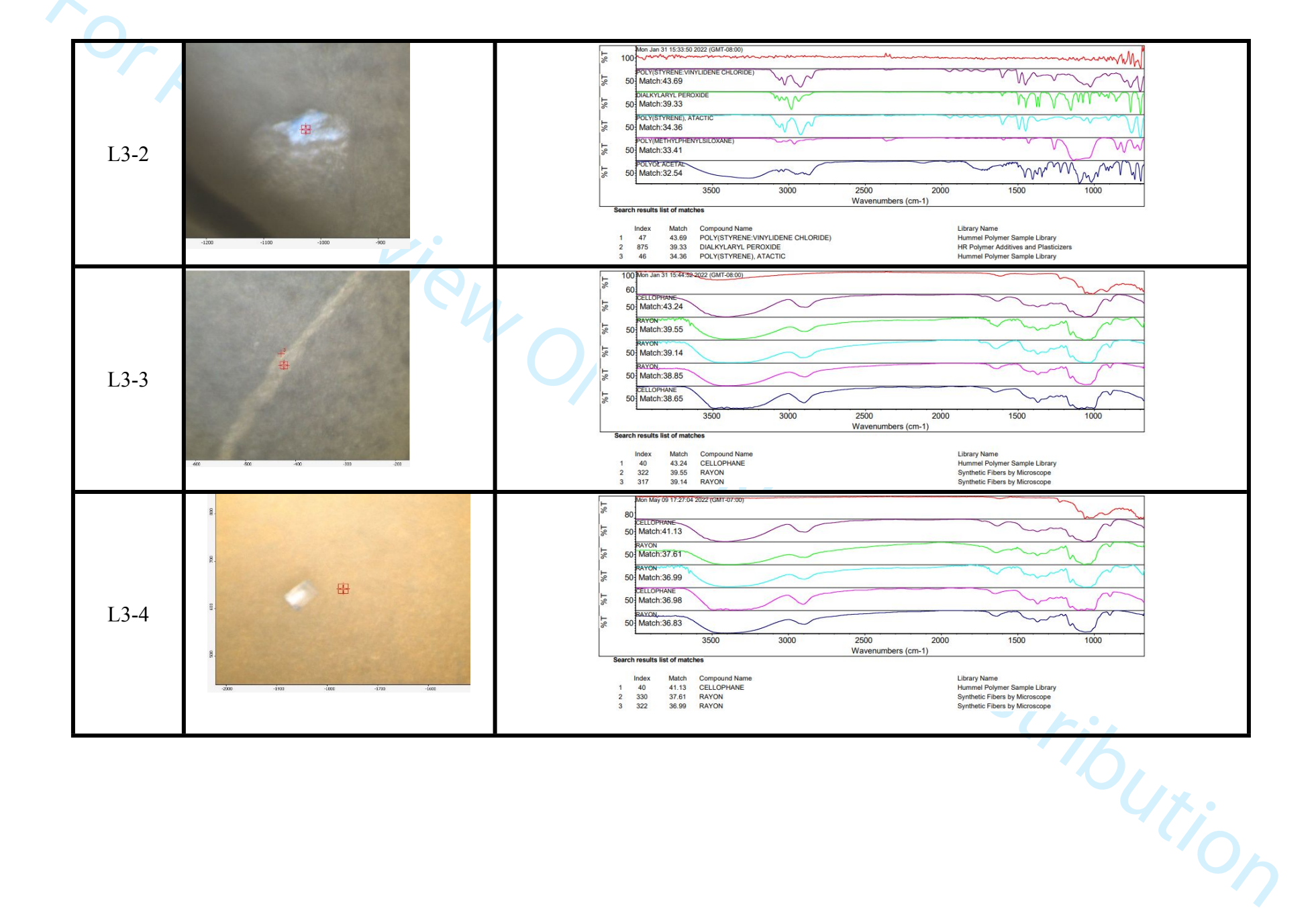
Table S4. FTIR-ATR particle analyses of samples from Laguna Pueblo, NM.

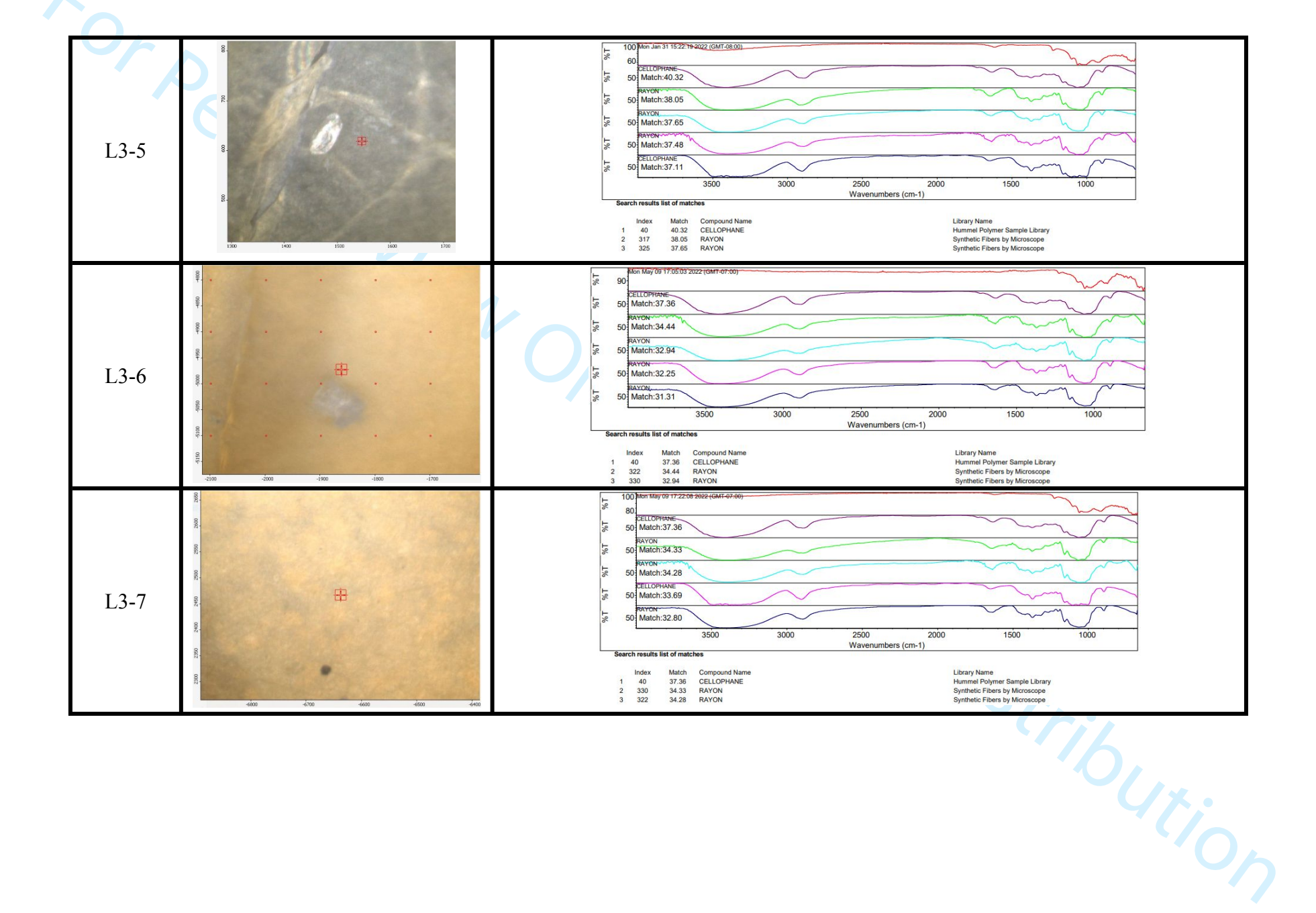


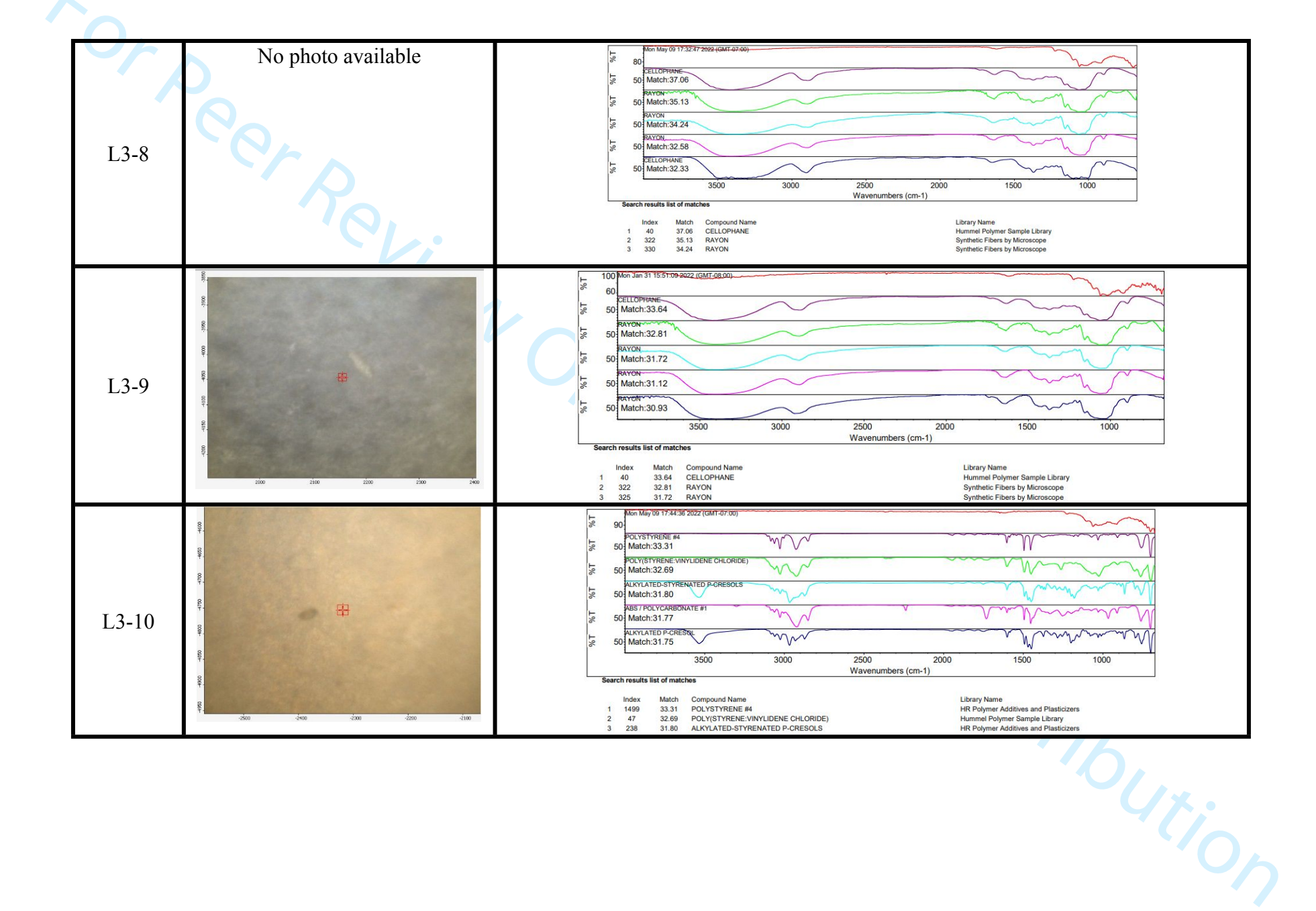


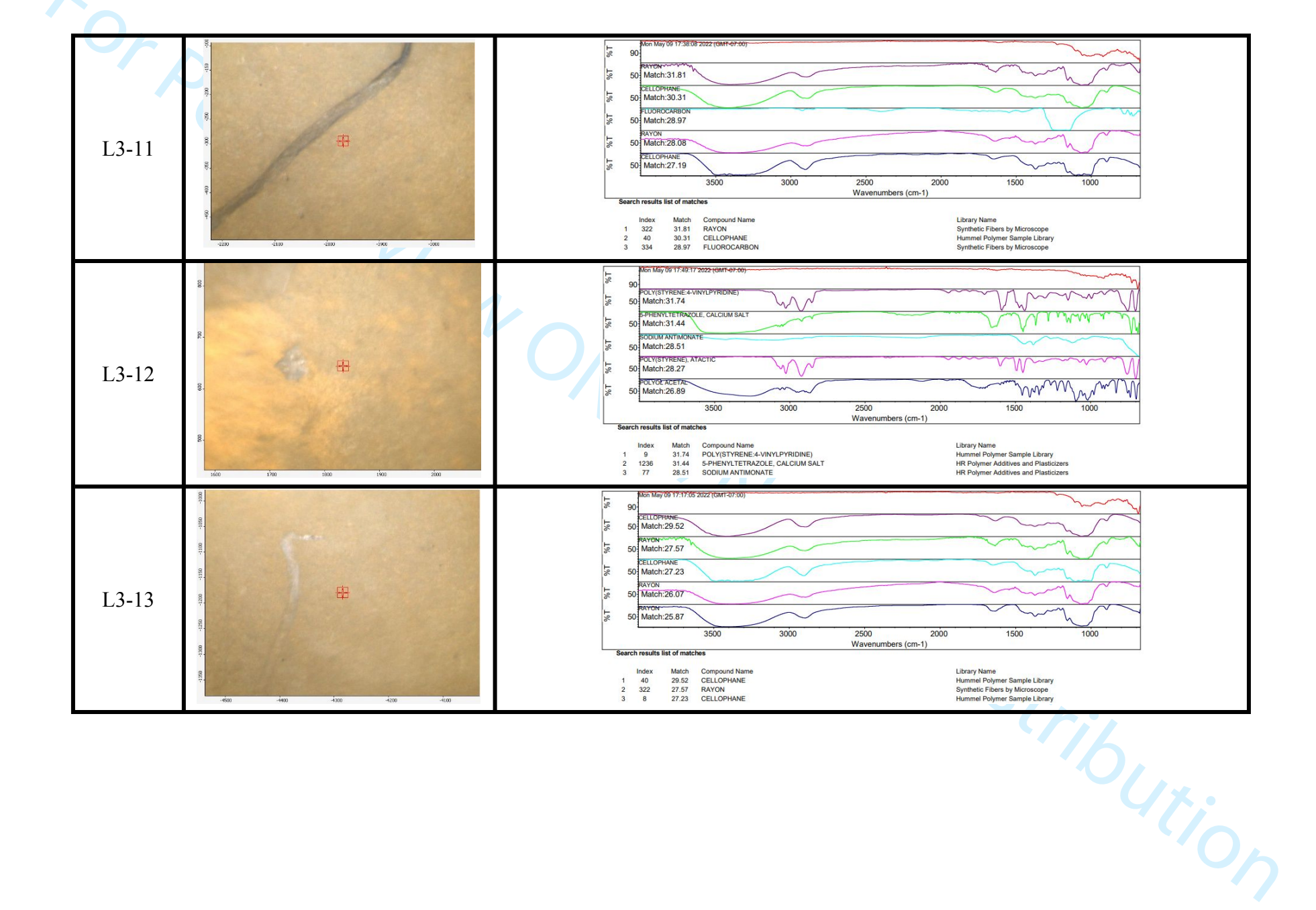


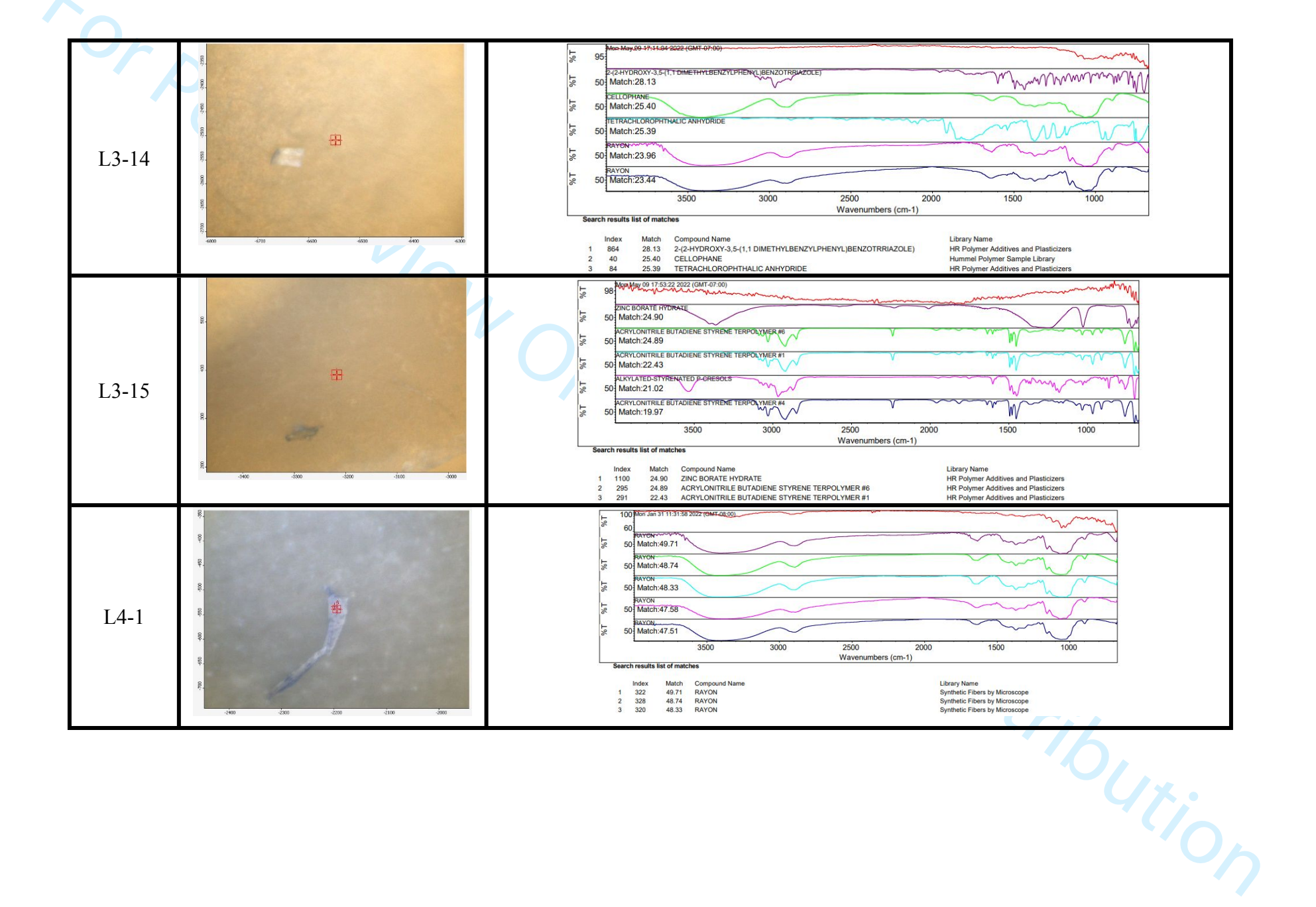


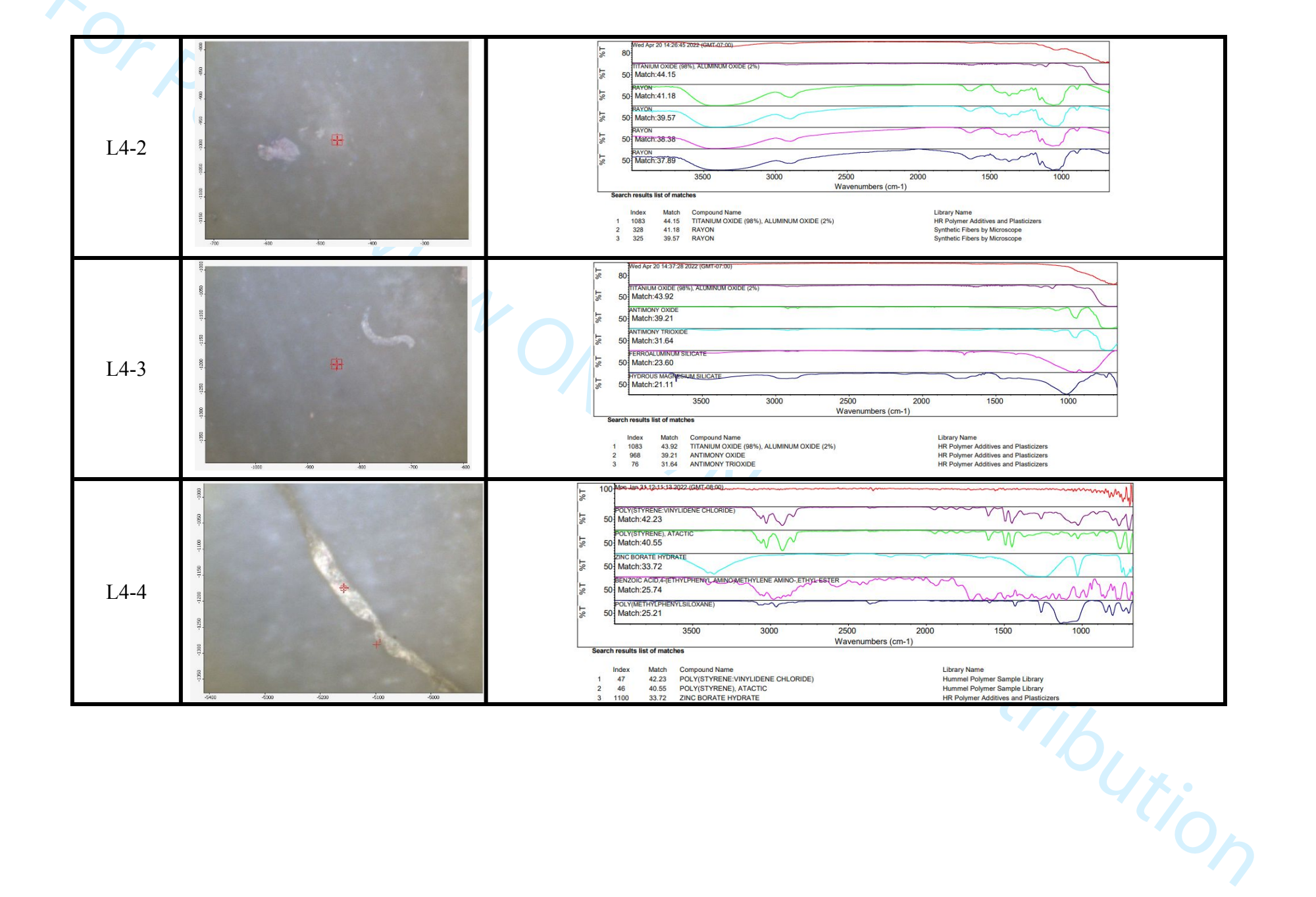


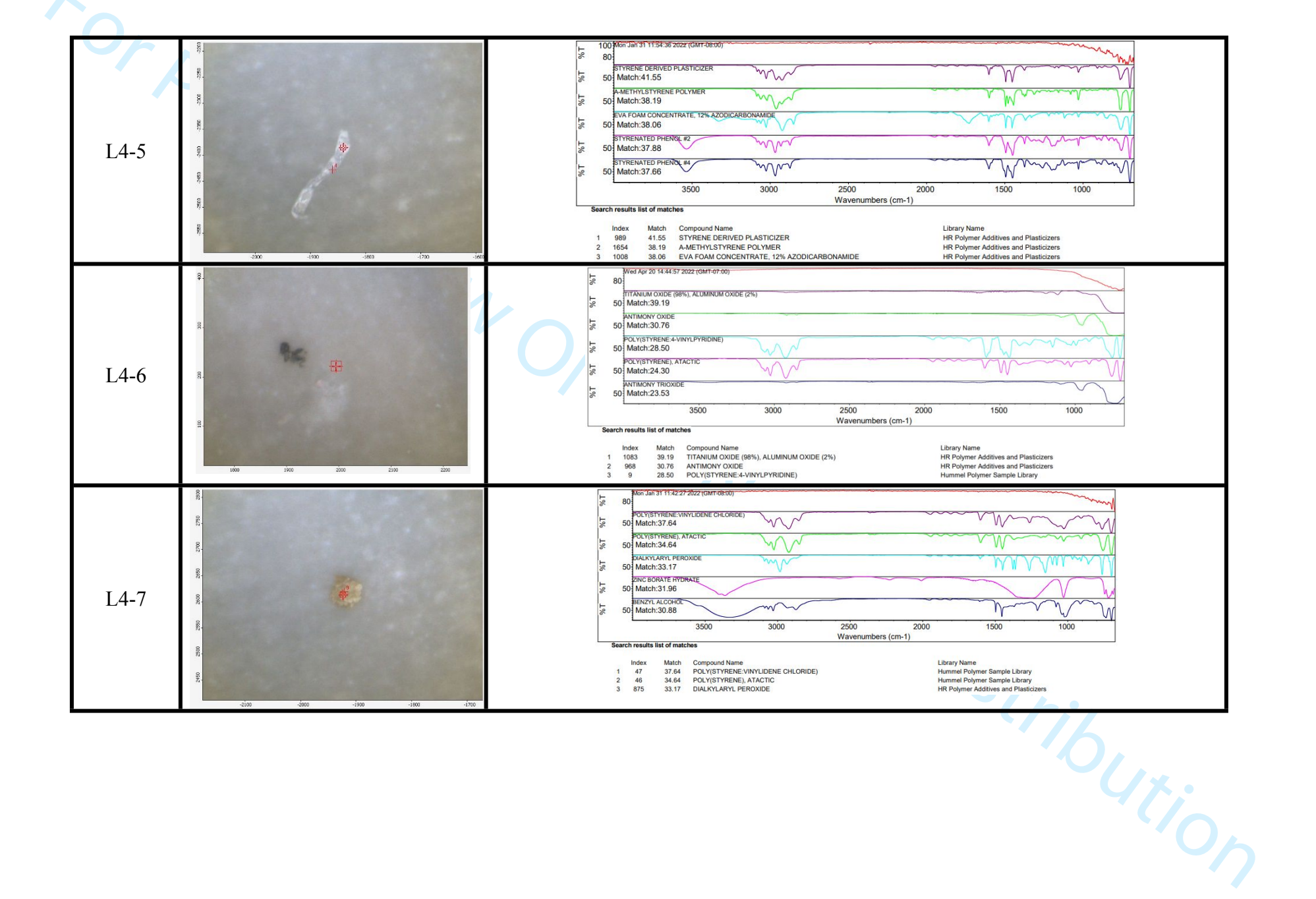


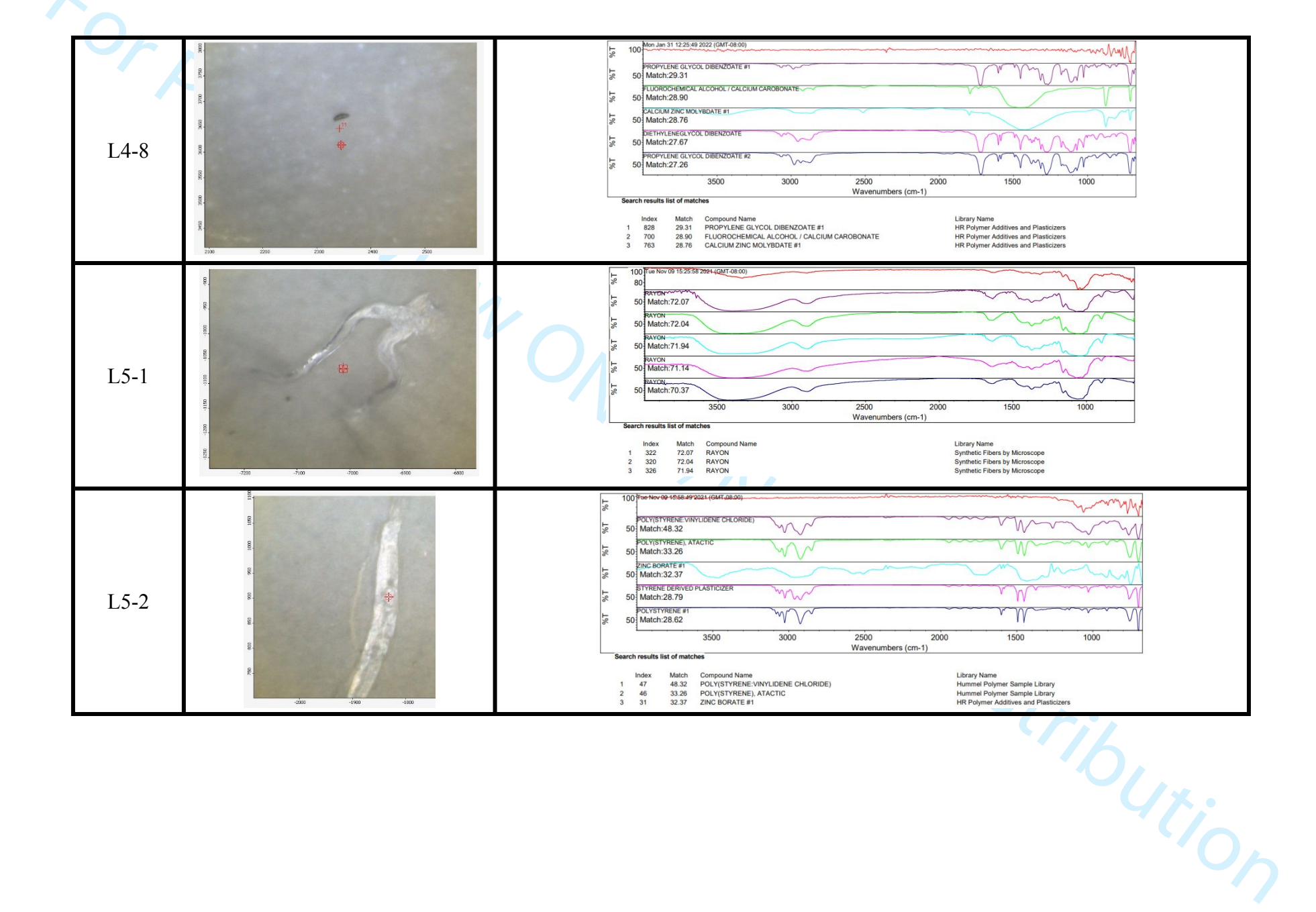


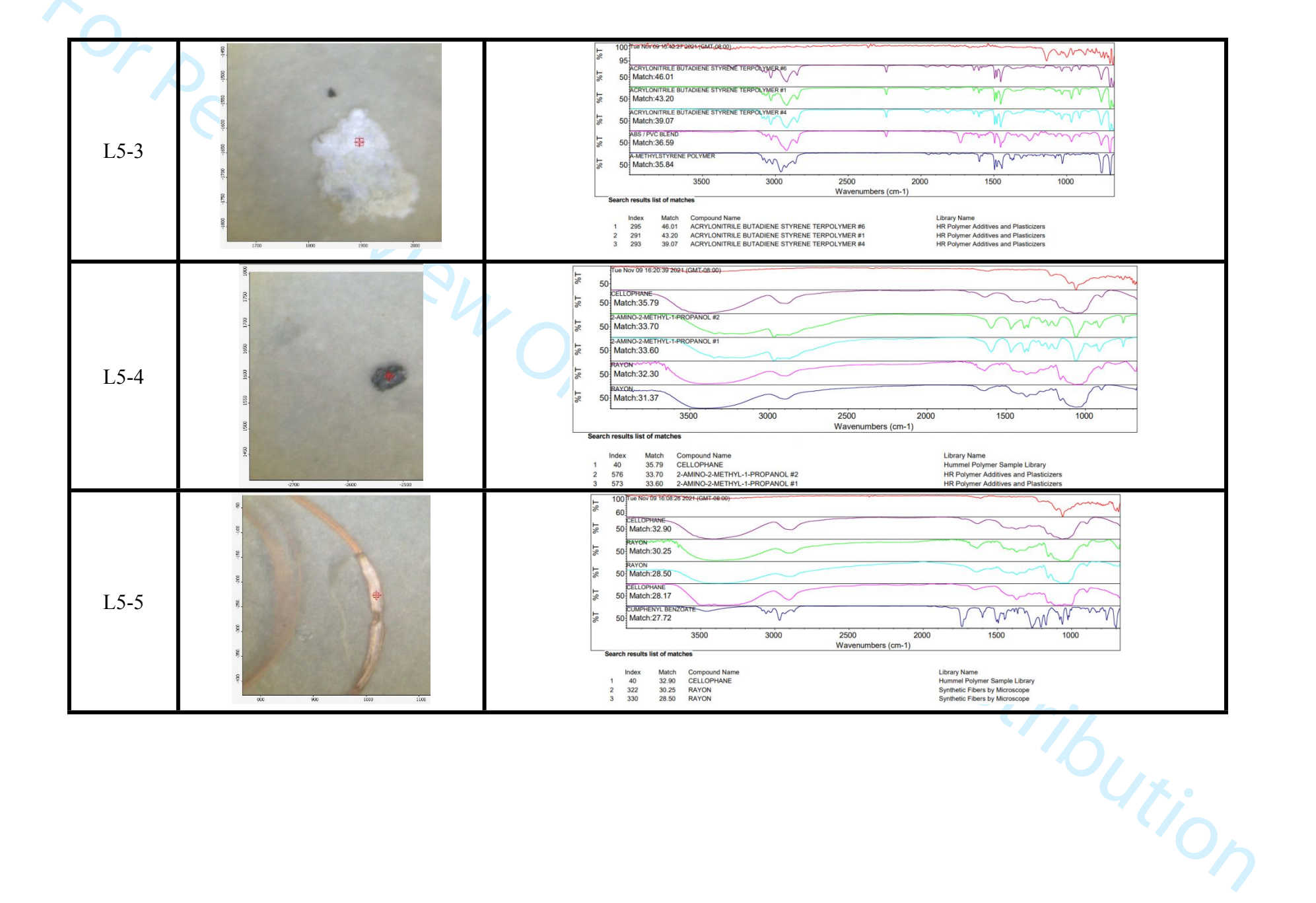


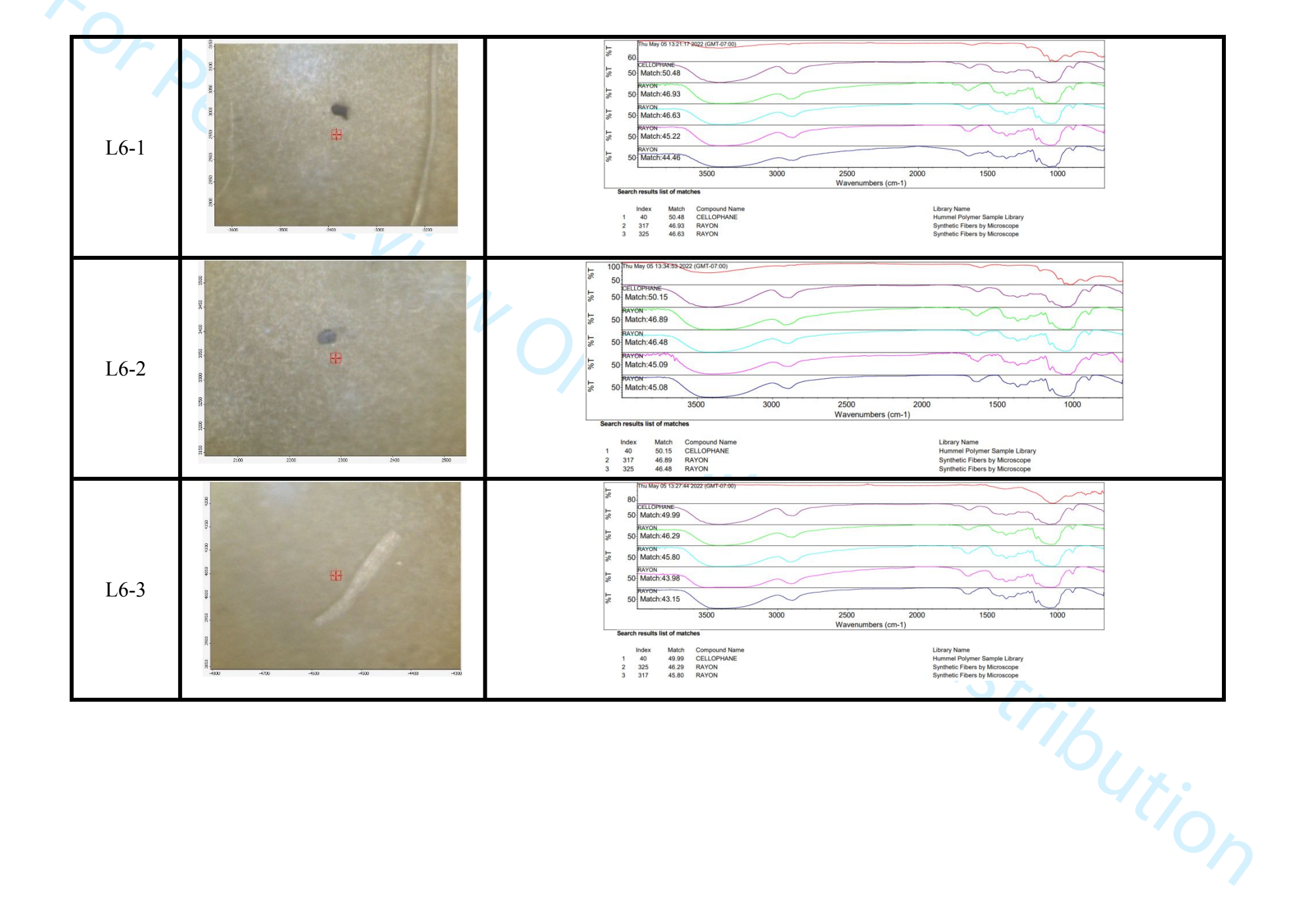


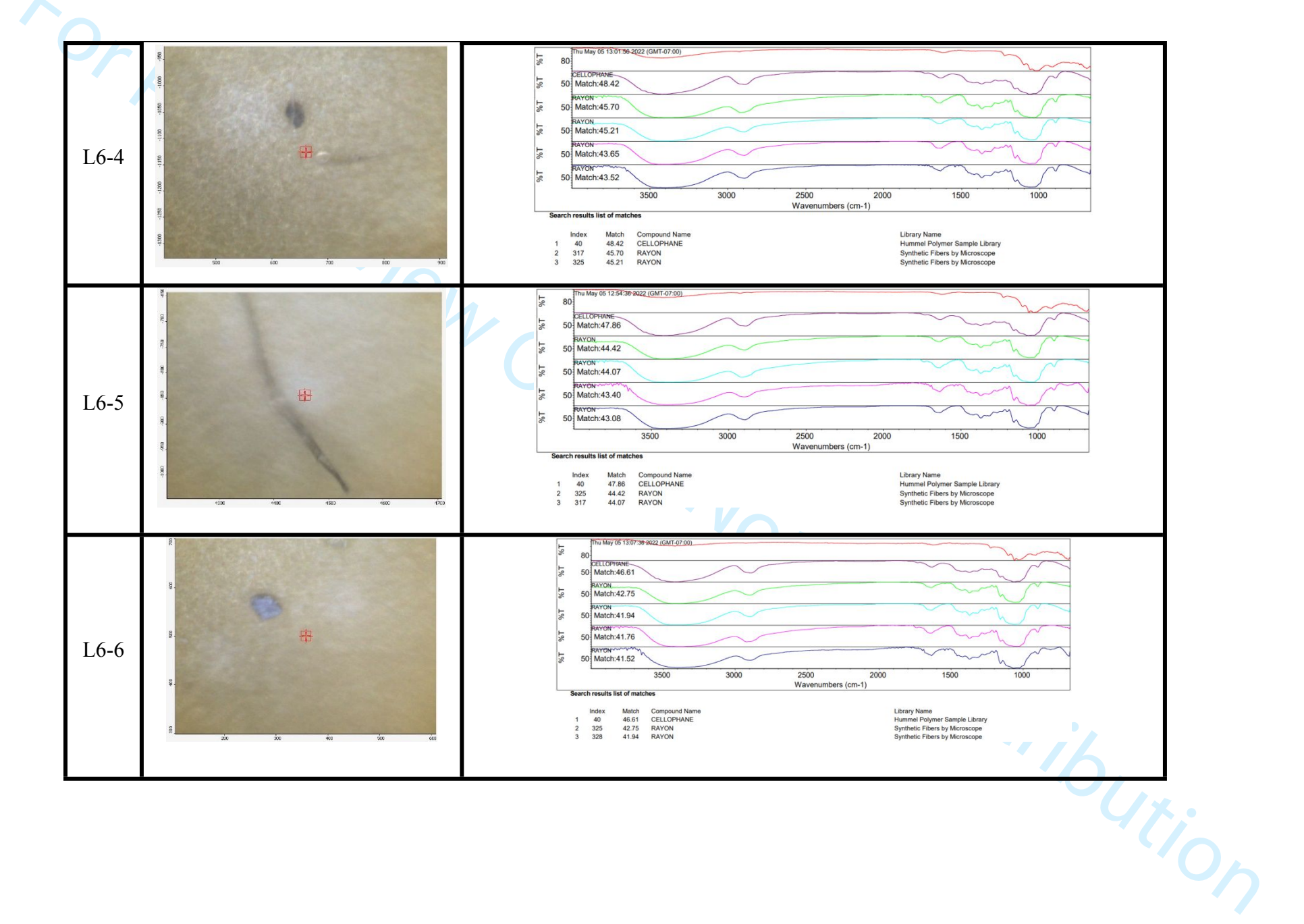


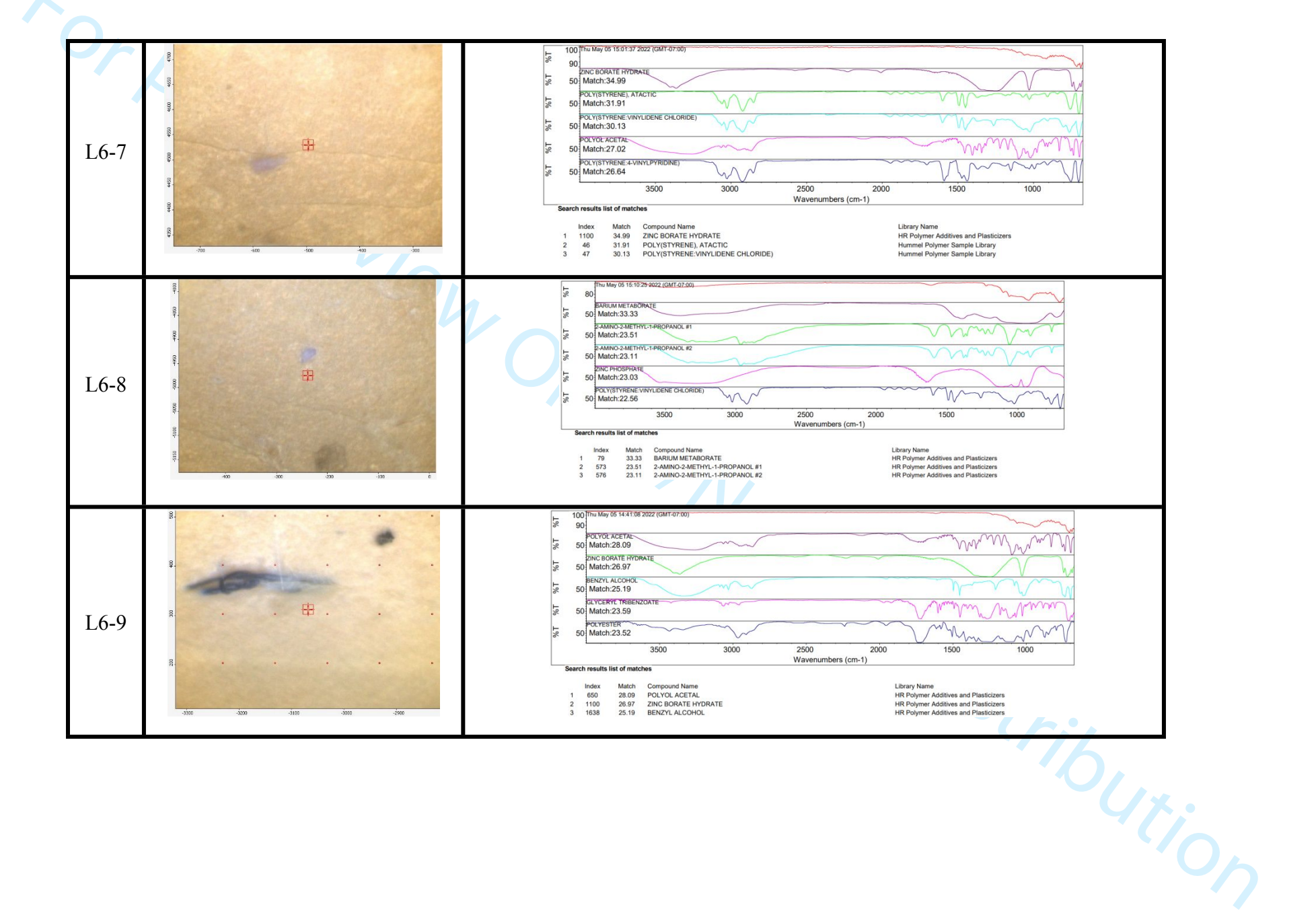












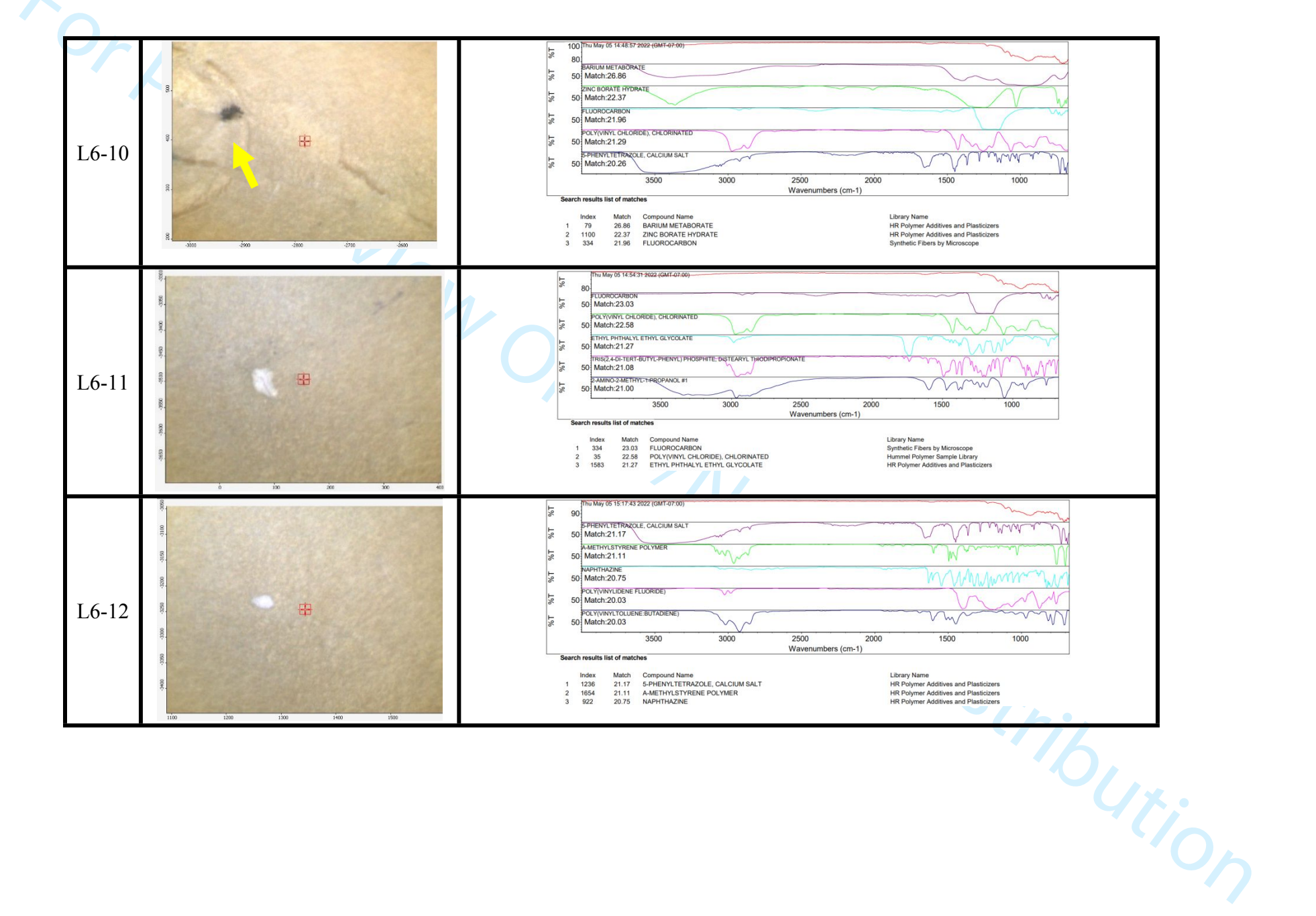
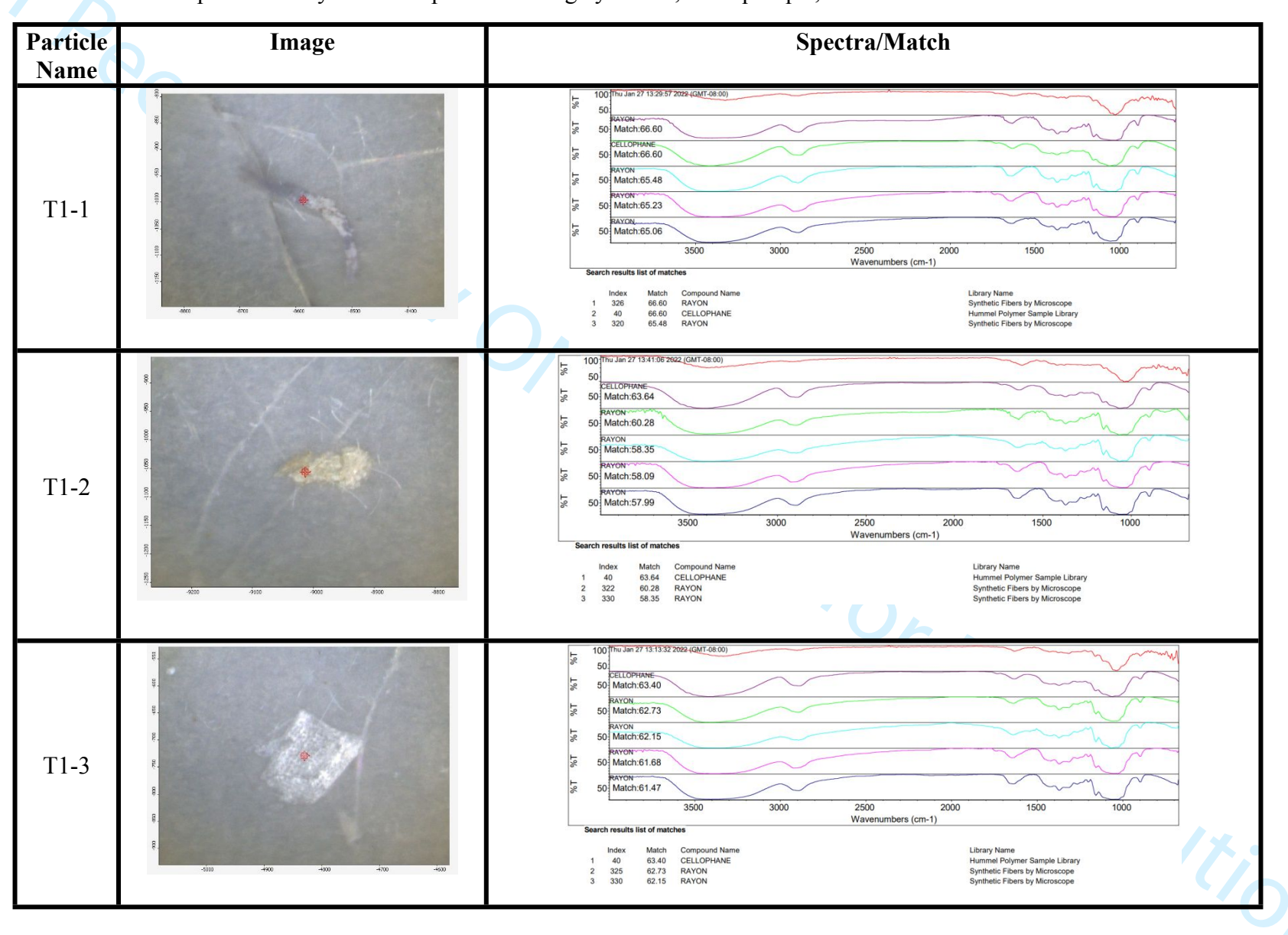
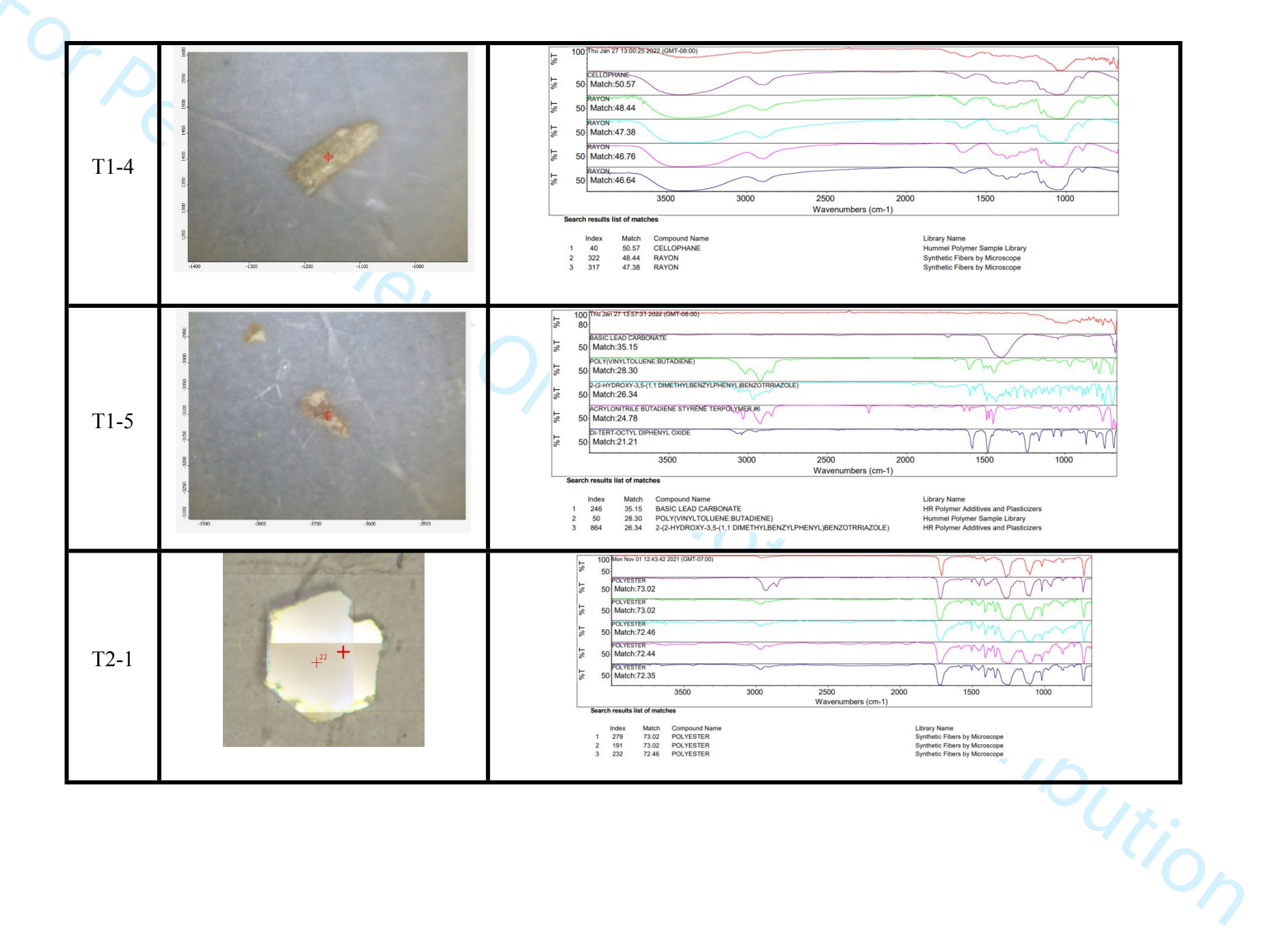
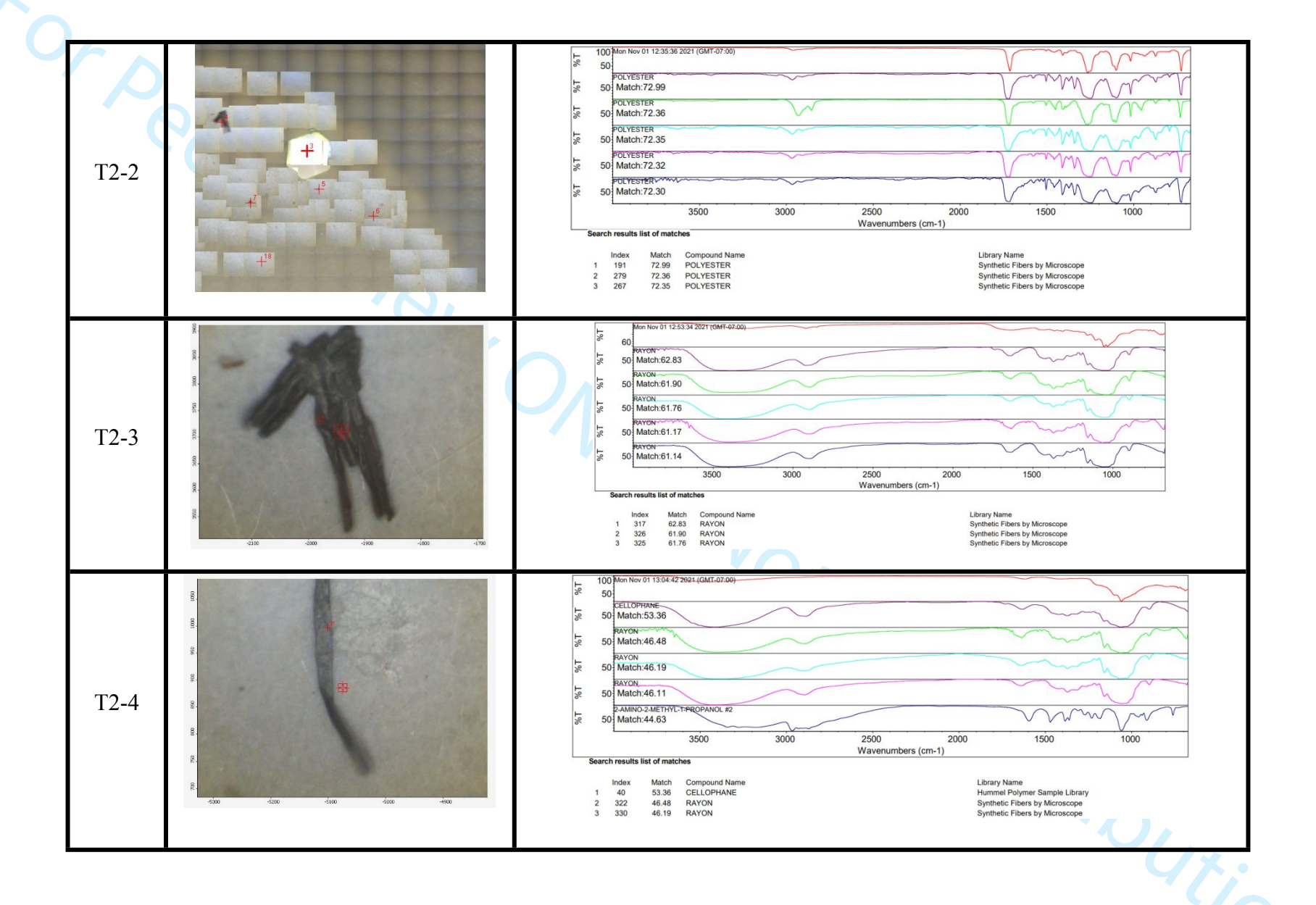
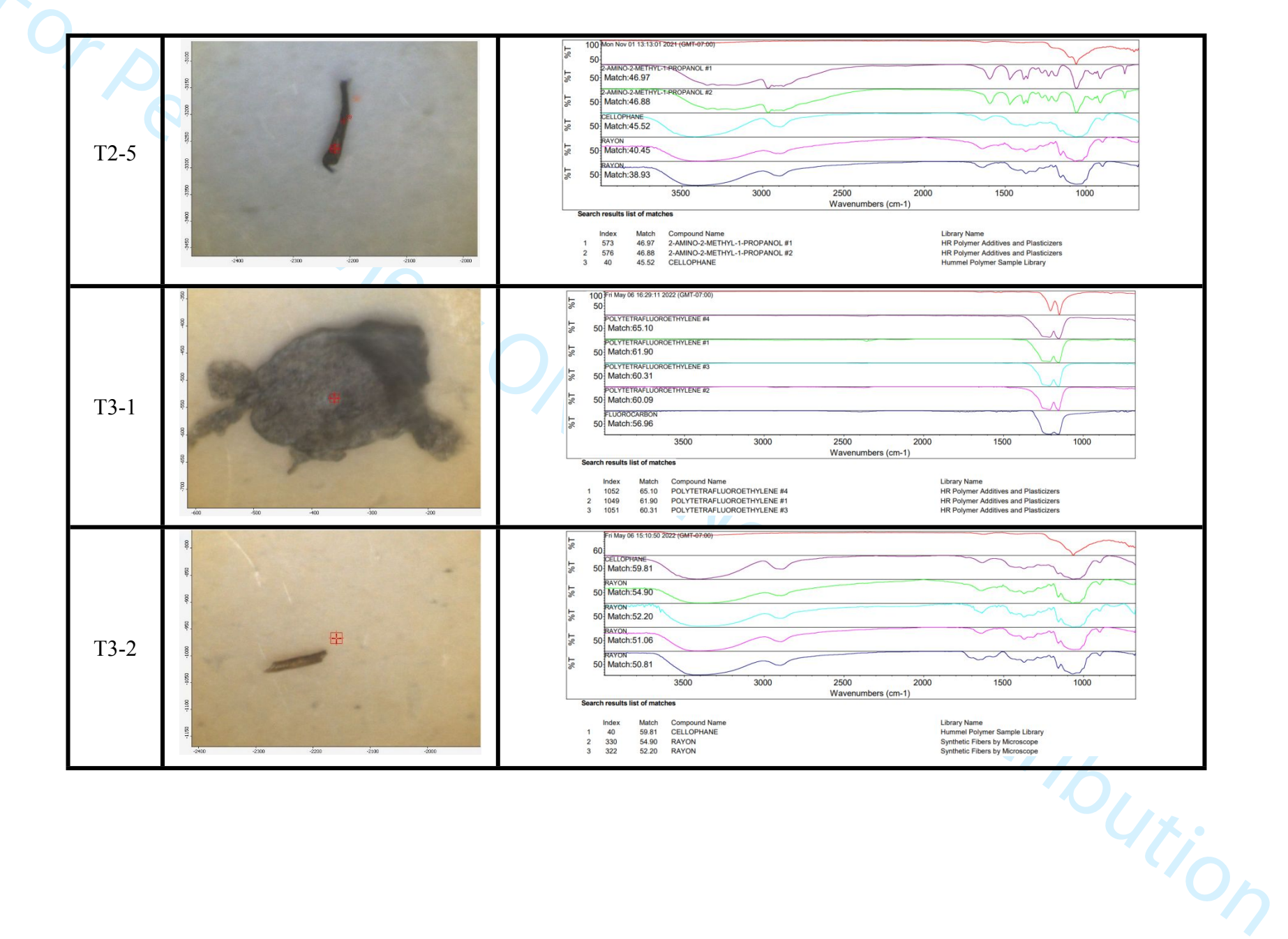


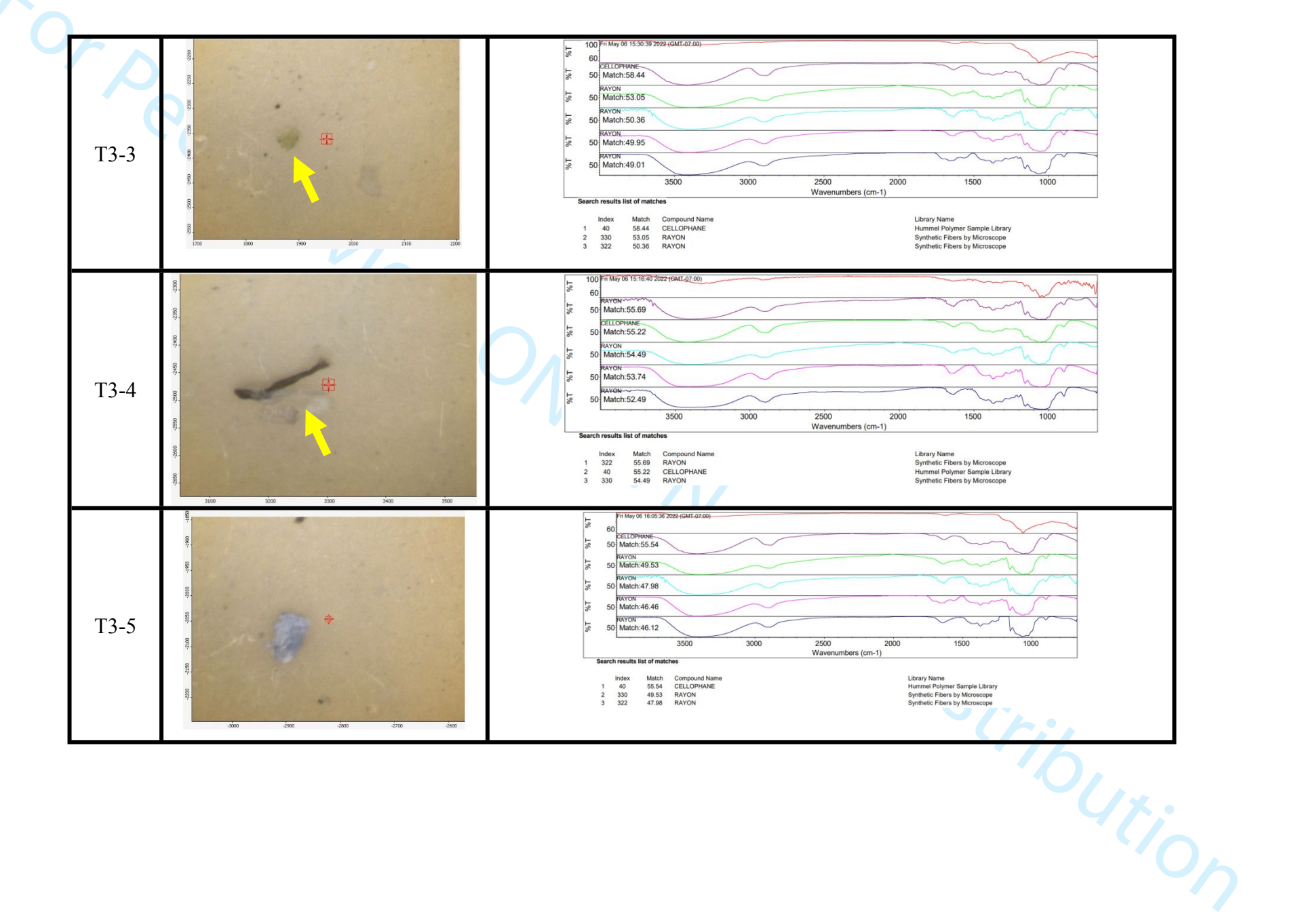
Table S5. FTIR-ATR particle analyses of samples from Tingley Beach, Albuquerque, NM.

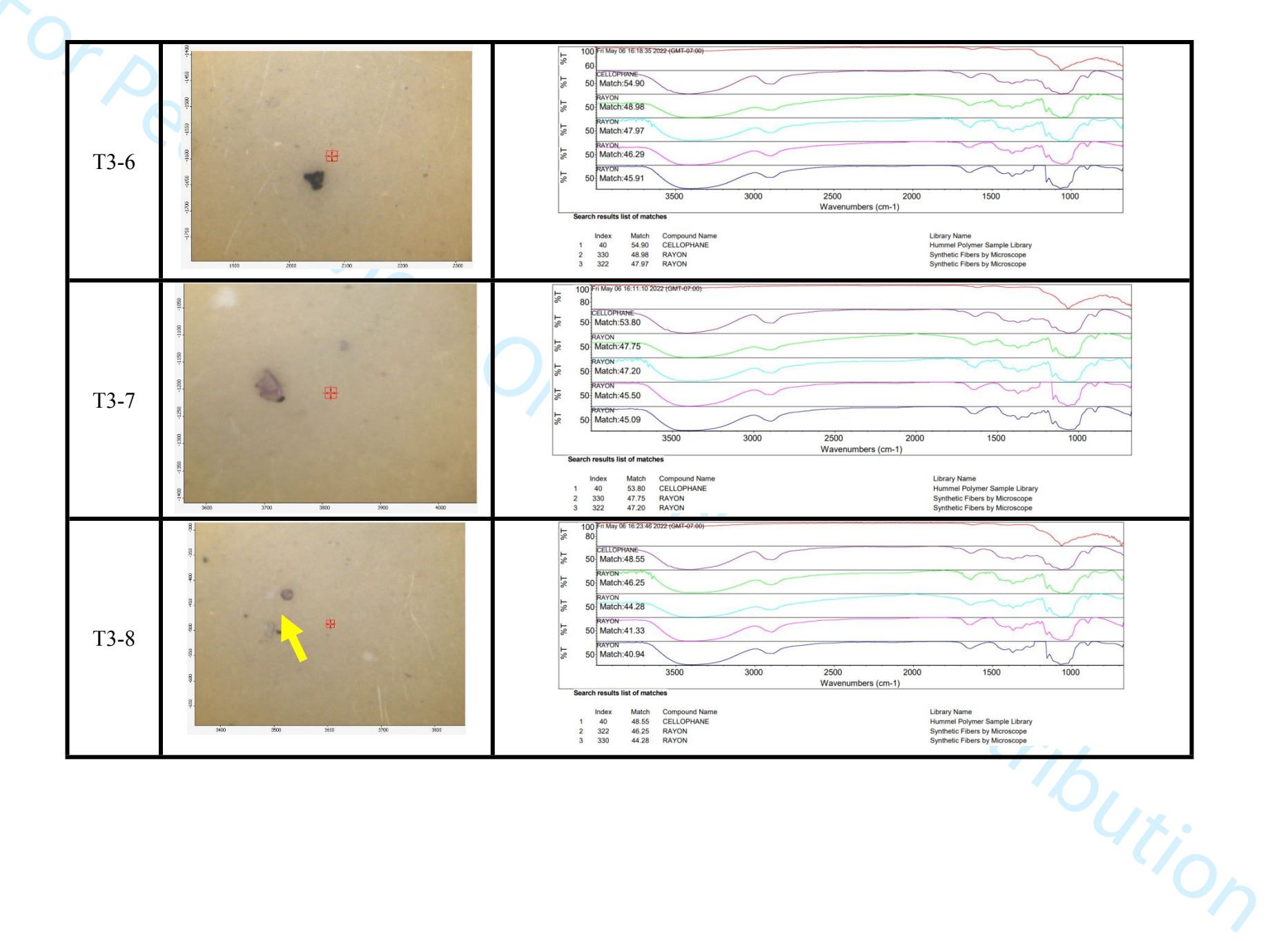


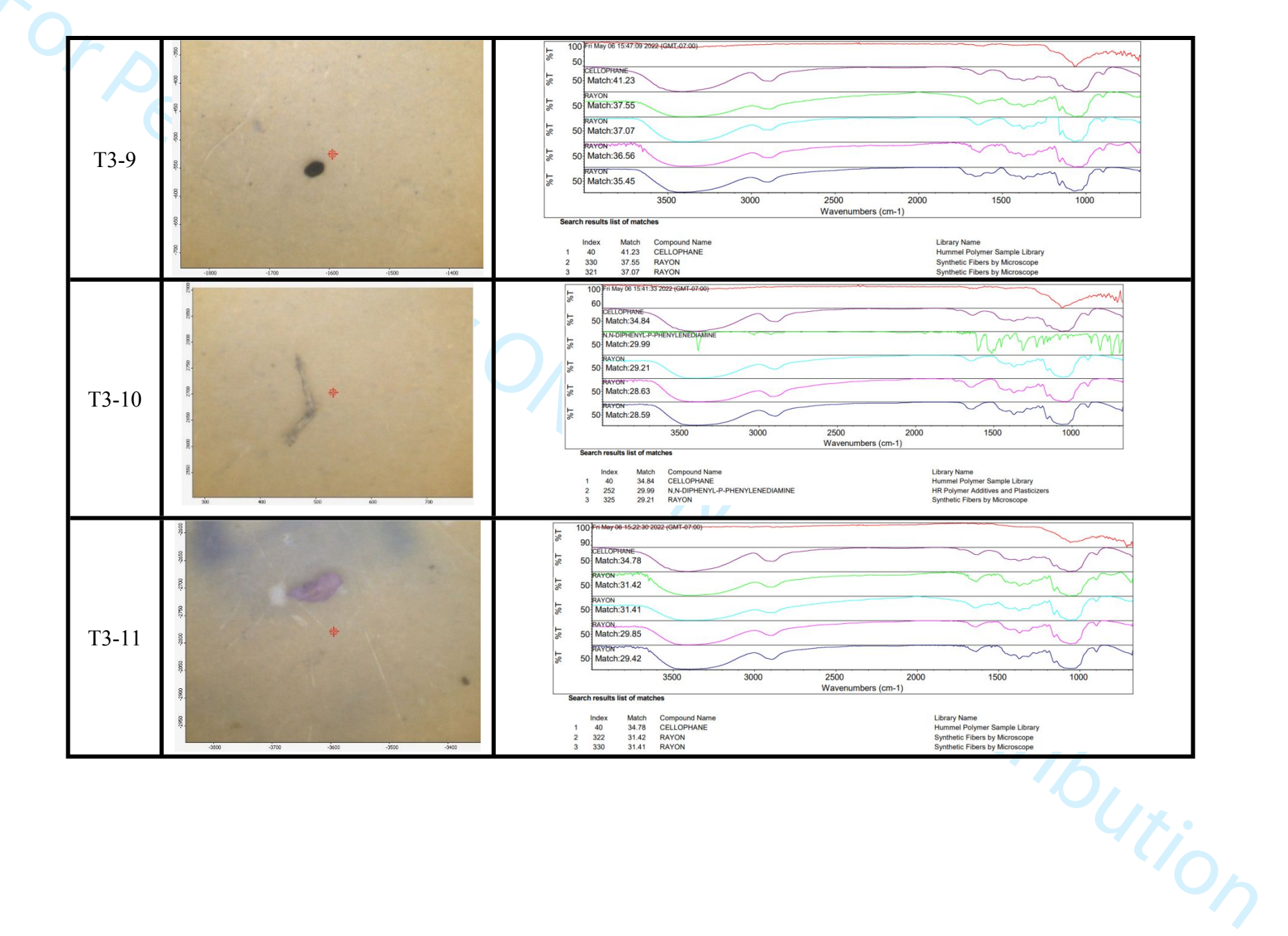












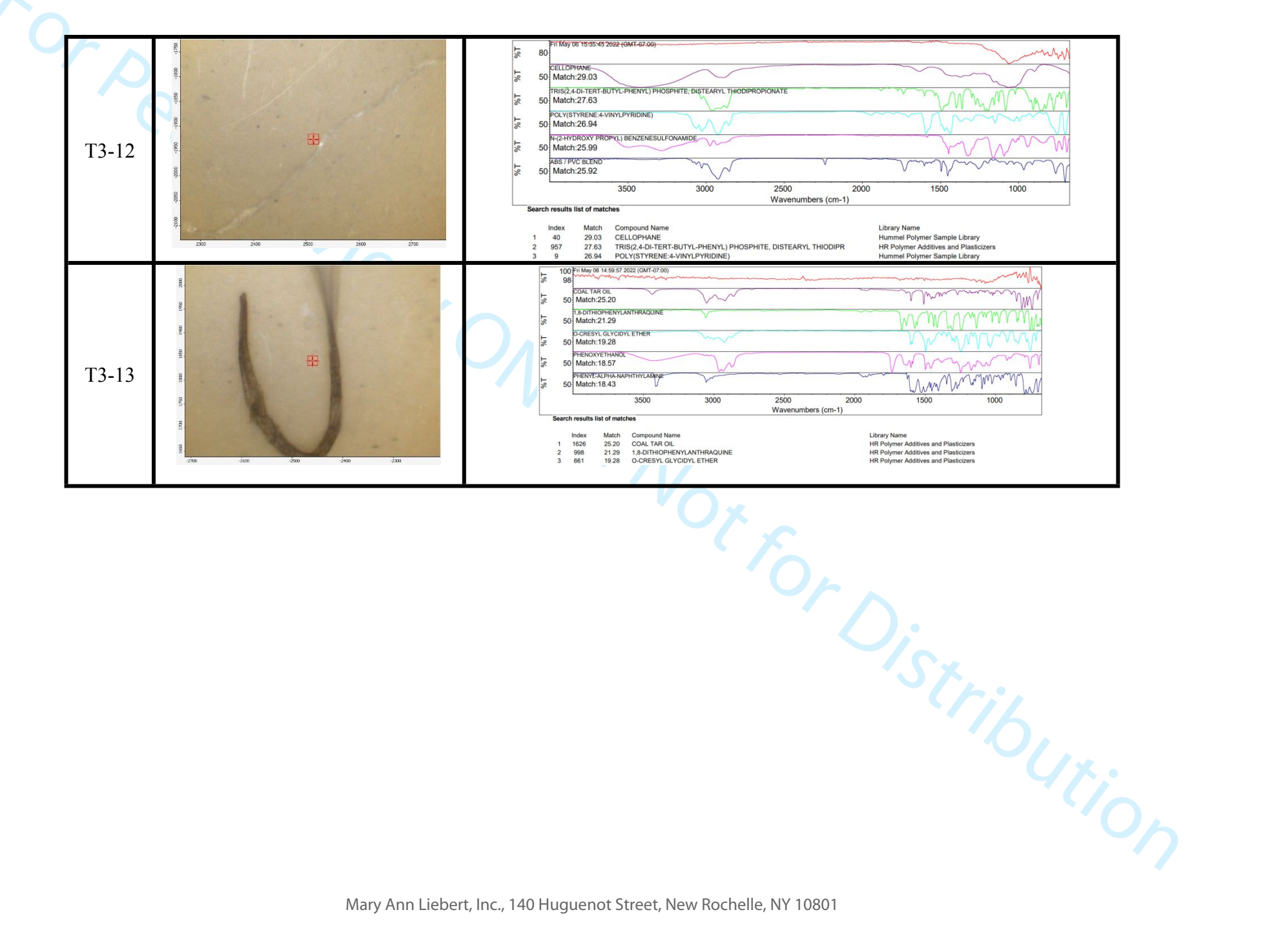
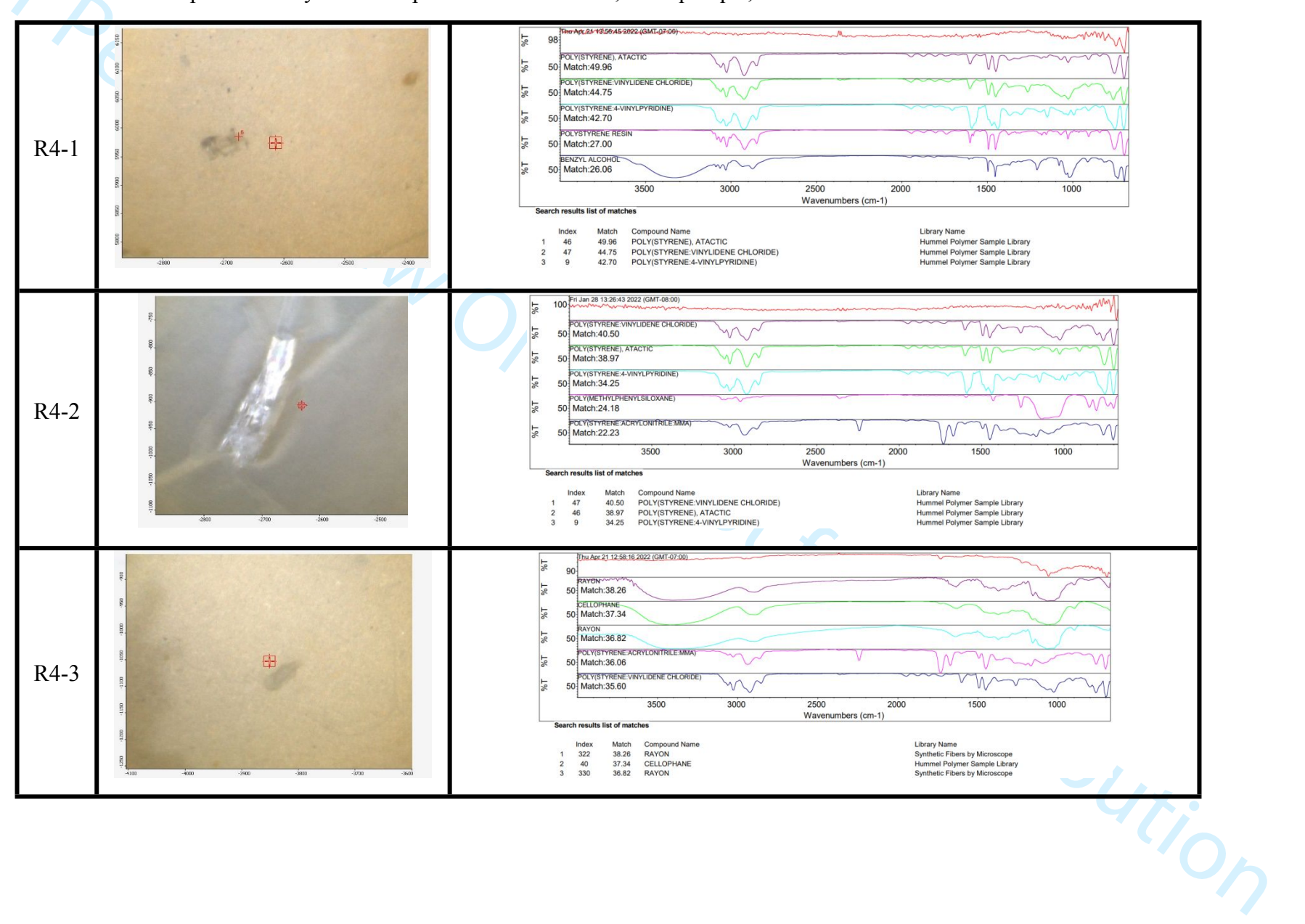
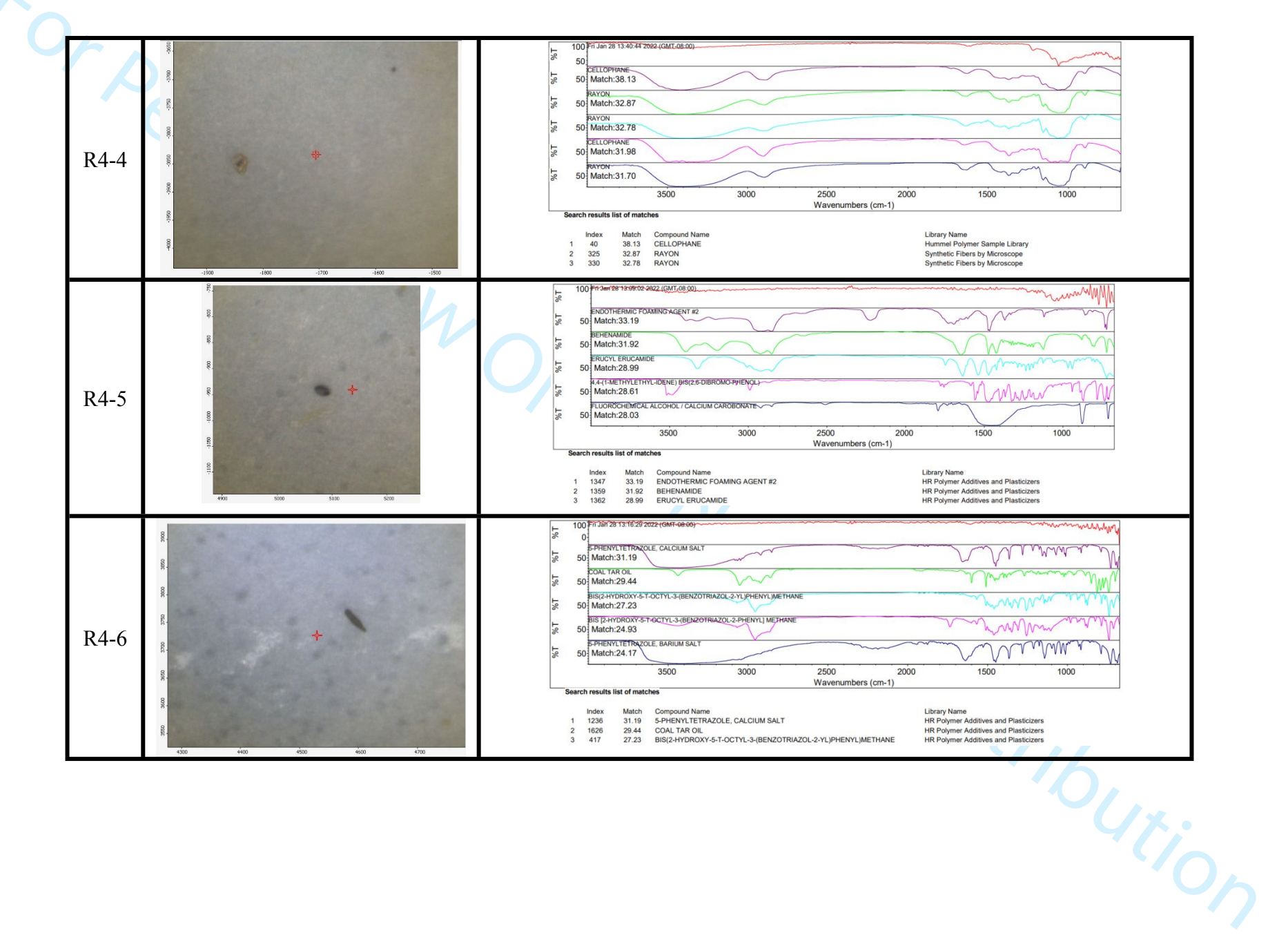
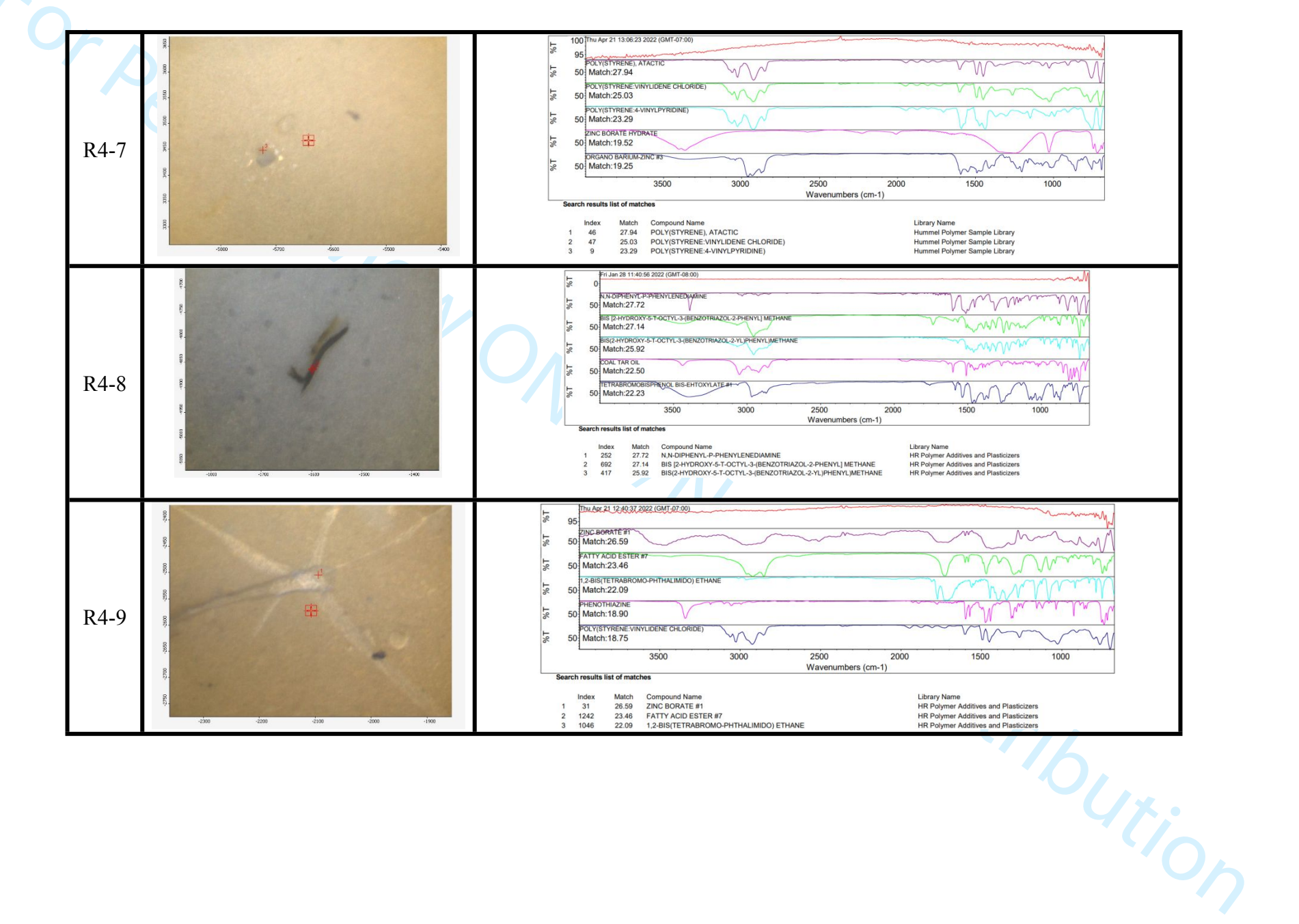
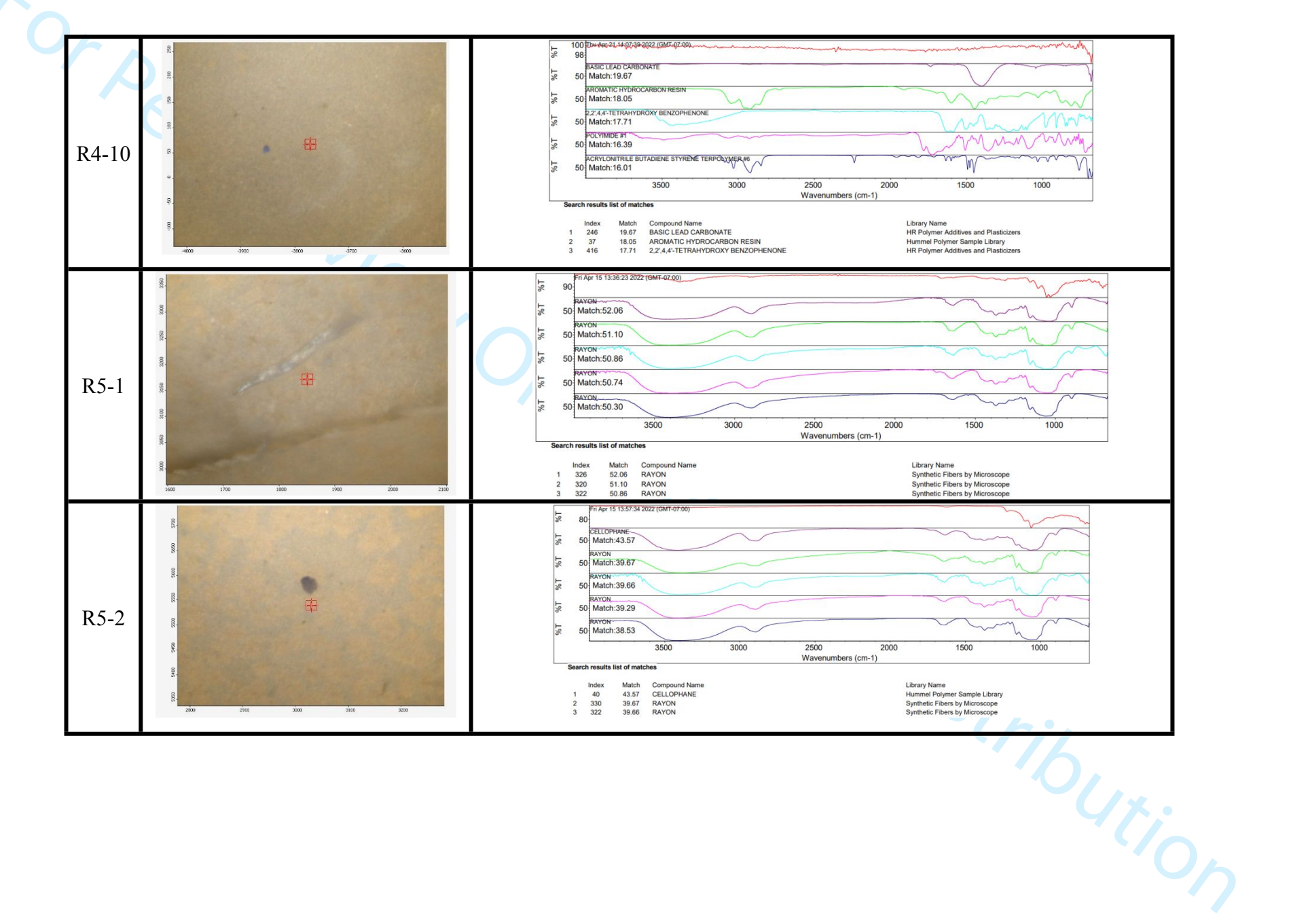


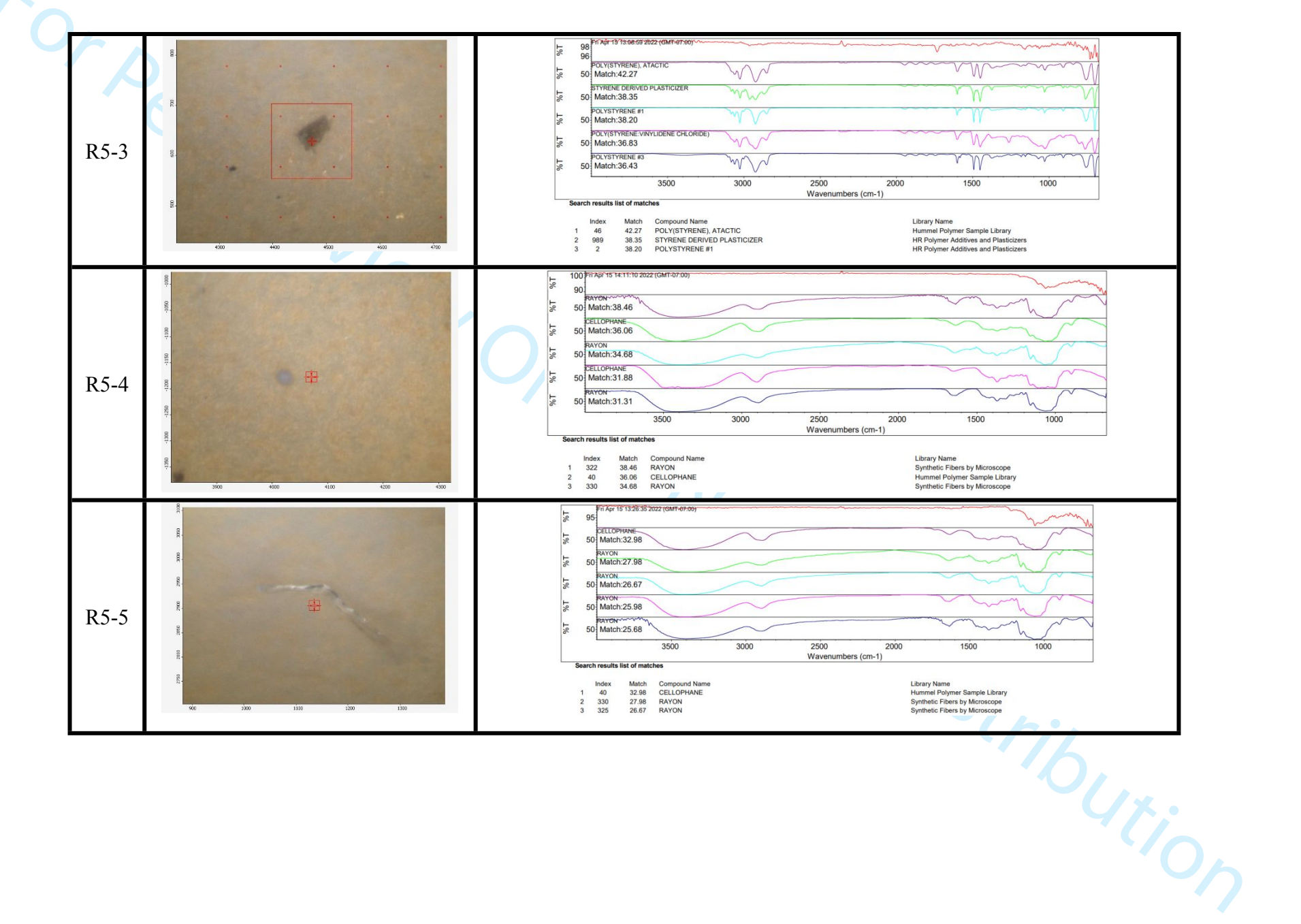
Table S6. FTIR-ATR particle analyses of samples from Rio Grande, Albuquerque, NM.

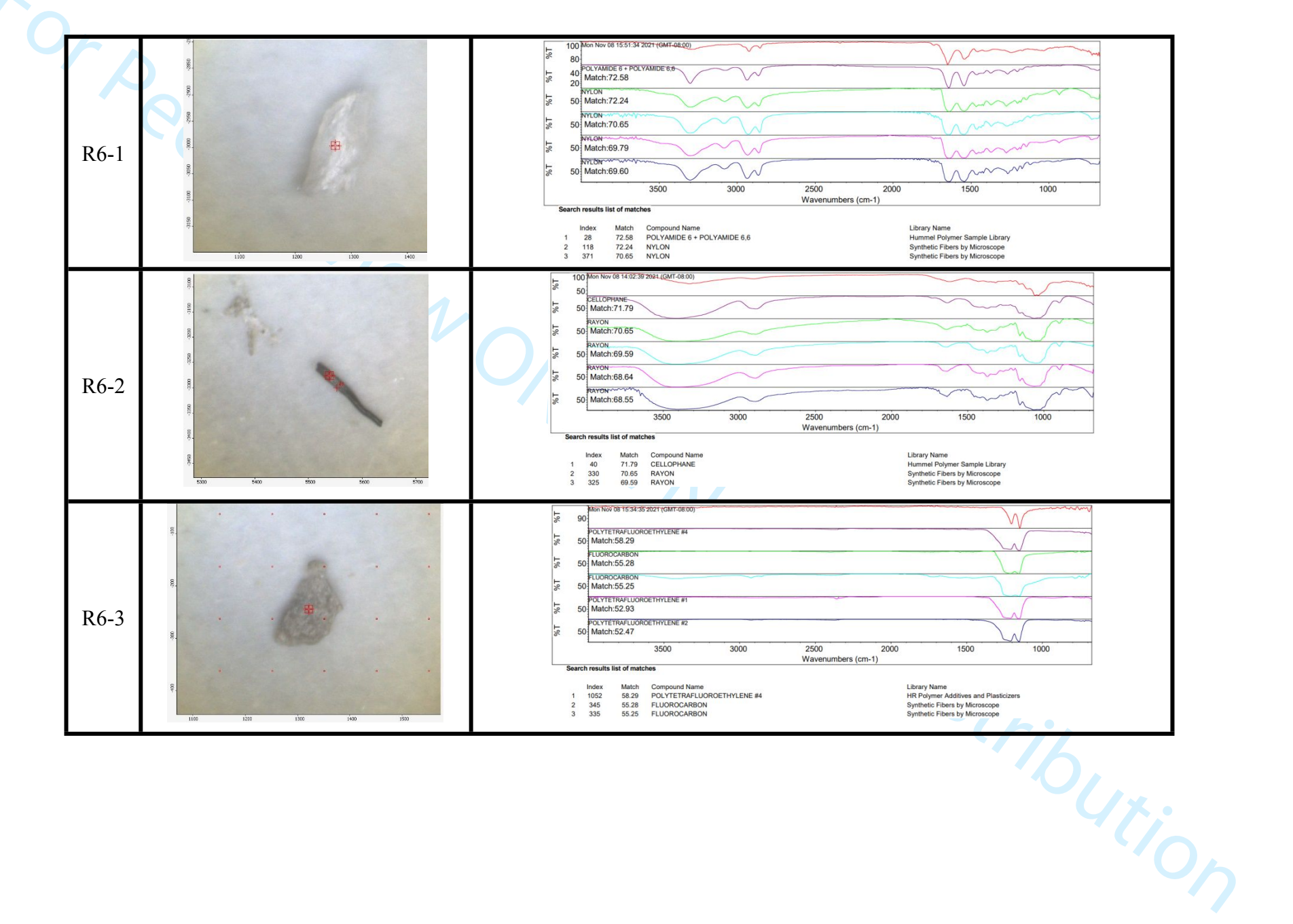


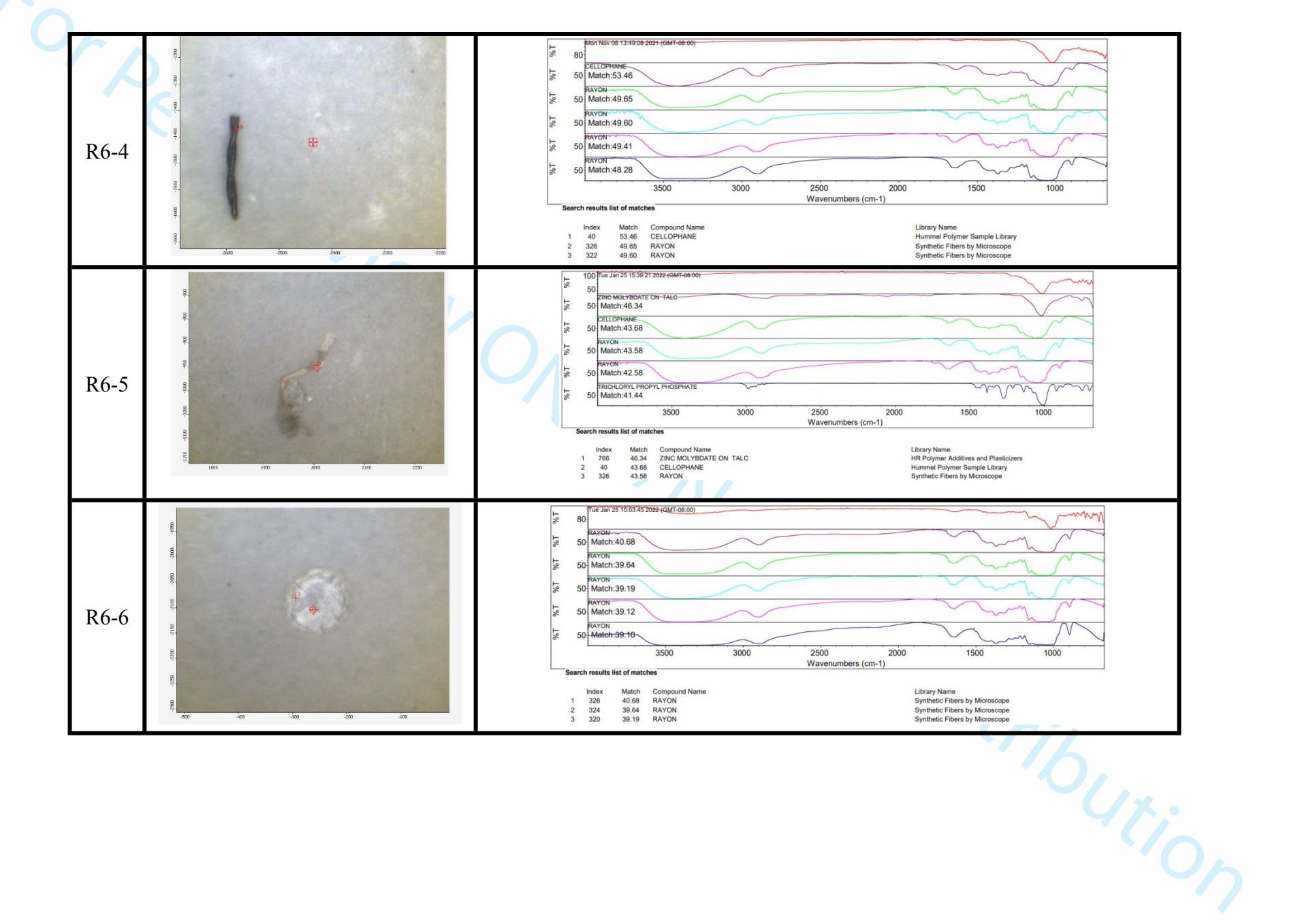


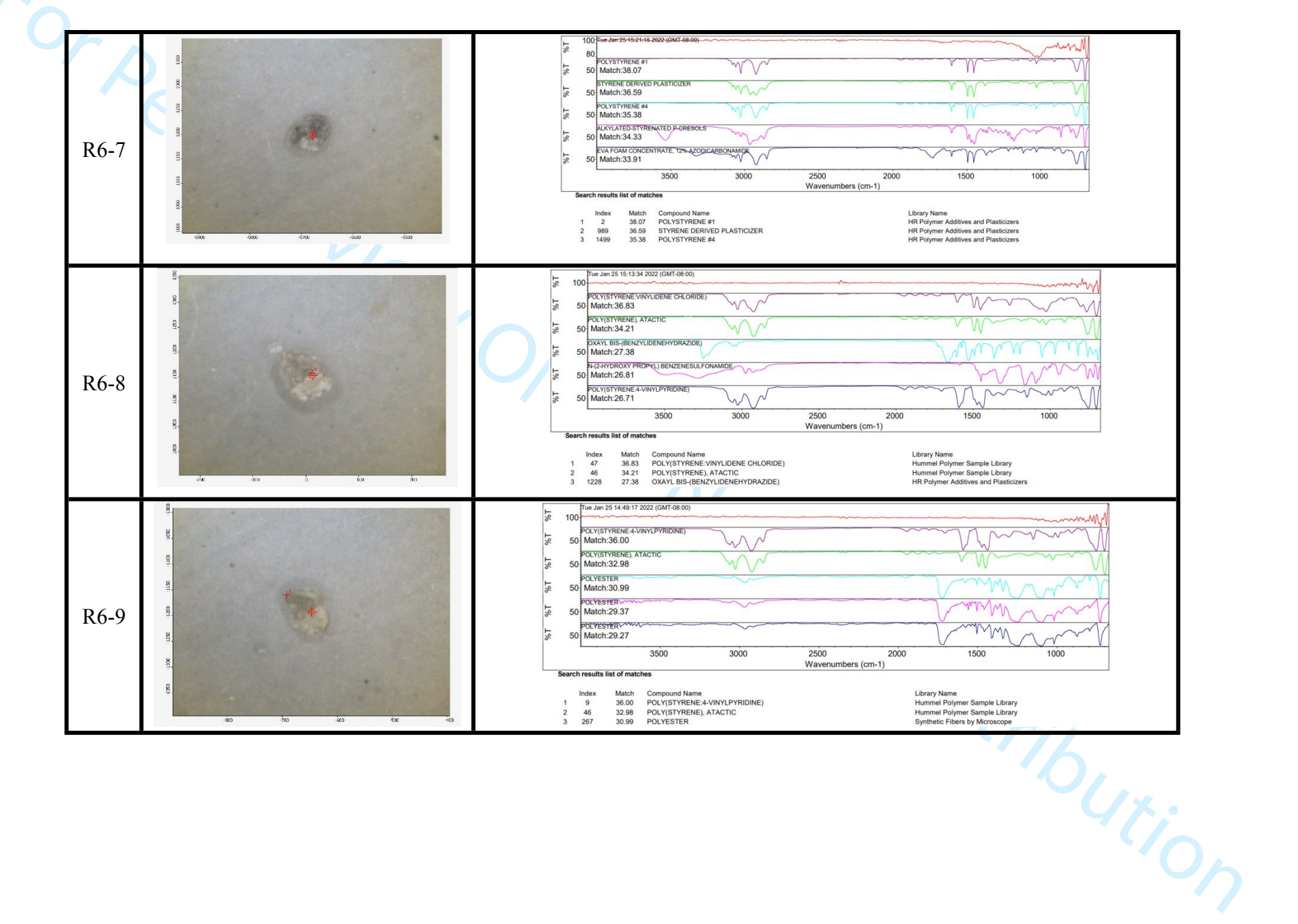












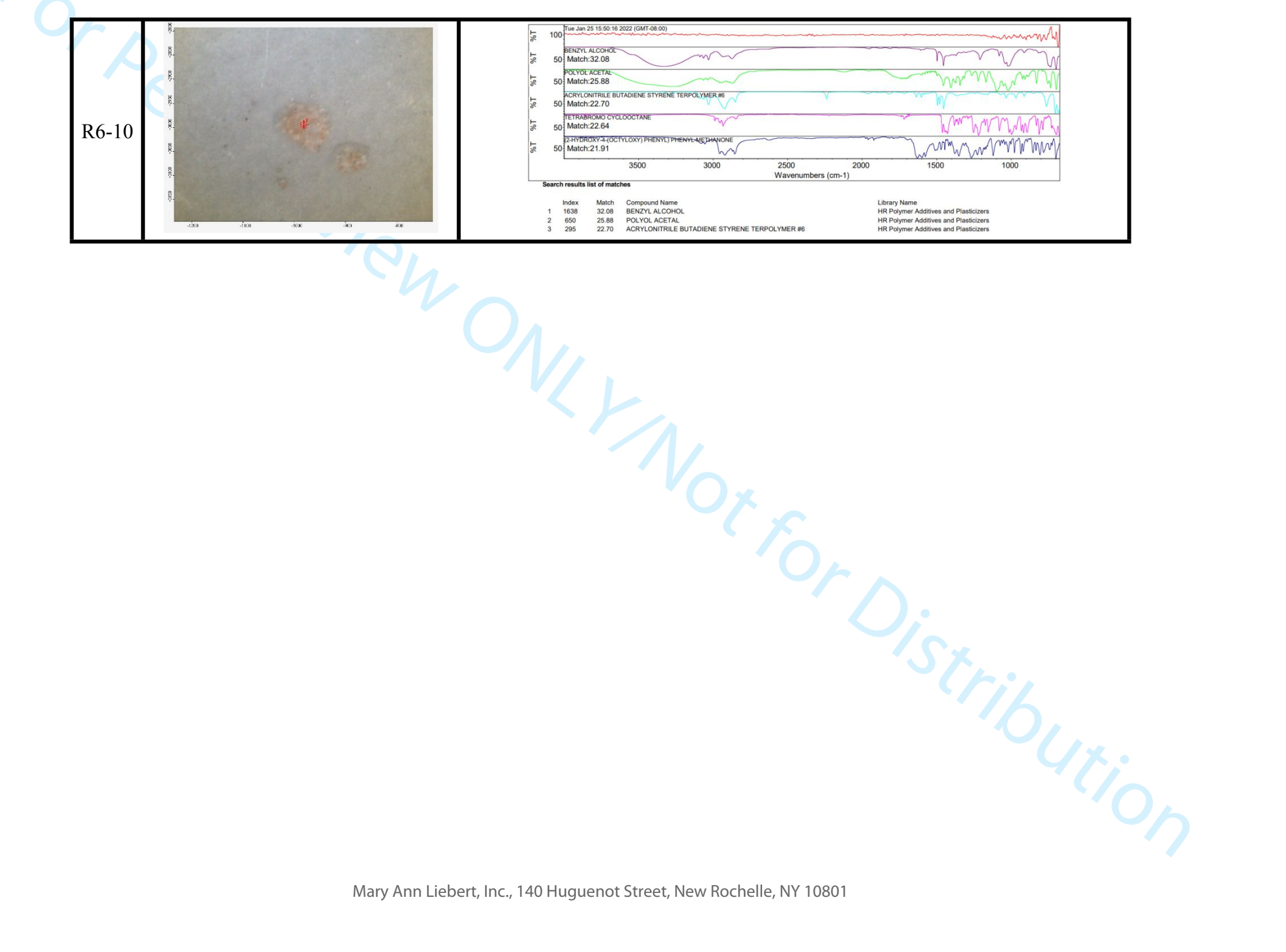
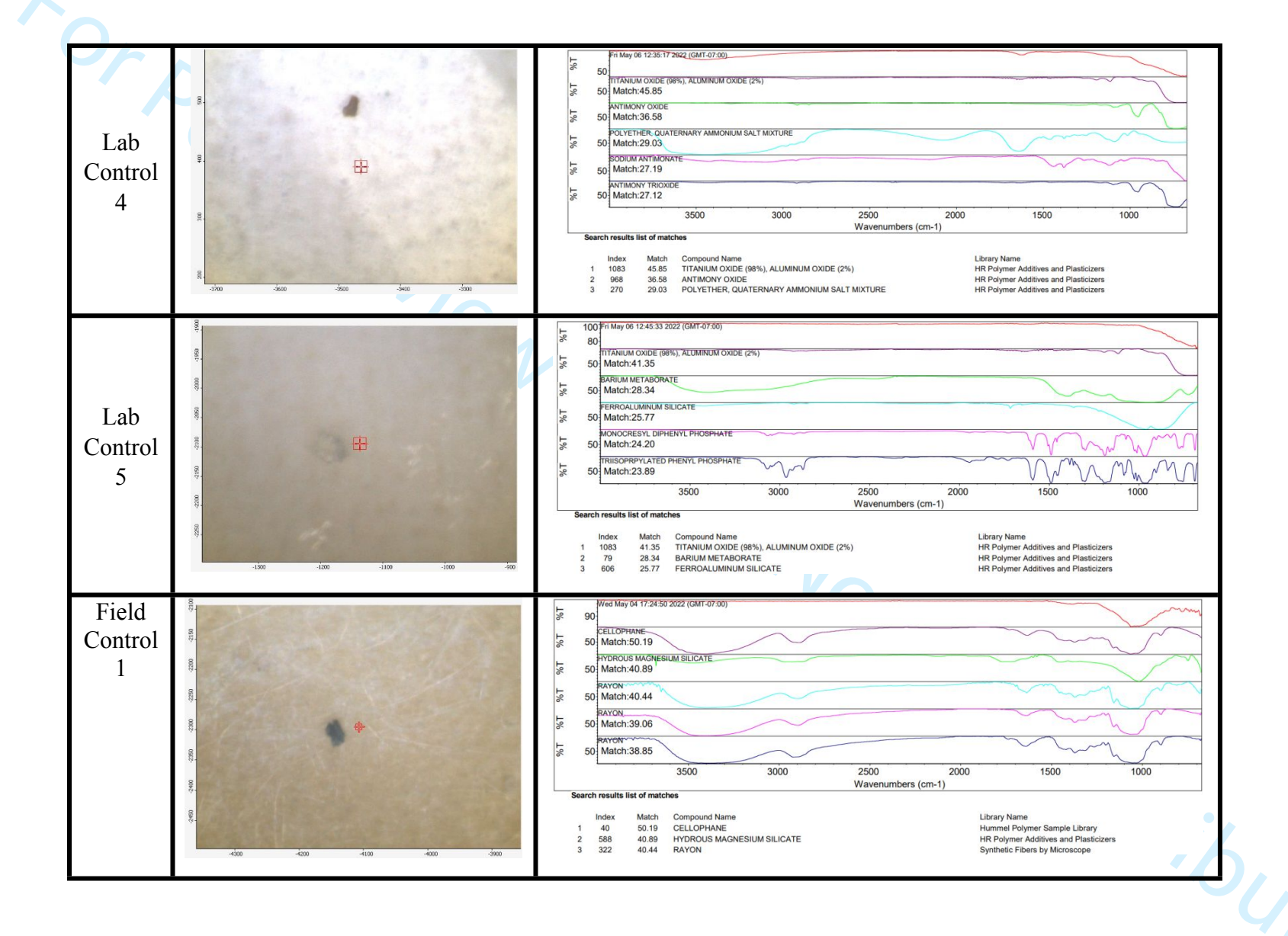
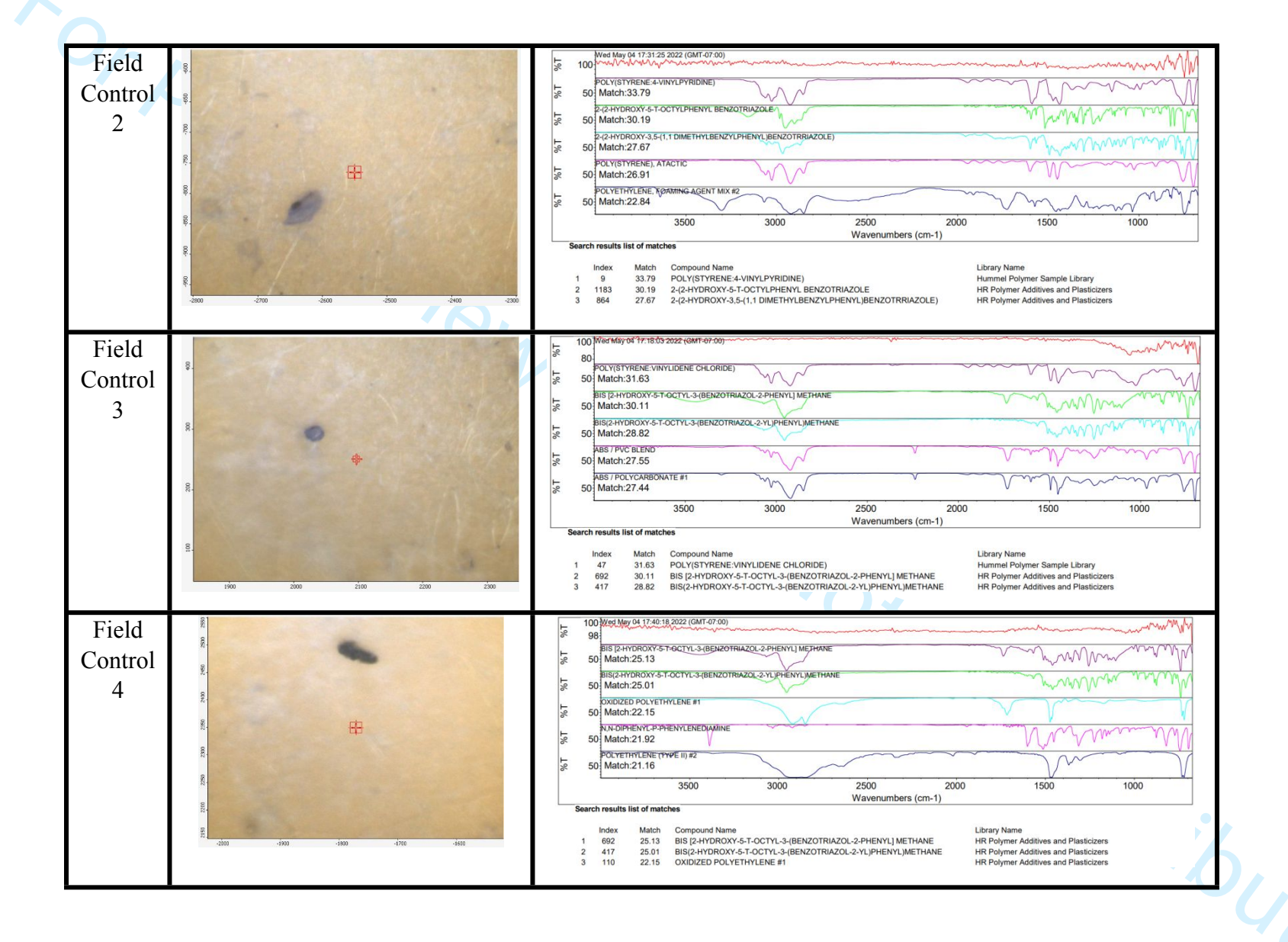
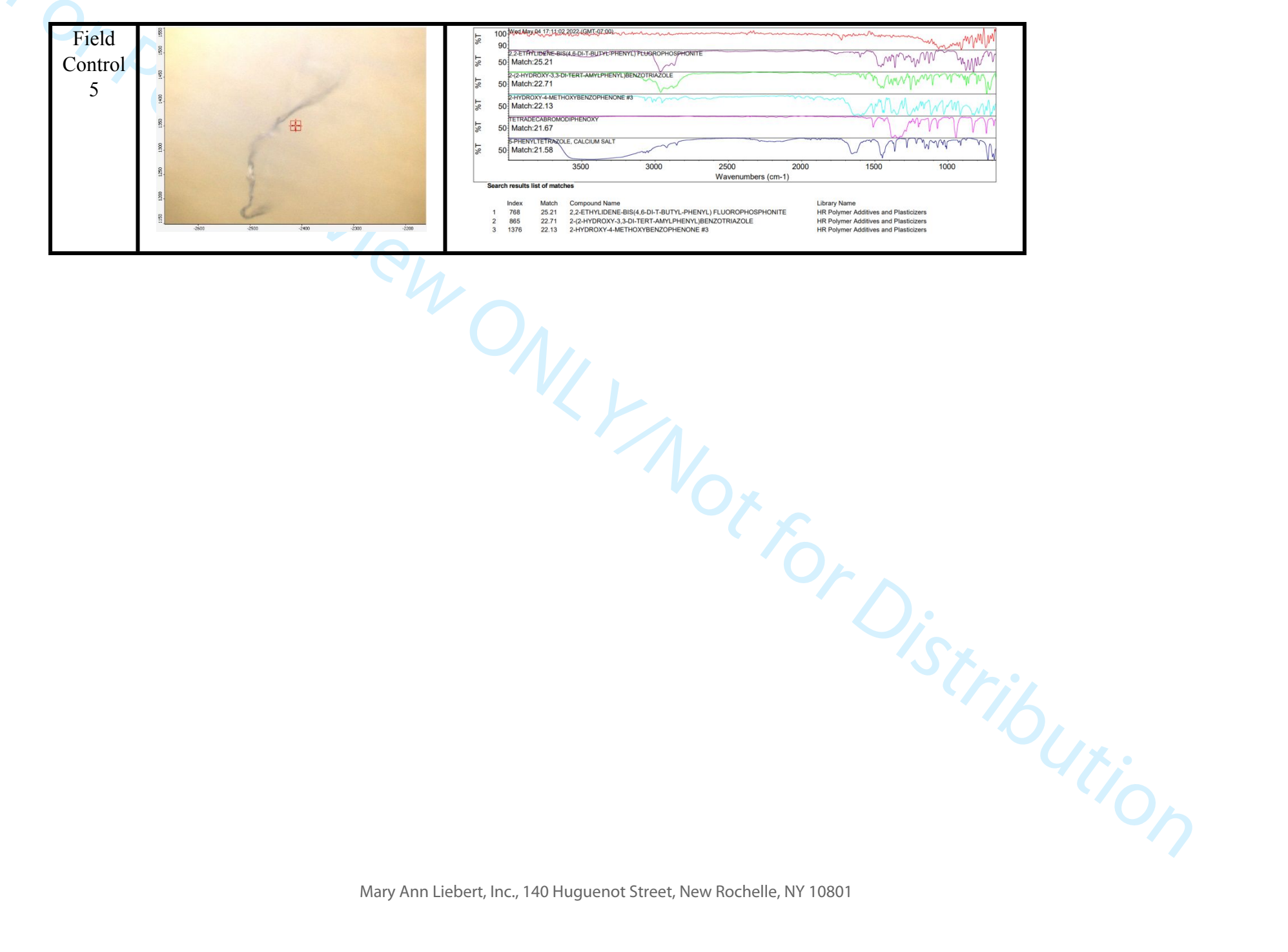


Table S6. FTIR-ATR particle analyses of controls.

Particle Name	Image	Spectra/Match		
Lab Control 1	000- 000- 000- 000- 000- 000- 000- 000	100 F17 May 06 12-52-09 2022 (CMT-07-00)		
Lab Control 2	8- 8- 8- 3- 3- 3- 3- 3- 3- 3- 3- 3- 3- 3- 3- 3-	100 Fit May 06 12:41:20 2992 (GMT-97.00)		
Lab Control 3	0001- 0001-	100 Fri May 06 13 D4-30 2022 (9MT-07-90)		







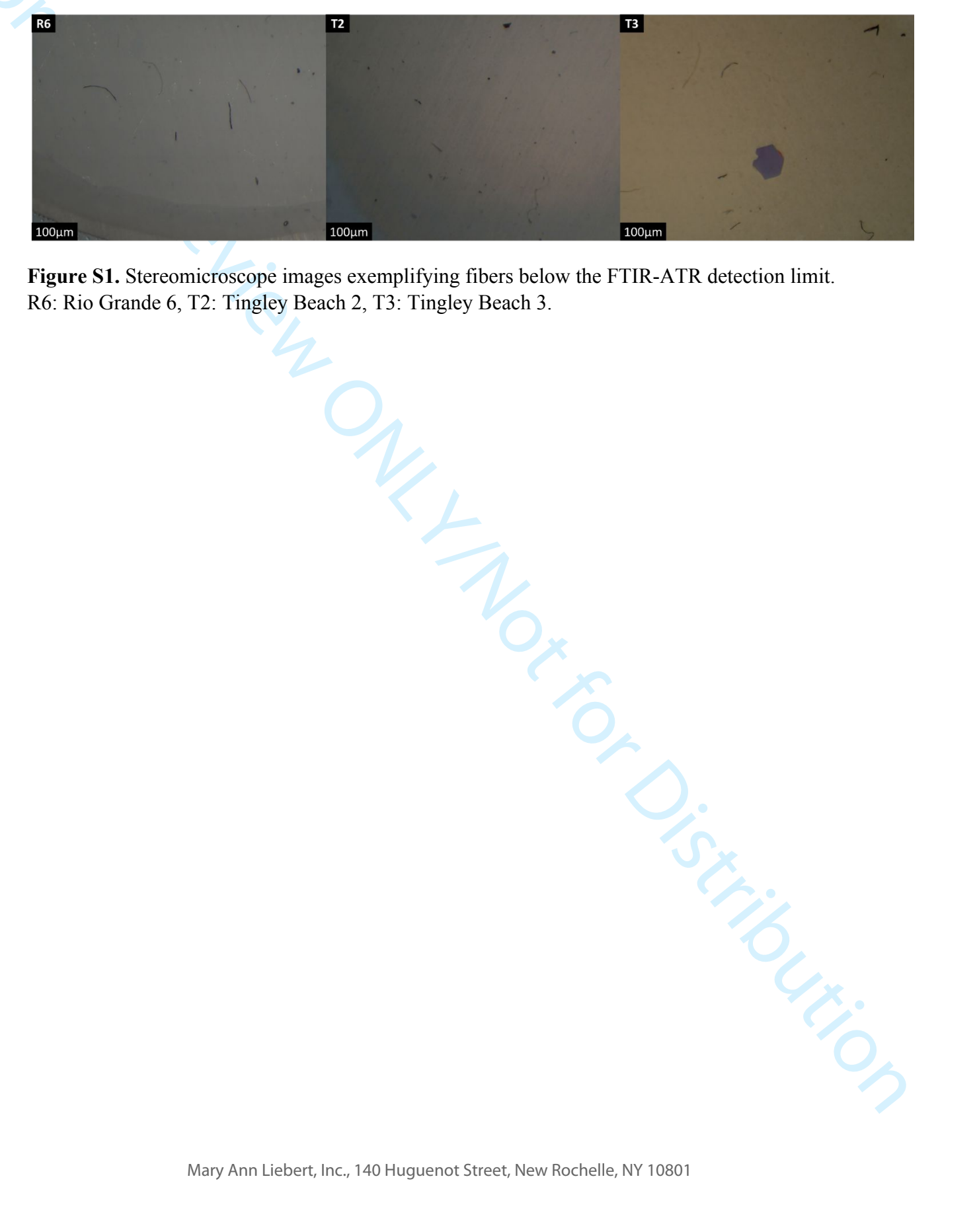


Figure S1. Stereomicroscope images exemplifying fibers below the FTIR-ATR detection limit. R6: Rio Grande 6, T2: Tingley Beach 2, T3: Tingley Beach 3.

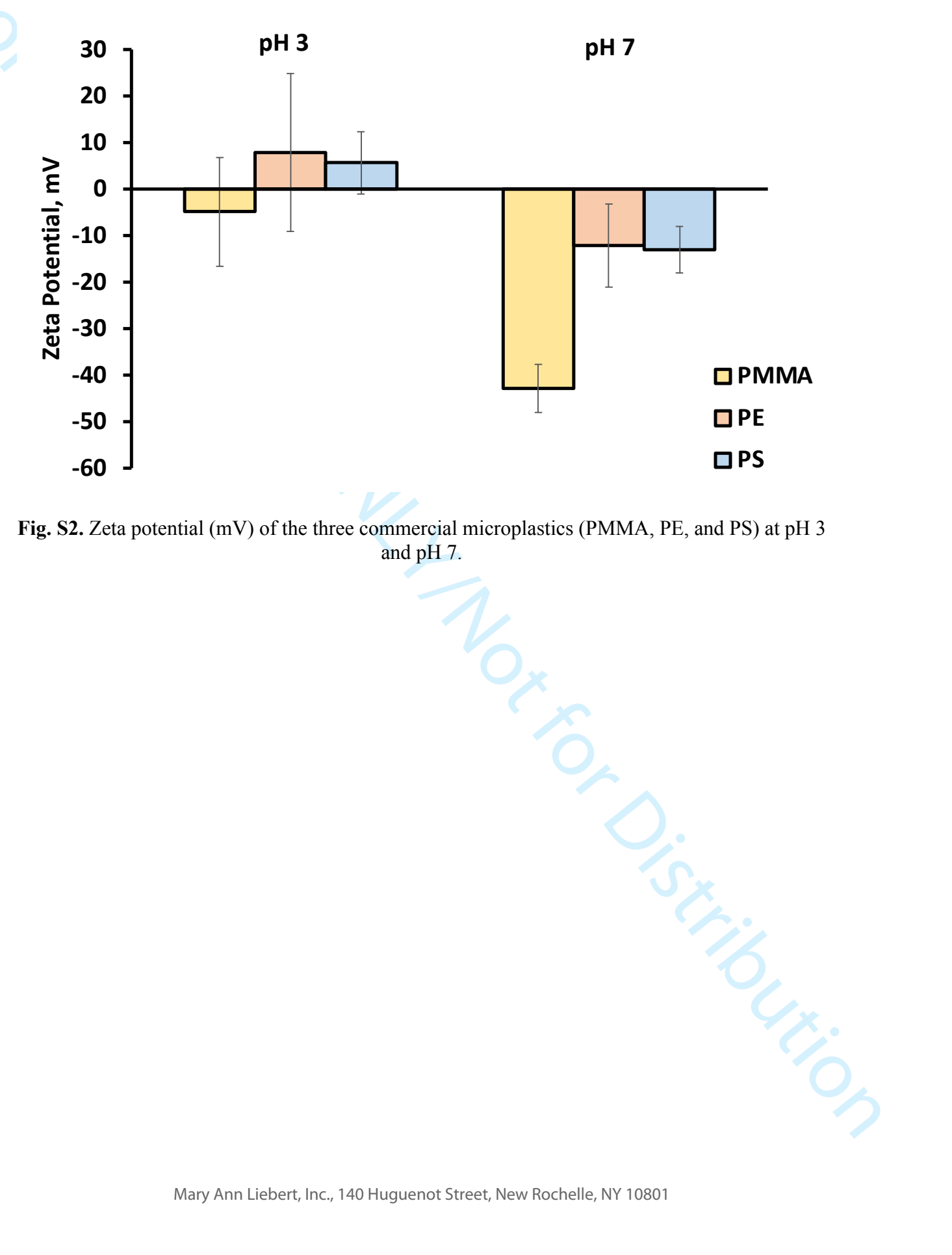


Fig. S2. Zeta potential (mV) of the three commercial microplastics (PMMA, PE, and PS) at pH 3

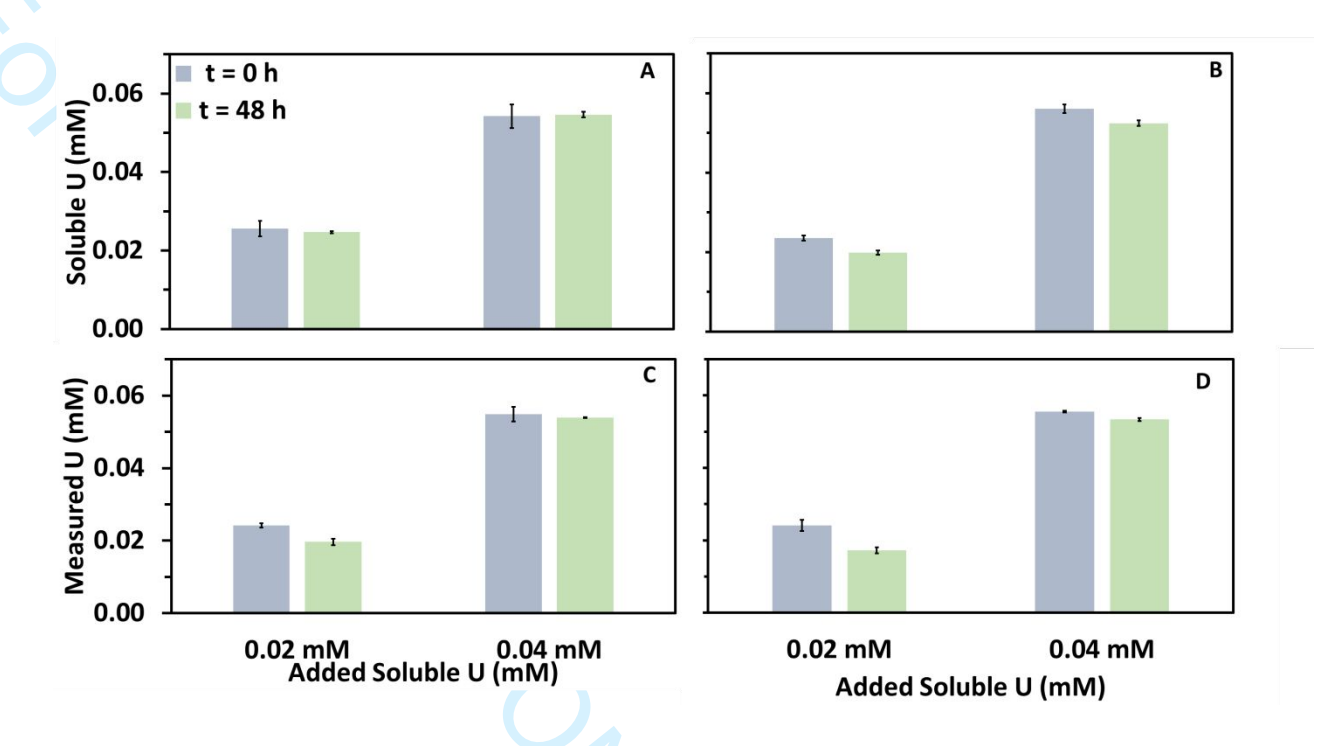


Fig. S3. Soluble U concentration of filtered solutions in batch experiments containing (A) PMMA, (B) PE, (C) PS, and (D) control (no microplastics) at pH 7 at 0 and 48 h. Error bars indicate standard deviation obtained from triplicates.

PRATA, J. C., ALVES, J. R., DA COSTA, J. P., DUARTE, A. C. & ROCHA-SANTOS, T. 2020. Major factors influencing the quantification of Nile Red stained microplastics and improved automatic quantification (MP-VAT 2.0). Sci. Total Environ., 719, 137498. MY, 49, 1362 YANG, D., SHI, H., LI, L., LI, J., JABEEN, K. & KOLANDHASAMY, P. 2015. Microplastic Pollution in Table Salts from China. Environ. Sci. Technol., 49, 13622-13627.